Biozentrum der Universität Basel

Doktorarbeit unter der Leitung von Prof. Dr. Markus A. Rüegg

Proteomic profiling of Duchenne muscular dystrophy: Protein patterns and candidate markers of disease

Inauguraldissertation

zur Erlangung der Würde eines Doktors der Philosophie
vorgelegt der Philosophisch-Naturwissenschaftlichen Fakultät
der Universität Basel

von
Claudia Andrea Escher
aus Zürich ZH

Zürich, August 2011

creative commons

Attribution-Noncommercial-No Derivative Works 2.5 Switzerland

---

You are free:

to Share — to copy, distribute and transmit the work

Under the following conditions:

Attribution. You must attribute the work in the manner specified by the author or licensor (but not in any way that suggests that they endorse you or your use of the work).

Noncommercial. You may not use this work for commercial purposes.

No Derivative Works. You may not alter, transform, or build upon this work.

- For any reuse or distribution, you must make clear to others the license terms of this work. The best way to do this is with a link to this web page.
- Any of the above conditions can be waived if you get permission from the copyright holder.
- Nothing in this license impairs or restricts the author's moral rights.

Your fair dealing and other rights are in no way affected by the above.

This is a human-readable summary of the Legal Code (the full license) available in German:
http://creativecommons.org/licenses/by-nc-nd/2.5/ch/legalcode.de

Disclaimer:
The Commons Deed is not a license. It is simply a handy reference for understanding the Legal Code (the full license) — it is a human-readable expression of some of its key terms. Think of it as the user-friendly interface to the Legal Code beneath. This Deed itself has no legal value, and its contents do not appear in the actual license. Creative Commons is not a law firm and does not provide legal services. Distributing of, displaying of, or linking to this Commons Deed does not create an attorney-client relationship.

Quelle: http://creativecommons.org/licenses/by-nc-nd/2.5/ch/deed.en Datum: 3.4.2009

Genehmigt von der Philosophisch-Naturwissenschaftlichen Fakultät auf Antrag von

Prof. Dr. Markus A. Rüegg
Dissertationsleitung

Prof. Dr. Ruedi Aebersold
Korreferat

Basel, 25. Mai 2010

Prof. Dr. Eberhard Parlow
Dekan der Philosophisch-Naturwissenschaftlichen Fakulät

TABLE OF CONTENTS

SUMMARY

Duchenne muscular dystrophy (DMD) caused by mutations in the dystrophin gene is a severe chronic muscle-wasting disease leading to early loss of ambulation in patients and to death by the third decade. Other muscular dystrophies exist including amongst others DMD's milder allelic form Becker muscular dystrophy and the heterogeneous group of limb-girdle muscular dystrophies that differ in age of onset, severity, and affected proteins.
In diagnosing muscular dystrophies, the assessment of multiple proteins in a muscle biopsy by immunohistochemical methods is considered the gold standard, as the identification of the underlying mutation is not always feasible or sufficient due to difficult genotype-phenotype prediction. The reproducibility and sensitivity of reverse protein arrays and their excellent correlation with immunohistochemistry and immunoblotting combined with minimal sample and antibody consumption make them an ideal approach for the assessment of muscular expression of multiple proteins in small biopsies. We have evaluated a set of antibodies currently used in standard diagnostic processes for muscular dystrophies on human muscle tissue and cultured primary human myotubes. We have found high correlations with Western blot data and reproducible significant differences in dystrophin, sarcoglycan, and dystroglycan expression between control and patient samples. Reverse protein arrays can quantitatively measure muscle proteins in as little as 10mg muscle tissue. This technology could be of interest not only in diagnostic processes, but especially for protein quantification of multiple, follow-up biopsies during clinical trials in upcoming therapy approaches when protein expression in muscle is considered an important outcome measure or biomarker.
Despite the precise and extensive knowledge about the dystrophin gene and its protein, precise molecular and cellular events that eventually lead to muscle fiber degeneration in DMD are poorly understood. Downstream pathogenic events in metabolic pathways and cellular signaling that are key factors causing the ultimate degeneration of muscle fibers in DMD and reflecting disease state can be elucidated using mass spectrometry-based proteomics experiments. Proteomic profiling of DMD muscle tissue and comparing the resulting pattern to other muscular dystrophies has revealed a set of proteins that are differentially expressed in DMD skeletal muscle, most prominently a drastic increase in the muscle-specific member of the small heat shock protein family HSPβ2. We are currently implementing a set of experiments to validate HSPβ2 as disease marker for Duchenne muscular dystrophy in cultured primary myotubes from DMD patients and, if applicable, in serum from DMD patients. HSPβ2 is a promising candidate that could be applied as signature molecule as part of a protein panel that can be used to assess disease state in DMD or therapeutic effects of novel drugs or treatments.

LIST OF ABBREVIATIONS

2DE	Two-Dimensional Gel Electrophoresis
ADP	Adenosine Diphosphate
ATP	Adenosine Triphosphate
BMD	Becker Muscular Dystrophy
CK	Creatine Kinase
CLB1	Cell Lysis Buffer
CV	Coefficient of Variation
DAP	Dystrophin-Asscociated Proteins
DGC	Dystrophin-Glycoprotein Complex
DIGE	Difference In-Gel Electrophoresis
DMD	Duchenne Muscular Dystrophy
DMEM	Dulbecco's Modified Eagle Medium
DRM	Desmin-Related Myopathy
DRP	Dystrophin-Related Protein
ECM	Extracellular Matrix
EDMD	Emery-Dreifuss Muscular Dystrophy
ESI	Electrospray Ionisation
FCS	Fetal Calf Serum
FKRP	Fukutin-Related Protein
GPD1L	Glycerol-3-Phosphate Dehydrogenase-Like Protein
HPLC	High-Performance Liquid Chromatography
HSP	Heat Shock Protein
IHC	Immunohistochemistry
kDa	Kilo Dalton
LGMD	Limb-Girdle Muscular Dystrophy
MALDI	Matrix-Assisted Laser Desorption Ionisation
MDC	Muscular Dystrophy, Congenital
MHC	Myosin Heavy Chain
MS	Mass Spectrometry
MLC	Myosin Light Chain
MTJ	Myotendinous Junction
MW	Molecular Weigth
NMJ	Neuromuscular Junction
PBS	Phosphate Buffered Saline
pI	Isoelectric Point
SGM	Skeletal Muscle Growth Medium
SR	Sarcoplasmic Reticulum
VDAC	Voltage-Dependent Anion Channel

1. INTRODUCTION

1.1. General Introduction

1.1.1. Human muscle – forms and development

Human muscle consists of three tissue forms: Smooth muscle, skeletal muscle and cardiac muscle. Skeletal muscle accounts for about 40% of total human body mass. Cardiac muscle and skeletal muscle are alternatively named striated muscle due to the characteristic striated appearance of I-bands and A-bands in polarizing microscopy. In contrast to other muscles, contraction of skeletal muscle is voluntary because it is controlled by the nervous system.
In the embryo, proliferating precursor cells from the dermatomyatome of the developing somite coalesce into cells that will differentiate into skeletal muscles. Upon the activation of muscle-specific genes, the cells become myoblasts (mononuclear undifferentiated muscle cells). Myogenic determination factors activate regulatory regions of genes that code for the skeletal muscle-specific structural and functional proteins. Calcium ions and adhesion molecules such as N-cadherin and the neural cell adhesion molecule (NCAM) induce the fusion of postmitotic myoblasts to multinucleated myotubes [1]. As myotubes grow further, the initially centrally located nuclei migrate to the periphery of the myotubes and the myofibrils are differentiated into muscle fibers. Induction of myogenin mRNA is the earliest known event accompagnying myogenic differentiation.

1.1.2. Skeletal muscle structure

Skeletal muscle is composed of parallel multinucleated muscle fibers and connective tissue. Muscle fibers consist of cylindrical myofibrils surrounded by a membrane of the sarcoplasmic reticulum (SR). Based on morphological, electrophysiological, biochemical and functional characteristics, muscle fibers can be classified as slow-twitch (type I) or fast-twitch (type II) muscle fibers. Fast-twitch muscle fibers can be further divided into subtypes IIa, IIb, and IIc according to their myosin heavy chain (MHC) type, number of mitochondria, and metabolism type [1]. Examples for slow-twitch muscle are cardiac muscles or the soleus, examples for fast twitch muscle include the quadriceps femoris or gastrocnemius. Muscles vary considerably in their contents of fast- and slow-twitch muscle fibers. In superficial muscle regions fast-twitch fibers are more abundant whereas in deeper muscle layers slow-twitch muscle fibers are predominant [2].
The parallel myofibrils in the single muscle fibers lead to a longitudinal striation visible in polarizing microscopy. Physical activity can enhance the number and diameter of myofibrils, whereas the number and mass of myofibrils decrease during inactivity (hypothrophy). Myofibrils are in turn composed of myofilaments (thick myofilaments: myosin and myosin-binding proteins C, H, and X (A-bands); thin myofilaments: actin, troponin and tropomyosin

(I-bands)) that account for their transverse striation in polarizing or phase contrast microscopy [1, 3]. Troponin and tropomyosin form a complex that plays a role in the regulation of muscle contraction upon Ca^{2+} activation [3]. The elementary contractile unit of skeletal muscle is the sarcomere exerting crucial functions as rapid and efficient shortening, switching on/off in milliseconds and precise self-assembly as well as structural regularity [3]. Sarcomeres extend from Z-line to Z-line in the I-bands (see Figure 1). In the middle section of the A-bands ranging over the thick filaments lies the slightly lighter appearing H-zone where myosin filaments have no globular structures. The H-zone contains the M-Line appearing as thin dark band containing creatine kinase (CK), myomesin, protein M, skelemin as well as cross-bridges of myosin filaments. Here, myosin filaments are precisely arranged in their parallel structure. One thick filament is composed of about 300 molecules of myosin II and associated non-myosin proteins [3]. F-actin being the main component of the I-bands is composed of 14 polymerized G-actin monomers each containing one myosin binding site arranged in a double-helical structure. One molecule of tropomyosin is attached to each seven actin monomers. Z-lines of α-actinin, myotilin, theletonin and other proteins divide the I-bands into two zones and mark the beginning and end of each sarcomere. Nebulin (connecting Z-lines and actin) and titin (connecting M-lines and Z-lines) parallel the thick and thin myofilaments and mediate longitudinal stability of the sarcomeres as well as length determination of the filaments [3].

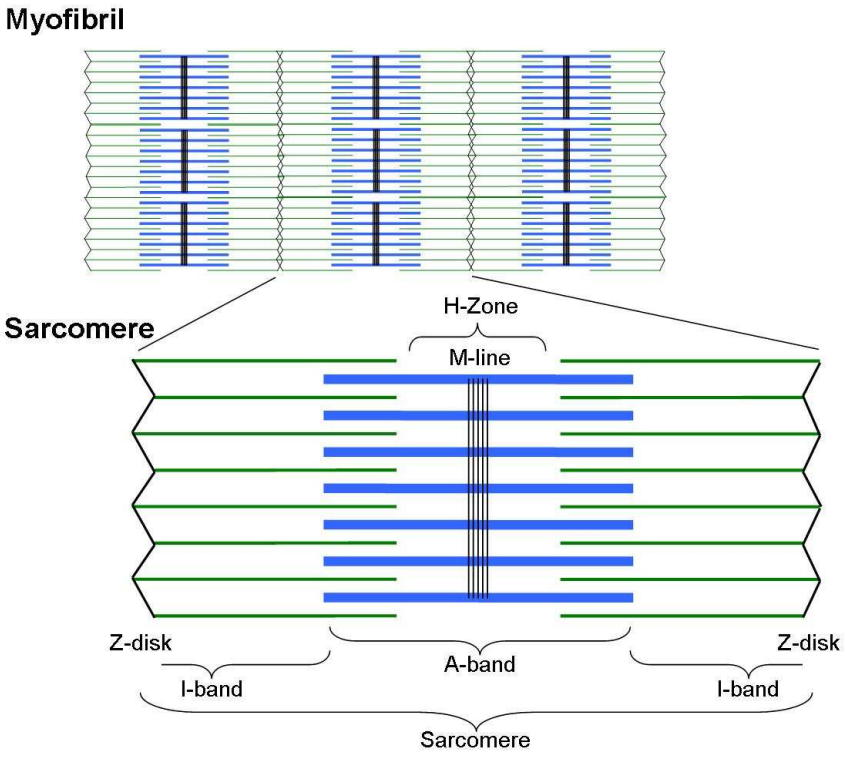

Figure 1: Schematic representation of the sarcomere extending from Z-band to Z-band in the myofibril

Space between myofilaments contains mitochondria, SR and glycogen. The cytoskeleton of muscle fibers consists of the endosarcomeric and the exosarcomeric part and is built from a complex three-dimensional scaffold of microtubules, cytoskeletal actin filaments and intermediate filaments. This scaffold maintains structural and mechanical integrity of the muscle fiber during contraction and exhibits high flexibility and stability. Intermediate filaments of the exosarcomeric cytoskeleton are divided into five classes: I contains the acidic cytokeratins, II the basic cytokeratins, III desmin, vimentin, synemin and paranemin, IV syncoilin, desmuslin, and nestin, and V lamins A/C and B. Desmin, the main intermediate filament protein in adult muscle, forms the cytoskeleton particularly at the Z-disk, but also extending longitudinally along the myofibrils and towards the plasmalemma. The >500kDa protein plectin is an intermediate filament linker connecting desmin (and probably also other intermediate filaments such as syncoilin and desmuslin) to the Z-disks and to the peripheral cytoskeleton. Intermediate filaments protect the muscle cells against mechanical stress. Other intermediate filament proteins are probably present in adult muscle, as the knockout of desmin does not have a great impact on myofibril alignment, and plectin localization at the Z-disks persists. Upon denervation, however, the levels of intermediate filament proteins in muscle fibers decrease.
Costameres are agglomerations of proteins localized subsarcolemmal at the Z-lines. They entirely surround the muscle fibers and thereby maintain the sarcolemma in the direction of the sarcomeres, protect sarcomeres from mechanical damage and partially transfer lateral force that is generated during contraction to the extracellular matrix (ECM) and other muscle fibers. Costameres contain cytokeratins, α-actin and β-spectrin (among others). Muscle fibers contain two independent membrane systems: the sarcoplasmatic reticulum and the transversal (T-) tubuli (invaginations of the sarcolemma). Nuclei in healthy human muscle are located in a subsarcolemmal position at the periphery of the muscle fibers.

Cytoskeleton in muscle plays an important role (structural and supportive) in force transmission and connection between myofibrils and sarcolemma (the basal lamina with the lipid bilayer undercoated by subsarcolemmal actin network). The lipid bilayer of the plasmalemma is mechanically not very stable and is protected from mechanical stress externally by the basal lamina and internally by the actin network. These two layers are strongly attached to each other across the plasmalemma at the costameres and between costameres by the dystrophin-glycoprotein complex (DGC) or integrins [4]. Integrins are heterodimeric cell surface receptors binding cytoskeletal elements and playing an important role in transmembrane signaling. In skeletal muscle, integrins are found in the lateral surface of muscle cells, especially at costameres stabilizing junctions and playing a role in muscle differentiation [4]. α7-integrin expression for example is restricted to a few cell types including

skeletal muscle. The cytoskeleton in muscle cells consists of four components: subsarcolemmal network, transverse connecting system, protein complex connecting myofibrils to sarcolemmal folds at myotendinous junction (MTJ), and microtubules. The structure-protecting transverse connecting system links myofibrils to the intermediate filament network and to the actin-based cytoskeleton of the muscle cell. Three multimolecular complexes are known: the focal adhesion type (integrins), the dystrophin/utrophin-based complex and spectrin-based membrane skeleton systems. The neuromuscular junction (NMJ) maintains high density of acetylcholine receptors and acetylcholinesterase as well as close proximitiy with motor nerve terminals. Dystrophin, utrophin and spectrin are highly expressed at the NMJ and probably stabilize it. The MTJ is responsible for longitudinal force transmission from the ends of the myofibrils to the tendons. As this site requires extreme mechanical stability, injury in DMD often occurs here.

1.1.3. Function of human skeletal muscle

Many modes of cellular movement require the interaction of actin filaments and myosin as motor protein. The highly coordinated contraction of skeletal muscle is also mediated by this interaction, through the actin-myosin sliding mechanism. It was thought early that during muscle contraction, filaments shorten and somehow fold internally in order for the muscle to contract. The observation that during contraction the A band remains constant in length led to the sliding-filament model, which is generally accepted today namely that filaments remain constant in length while the muscle contracts [3]. Muscle contraction transmits metabolic energy that is stored in the muscle cells into mechanical work [5].

Actin and myosin are responsible for this transduction of chemical energy to mechanical force during muscle contraction. By hydrolyzing adenosine triphosphate (ATP), the proteins are linked with the energy source for contraction [3]. When no ATP is present myosin (thick filament) is stably bound to actin via its globular subunit, the head domain (state of rigor mortis). In relaxed muscle state, tropomyosin and troponin prevent the myosin heads from stably binding to actin. Most myosin heads have ATP or adenosine diphosphate (ADP) and orthophosphate (P_i) bound [5]. Generally, when ATP binds to the myosin head, myosin is detached from the thin actin filament. Hydrolysis of the ATP to ADP induces a conformational change at the myosin head, which then binds to a subunit of the thin filament further to the direction of the Z-line. P_i is released from the ATP binding site which induces a second conformational change back to the initial state of the myosin head thereby causing the actual contraction as the myosin head keeps bound to the thin filament resulting in the filaments being pulled past each other.

Intracellular Ca^{2+} release to the sarcoplasm mediated by transverse tubular system channels and SR initiates muscle contraction (via the direct interaction of dihydropyridine receptors (DHPRs) opening the ryanodine receptors (RYRs, reviewed in [6])). Time- and voltage-

dependent sodium and potassium channels ensure the propagation of the action potential in muscle similar to the one in nerve.The intracellular membrane system SR and the transverse tubules are key players in the Ca^{2+} movements controlling muscle contraction. SR actively pumps, sequesters and releases Ca^{2+} thereby initiating and terminating muscle contraction [7]. The electrically excitable membrane at resting potential (reversal potentials for potassium and sodium through the membrane) receives signals from the motor nerve. This is transferred to the NMJ, where action potentials (all-or-nothing signal) propagate along the myofiber membranes. In order to achieve a synchronous contraction the excitation spreads along the transverse tubular system into the depth of the fibers. When muscle contraction is over, calcium is pumped back to the SR and stored by calcium-buffering proteins or it is taken up by the mitochondria in the sarcoplasm [6].

1.1.4. Regeneration

Muscle tissue has an outstanding capacity for self-repair. Regenerating muscle can be identified histochemically according to features as basophilic cytoplasm or large dark nuclei. Fetal myosin isoforms as well as intermediate filament proteins desmin and vimentin are expressed in regenerating muscle. Along with maturation of the muscle fiber, adult myosin isoforms are expressed, vimentin expression is no longer visible and desmin expression is extenuated. As the growth of fibrous tissue in muscle after damage represents a major obstacle to regeneration of muscle organization, the government of collagen proliferation seems to be an important factor [8]. Upon injury, damaged muscle cells become necrotic and macrophages remove cellular debris. In the phase of regeneration, satellite cells become mitotically activated, replenish the pool of satellite cells and fuse either to existing myotubes or form new myotubes (reviewed in [9]). The fusion of satellite cells to form primary myotubes is independent of nerves, but as soon as secondary myotubes have to be formed innervation is required. If the muscle is not rapidly renervated, severe atrophy occurs [10]. In muscular dystrophy, cycles of degeneration and regeneration are considered a characteristic feature of the disease.

The dysferlin protein plays a role in membrane repair. Since muscle fibers are subject to high mechanical stress, membrane damage occurs quite frequently. Dysferlin-carrying vesicles are then carried to the site of disruption with a high Ca^{2+} concentration and provide a “patch” for membrane repair. Mutations in the dysferlin gene lead to Myoshi myopathy (MM) or LGMD2B where the cause of muscle damage is a defect in mucle membrane maintenance rather than a structural problem like in most other muscular dystrophies [11].

1.1.5. Muscle proteins

1.1.5.1. Myosin and Actin – the contractile proteins

Myosins are a large superfamily of about 15 classes of motor proteins which interact with actin, hydrolyze ATP and generate cell movement [12]. As the myosin II class was discovered long before the other classes, it is referred to as “conventional” myosin. Members of myosin class II are hexameric rod-like proteins consisting of two heavy (223kDa) and four light chains (15-22 kDa) found in skeletal muscle cells as well as in non-muscle cells. Both the heavy chains form filaments by assembling a rod-like coiled-coil domain with two light chains attached at a globular structure at both their respective amino ends [3]. These globular structures do contain the ATP binding sites as well as cross bridges to establish the actin/myosin contact. Therefore, myosin has enzymatic (head) and structural (tail) properties. The myosin head accounts for about 130kDa divided in three domains with the smallest domain lying at the junction with the tail and associating with the light chains [3]. Myosin heads in vivo (in the presence of ATP and in the absence of Ca^{2+}) are highly organized in a helical order, in vertebrates, the number of coaxial helices is three. Upon activation or upon ATP depletion, the array of the heads gets disordered.
In adult mammalian skeletal muscle, four MHC isoforms are known: the “slow” β-MHC (MHCIβ), and the “fast” IIa-, IIb-, and IIx-MHC. Major myosin light chain (MLC) isoforms in mammalian skeletal muscle are the “slow” MLC1s and the “fast” MLC1f and MLC3f [13, 14]. The MHC isoform profiles may serve to classify muscle fibers into either pure fiber types or so-called hybrid fiber types containing a specific combination of MHCs [14]. Such fiber-type patterns of expression are seen as well for MLCs and other muscle proteins such as α-actinin, troponin, various Ca^{2+}-regulatory proteins and others [14]. Myosin forming the thick myofibrillar filament accounts for about 54 percent of myofibrillar protein [3].
In normal muscle fibers there is little co-expression of slow and fast myosin isoforms whereas in dystrophic muscle, co-expression of slow, fast and fetal myosin can occur in the very same muscle fiber indicating some extent of abnormality [15].

Actin is a globular protein (G-actin, molecular mass 42 kDa) self-associating to the thin myofibrillar filament (F-actin) and accounting for 20 percent of myofibrillar total protein [3]. F-actin filaments are built up from two strands of actin subunits twisted around each other forming a double helix with one turn of each helix containing 13-14 actin subunits. Major differences in sequence between skeletal, cardiac, smooth muscle and nonmuscle actins are found near the N-terminus and polymers from sarcomeric actins are stabler than those from cytoskeletal actins [3].

1.1.5.2. The dystrophin-glycoprotein complex (DGC)

The DGC was first purified from rabbit skeletal muscle membranes in 1990 by Kevin Campbell and co-workers [16]. Four wheat-germ agglutinin-binding proteins with molecular weights (MW) of 156kDa (α-dystroglycan), 50kDa (α-sarcoglycan), 43kDa and 35kDa were shown to co-purify with dystrophin. The DGC provides a structural link between the cytoskeleton and the ECM, but also has an important role as a receiver and transducer of cell signals [6]. It contains extracellular proteins (α-dystroglycan), cytoplasmic proteins (syntrophins, dystobrevins), and transmembrane proteins (sarcoglycans, β-dystroglycan, sarcospans, see Figure 2). Other associated proteins are caveolin-3 and neuronal nitric oxide synthase (nNOS). These proteins are expressed along the sarcolemmal membrane and therefore also at the NMJ and the MTJ. Other proteins such as utrophin, dystrobrevin-1, β2-syntropin, and unique laminin forms in contrast are exclusively expressed at the NMJ (for a review see [17]).

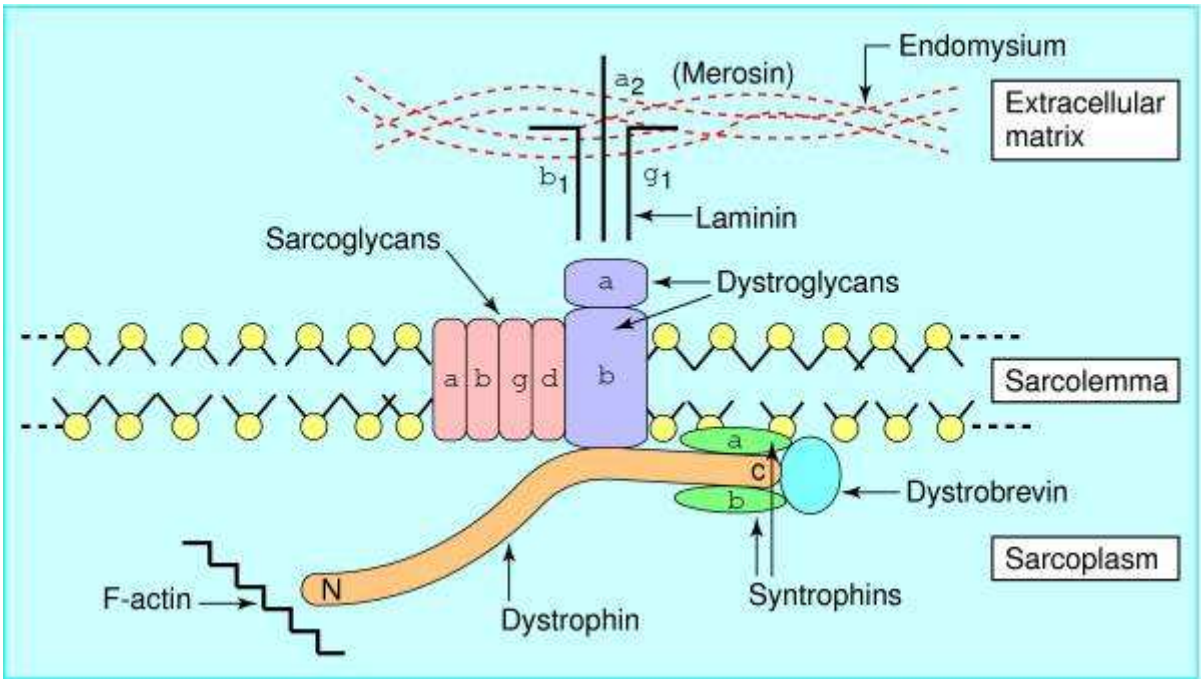

Figure 2: Dystrophin-glycoprotein complex. Figure taken from Emery, A.E.H, BMJ 1998 [18].

1.1.5.3. Dystrophin

In 1987, the dystrophin protein was shown to be the protein product of the DMD gene by Hoffman et al. [19]. Dystrophin in skeletal muscle (tissue-specific isoforms are known) is a large subsarcolemmal cytoskeletal protein [20]. The large cytoskeletal protein associates tightly with sarcolemmal glycoproteins through its carboxy-terminal domain and binds F-actin through its amino-terminal domain thereby anchoring the sarcolemma to the cytoskeleton of the muscle cell (reviewed in [21, 22]). Disruption of this link caused by the absence of dystrophin renders the sarcolemma susceptible to damage after muscle contraction and

results in necrosis. The actin-binding amino-terminal domain (exons 1-8) is highly similar to the actin-binding domains of spectrin or α-actinin. The rod-like domain (exons 9-62, also called triple-helical-repeat domain) accounts for most of the molecular mass of dystrophin and resembles the rod-like domains of spectrin and α-actinin. However, dystrophin forms a rather “nested” structure and unlike spectrin residues, not an antiparallel dimer (due to the lack of outer hydrophobic residues). The cysteine-rich domain (exons 63-69) shows high homology to the C-terminus of α-actinin, its N-terminus forms together with the C-terminus of the rod-like domain the site of a WW domain required for the binding to β-dystroglycan. The highly conserved across species C-terminal domain of the dystrophin protein (exons 70-79) has two α-helical coiled-coil domains similar to utrophin and binds to dystrobrevin (reviewed in [22]). The tight membrane association of dystrophin is mediated through the dystrophin-associated protein complex (DAP) and dystrophin is linked to the ECM via the dystroglycan complex.

Dystrophin is missing in DMD and often reduced in BMD patients. As in DMD, dystrophin is often completely absent and/or lacks the carboxy-terminus and in BMD the carboxy-terminus is often preserved, antibodies that are specific for the C-terminus of dystrophin are particularly useful for the immunohistochemical (IHC) distinction of DMD and BMD. The amino- and the carboxyterminus seem to be particularly important for dystrophin function as mutations in these regions usually lead to a more severe phenotype [23].

1.1.5.4. Sarcoglycans and Dystroglycans

Dystroglycan α- and β-subunits are encoded by a single mRNA and posttranslationally cleaved [24]. α-dystroglycan is a highly glycosylated ECM protein of 156kDa found by Campbell and co-workers in 1990 along with the discovery of the DGC [16]. It links laminin in the ECM and dystrophin (via β-dystroglycan). Brancaccio et al. showed a dumbbell-shaped structure of chick α-dystroglycan with globular domains at the N-terminus and the C-terminus, and a mucin-like motif in the cental region [25]. A-dystroglycan contains several N-linked glycans [26] and extensive O-linked glycosylation in the mucin region [25]. Therefore, it is difficult to analyze using SDS-PAGE as glycosylated proteins often migrate as smeared bands in the gel. β-dystroglycan is a transmembrane protein linking the sarcolemma to intra- and extracellular structures [27]. Expression of β-dystroglycan seems to parallel the expression of dystrophin and shows a uniform and strong expression pattern where a “complete” dystrophin protein is expected (such as in healthy muscle or in revertant fibers in BMD or DMD patients) [28].

α-, β-, γ-, and δ-sarcoglycan in skeletal muscle form a transmembrane complex at the sarcolemma with a role in sarcolemmal stability and probably involved in cell signaling upon

mechanical perturbations [29]. Defects in sarcoglycans are the cause of various LGMDs and alternatively named sarcoglycanopathies. Identical mutations do not necessarily lead to the same severity of the disease [1]. α-sarcoglycan is a 50kDa dystrophin-associated membrane glycoprotein found by Campbell and co-workers in 1990 after the description of the DGC [16], and originally named 50DAG. At the time, a (secondary) α-sarcoglycan deficiency in muscle from *mdx* mice could not be demonstrated due to antibodies with low affinity [16]. In 1992, Matsumura et al. found an α-sarcoglycan deficiency in SCARMD patients [30], later this was demonstrated to be a secondary deficiency by linkage analyses when SCARMD was linked to chromosome 13 and the α-sarcoglycan gene was mapped to chromosome 17 [31] with several mutations causing primary deficiencies in α-sarcoglycan (LGMD2D, primary adhalinopathy) [31, 32]. Deficiencies in the other sarcoglycans lead to LGMD2E (β-sarcoglycan), LGMD2F (δ-sarcoglycan) and LGMD2C (γ-sarcoglycan). Other sarcoglycans found in smooth muscle are ε- and ζ-sarcoglycan [33].

1.1.5.5. Other Muscle Proteins

Utrophin

The 395kDa utrophin (dystrophin related protein, DRP) is structurally and functionally similar to dystrophin. The N-terminal amino acid sequence is highly conserved between DRP and dystrophin, and DRP also binds F-actin *in vitro* although with a higher affinity for nonmuscle actin. The expression pattern in vivo varies greatly. DRP is expressed in myoblasts during development [34], and in adult striated muscle becomes restricted to satellite cells, the NMJ and the MTJ (reviewed in [22]). Utrophin is expressed at higher levels in DMD patients independently of regenerating fibers [35, 36]. It has been hypothesized that utrophin could compensate for the missing dystrophin in DMD patients, and methods to induce utrophin upregulation have been suggested as therapeutic approaches to the cure of DMD. But even though in DMD and BMD patients a greater proportion of muscle fibers is labelled with utrophin antibody, β-dystroglycan does not seem to be incorporarted stably in the sarcolemma, suggesting that utrophin is not able to fully compensate for the lack of dystrophin in these patients [28].

Calpain-3

Calpain-3 is the muscle-specific member of the calpains (intracellular cysteine proteases). Calpain-3 is localized near Z-lines in sarcomeres and interacts with titin filaments [1]. Mutations in the calpain-3 gene normally cause absence or reduction in calpain-3 protein and LGMD2A [1], but it has been shown that a considerable number of patients show normal levels of non-functional calpain-3 indistinguishable from controls on Western blots [37]. The proteolytic activity of calpain-3 induces actin cytoskeleton and focal adhesion (subcellular

macromolecules that mediate regulatory effects such as cell anchorage of ECM adhesion on cell behaviour) disorganization. While the ubiquitous calpains (m-calpain and μ-calpain) are heterodimers of a large and a small subunit, calpain-3 shows similar structures to the large subunit of these calpains and carries specific additional sequences (insertion sequences, IS). IS1 contains the autolytic sites and IS2 carries a nuclear translocation signal and a titin-binding site. Autolysis in the catalytic site (IS1) is necessary for calpain function as was demonstrated in [38] by expressing calpain-3 isoforms with spliced out exon 6 (containing two autolytic sites) and Capn3^{Y274A}, an isoform that is unable to be processed. Rather than forming a heterodimer with the small subunits of other calpains, calpain-3 forms a homodimer through its penta-EF-hand domain (protein domain IV) [39] . EF-hands are common calcium-binding motifs (helix-loop-helix). Other authors state that IS1 and IS2 are both essential for calpain-3 autolysis [40].
Autolysis of calpain-3 leads to the generation of a 34kDa N-terminal fragment and a 55-60kDa C-terminal fragment. The authors of [38] could not find specialized functions for these fragments, as all the fragments (34kDa, 55kDa, and 60kDa) induced normal cell spreading and stress fiber formation when expressed alone or in combinations in mouse myoblast cells. When enzymatically inactive (C129S) calpain-3 is purified, it elutes from columns at times corresponding to a MW of 180kDa, suggesting that it is forming a dimer in skeletal muscle [40].

α-actinin

α-actinin (ACTN) is an evolutionarily conserved F-actin crosslinking protein anchoring actin to intracellular structures that in humans is present in at least four isoforms encoded by distinct genes. ACTNs are major components of the cytoskeleton and are present in many cell types as homodimers mainly localized along actin-containing microfilament bundles, whereas the skeletal muscle isoforms ACTN2 and ACTN3 localized at the Z-disk can form homo- or heterodimers [41]. ACTN2 is found in skeletal and cardiac muscle and ACTN3 is skeletal muscle specific [42]. Generally, α-actinins have an important role in the organization of microfilament bundles, in anchoring actin filaments specific sites within the cell, and in assembling microfilaments in cell-cell contact areas [41, 43] .The skeletal muscle α-actinin isoforms are involved in anchoring myofibrillar actin thin filaments to the Z-disk and arranging the them in a lateral array [3, 41].

Emerin

Emerin is a 34kDa nuclear membrane protein found in skeletal and cardiac muscle as well as in a range of other tissues [44, 45]. Mutations in the STA gene lead to Emery-Dreifuss muscular dystrophy (EDMD). Manilal et al. [45] reported emerin staining only at the nuclear membrane (using a panel of 12 antibodies) in all tissues tested. They furthermore found

emerin staining in EDMD nuclei not to be reduced only in myofiber nuclei but also in nuclei of blood vessel smooth muscles.
Emerin absence in immunostainings is assumed to be specific for EDMD [46].

FKRP (fukutin-related protein)
FKRP function is still unclear. In intact skeletal muscle it is localized at the sarcolemma and seems to have a direct interaction with α-dystroglycan [47]. Co-enrichment and co-sedimentation with dystroglycan, but not with dystrophin or sarcoglycans, have been shown [47]. Mutations in the FKRP cause congenital muscular dystrophy type 1C (MDC1C) [48] and its allelic disorder LGMD2I [49, 50] and are associated with a wide clinical spectrum [51]. MDC1C (onset in the first weeks of life) is clinically characterized by severe weakness of the muscles of the shoulder girdle, hypertrophy of leg (calf and thigh), and severe respiratory involvement that leads to respiratory failure in the second life decade [48]. Brain structure and intelligence are usually normal, cardiac muscle on the other hand seems to be involved, as several patients show signs of heart involvement [48]. A severe reduction in α-dystroglycan immunolabelling and an inconclusive reduction in laminin-α2 immunolabelling are additional features of MDC1C, Brockington et al. [48] conclude from IHC findings that the reduction in laminin-α2 is probably the secondary reduction. General basement membrane organization doesn't seem to be globally perturbed as the expression of perlecan is preserved [48]. FKRP appears to be directly involved in α-dystroglycan glycosylation, as other components of the DGC still are normally glycosylated in MDC1C patients. The onset of LGMD2I takes place much later than MDC1C with variable phenotypes ranging from relatively mild to DMD-like [50].

1.1.6. Muscular Dystrophy
Diseases of skeletal muscle are characterized by atrophy, weakness and paralysis and are considered a field of neurology. Muscular dystrophies (MD) are a clinically and pathogenically very heterogenous group of genetically determined myopathies varying in age of onset, involved muscles, and severity of the disease that lead to progressive primary degeneration of muscle fibers. It was recognized quite early (end of the 19th century) that the progressive muscular dystrophies, a term that was established by Wilhelm Erb, do differ from progressive muscular atrophies by concurrence of hypertrophy and atrophy (abnormalities of muscle fiber diameter) [1]. In all muscular dystrophies muscle fibers are lost slowly but gradually. This is particularly severe in DMD. As the muscle fibers disappear they are replaced by either perimysial or endomysial connective tissue depending on the nature of the myopathic disorder and on the severity of muscle fiber loss [8]. Inflammation is seen in various types of myositis, in muscle abscesses, vasculitis, polyarteritis nodosa and other muscle disorders. Inflammatory cells are also detected around and within necrotic muscle

fibers (macrophages), sometimes even in non-necrotic muscle fibers (lymphoid cells, in fewer cases macrophages) [8].
Even though DMD is considered a non-inflammatory myopathy, some nonnecrotic muscle fibers are invaded by lymphocytes and macrophages (reviewed in [8]).
Necrosis occurs in muscles upon various pathogenic stimuli and results in the injury of all organelles in a muscle fiber or to a segment of a fiber. In segmental necrosis contractile substance of a sarcomere is homogenized and the striation is destroyed. The sarcolemma is no longer visible and fiber contents are normally removed by phagocytes while the remaining fiber may survive and appear normal [8]. Complement activation is seen during muscle fiber necrosis.
The classification of muscular dystrophy is an ongoing process. Classification according to clinical features does not necessarily reflect the underlying pathogenetical aspects and, on the other hand, classification according to mutation can also be misleading in cases where mutations in one gene can result in different phenotypes (e.g. mutations in the dysferlin gene causing LGMD2B or Miyoshi myopathy [1]).

1.1.6.1. Forms of muscular dystrophies

All muscular dystrophies lead to genetically determined muscle weakness and muscle wasting, which is probably the only common feature of the disease category that has a wide range of clinical presentations, other tissues that are affected, and involved genes and proteins [52]. Forms of muscular dystrophy include the Duchenne/Becker type muscular dystrophy (DMD/BMD), the congenital muscular dystrophies (CMD), the Emery-Dreifuss syndrome, the facioscapulohumeral muscular dystrophy, the oculopharyngeal muscular dystrophy, the large group of limb-girdle muscular dystrophies (LGMDs), distal muscular dystrophy and myotonic dystrophy. The incidence for the x-linked DMD is particularly high with 1:3500 (males), for its allelic milder form BMD it is around ~3:100'000 [1, 53], for congenital muscular dystrophies: 1:20'000-1:50'000 (estimate from Leiden Muscular Dystrophy, *http://www.dmd.nl*, accessed in March 2010), for facioscapulohumeral muscular dystrophy: 1:20'000-1:400'000, for oculopharyngeal muscular dystrophy: around 1:200'000 in France (more common in Canada, 1:1000 in the region of Quebec).
The LGMDs often have similar clinical characteristics such as paresis (weakness) and atrophy of muscles of the shoulder girdle and pelvis with a manifestation from the first years of age to the second decade, rarely later [1]. In general, the progress of autosomal-dominant forms (LGMD1) is slower and the prognosis is better than for autosomal-recessive forms (LGMD2). LGMDs do normally not progress very fast but some cases with drastically reduced life expectancy similar do DMD patients have been described [1]. Serum CK is elevated 30-100 times in autosomal-recessive forms and only slightly (in single cases up to 25fold) in autosomal-dominant forms [1]. Sarcoglycanopathies vary considerably in disease

severity. LGMD2C and LGMD2F but also LGMD2D can show severities similar to DMD and cardiac involvement has been found in all sarcoglycanopathies [1]. In contrast to the other muscular dystrophies, where the molecular cause of the disease is an absence or a reduction in a protein, some forms of surplus protein with an excess of the relevant proteins are known. In the two forms of desmin-associated myopathies, the primary desminopathy with a mutation in the desmin gene and the α-B-crystallinopathy with a mutation in the gene encoding for α-B-crystallin, an accumulation of desmin is seen in the muscle cell [1].

1.1.6.2. DMD/BMD

The clinical spectrum of dystrophinopathies is very broad due to the high number of possible mutations in the large dystrophin gene. In addition to the major allelic disorders DMD and BMD, other phenotypes are known such as cardiomyopathy with mild muscle weakness, myalgias, fatal X-linked dilated cardiomyopathy and others [22]. Very likely, DMD was first described in the first half of the nineteenth century. Duchenne's observations were published in 1861.

Diagnosis of DMD in boys is often made before the patient is 6 years old. Motoric development seems to be slow and children may appear clumsy with a waddling gait (Trendelenburg's sign). Running or climbing stairs becomes difficult and boys show a characteristic behaviour holding on to their own thighs when standing up (Gowers-Sign). Shoulder-girdle involvement becomes apparent early due to weakness of the torso and distal extremities with protruding shoulder blades. Atrophies and weakness (pareses) are often symmetrical, and facial muscles normally are not involved. Serum CK is significantly elevated, often >1000 units/L already at birth [54]. Contractures are frequent (e.g. in M. tibialis posterior [1]), hypertrophy is often seen in the early stadiums of DMD (especially in calves, muscles of the tongue, M. deltoideus and M. quadriceps femoris) [55], and muscle reflexes are weak or can no longer be triggered (except for the Achilles tendon reflex which can be preserved after the 10^{th} year of life). Cardiac involvement is very frequent (near 100% in patients over 18 years of age) but there is no apparent correlation between the severity of the muscle disease and the severity of heart involvement. Cardiac symptoms are manifested in only about 50% of the patients over 18, most probably due to low heart stress because of low activity of the patients. Pulmonary problems are mostly the cause of death in DMD patients while cardiac problems account for only about 10% of deaths. Intelligence may be lowered in DMD patients. Prognosis for DMD patients is a chronic progressive course of the disease with a possible phase of recovery in the pre-school age, most possibly due to a discrepancy between muscle growth and dystrophic processes [1].

BMD is characterized by a later onset of the disease and a more benign course with a higher life expectancy showing initial symptoms in the pelvic girdle and later in the shoulder girdle. BMD phenotypes vary considerably with a mild course when the deleted region of the protein

is in the middle region whereas deletions causing changes in the N-terminal region of the dystrophin protein cause severe phenotypes with an early walking disability. Defects in the proximal rod-like domain often cause stronger myalgia and muscle cramps and distal defects cause an intermediate phenotype. Nonsense-mutations of exons 30, 44 and 74 lead to intermediate phenotypes between DMD and BMD. Cardiac involvement is seen in over 50% of BMD cases and serum CK is elevated about 10-50 fold compared to controls [1].
Female carriers do show in about 10% of the cases (mild) clinical manifestations such as calf hypertrophy, myalgia or mild weakness and atrophy in the pelvis- and shoulder-girdle, sometimes even cardiac involvement. In very rare cases a DMD phenotype is seen in females, when both X-chromosomes show a mutation in the region of Xp21, the patients suffer from the Turner-syndrome (only one functional X-chromosome), an X-autosomal translocation, often with an inactivation of the X-chromosome or in very few cases due to failure of inactivation of the maternal X-chromosome [22]. Serum CK is elevated in about 95% of the female carriers. Overall dystrophin deficiency in DMD carriers is usually mild, and immunohistochemically female carriers often show a mosaic-like pattern of dystrophin-positive and -negative fibers [1, 8].

1.1.6.3. Molecular cause of DMD

Even before the dystrophin gene was discovered, elevated intracellular free Ca^{2+} levels were found in DMD patients (reviewed in [6]). Damage of the sarcolemma leads to excessive intracellular Ca^{2+} having two effects in the opposite direction: activation of the dysferlin membrane repair system which is desirable, but also activation of proteases (calpains), increased reactive oxygen species, and disturbed mitochondrial function (reviewed in [6, 9]). Experiments on the subproteome of Ca^{2+}-binding binding proteins have shown strong evidence for calcium dysregulation being a key factor in the pathophysiology of muscular dystrophies [9, 56]. Two hypotheses on how the absence of dystrophin ultimately leads to myofiber death exist: The structural hypothesis says that dystrophin provides a mechanical link between the ECM and the actin cytoskeleton and hence its absence causes instability of the sarcolemma and susceptibility during muscle contraction whereas the signaling hypothesis suggests disturbed cellular signaling in muscle cells due to dystrophin absence, which is the cause for muscle damage [52]. The expression of a short form of dystrophin (Dp116) lacking the N-terminus and most of the rod-like domain but with the WW-domain interacting with β-dystroglycan in *mdx* mice did not improve the dystrophic phenotype [57]. The authors suggested therefore that even though non-structural functions of dystrophin and DGC proteins were likely because of the ubiquitous expression of isoforms of these proteins, a mechanically functional dystrophin would be necessary in order to avoid a dystrophic phenotype.

Absence or reduction of dystrophin protein causes secondary reductions in sarcoglycans and dystroglycans [58] and this disintegration of the DGC initially triggers the pathogenesis of DMD. Subsequent secondary substantial alterations of energy metabolism, cellular signaling and ion homeostasis regulation are the likely key factors causing muscle fiber death. Decreased rates of mitochondrial oxidative phosphorylation rates and a substantial alteration of mitochondrial protein composition were observed in quadriceps muscle fibers of *mdx* mice which were not found in cardiac muscle or regenerating fibers [59]. Mitochondrial protein composition showed drastically decreased hemoproteins in mitochondria, which leads to elevated steady state redox states of the mitochondrial NAD-system that were observed in quadriceps muscle fibers of *mdx* mice but not in cardiac muscle or regenerating fibers [59] The lowered activity of respiratory chain-linked enzymes and the decreased rates of mitochondrial respiration are evidence for an inhibition of the respiratory chain. Oxidative stress has been shown to be enhanced in *mdx* mice where nNOS that normally produces NO reacting with free radicals is reduced. Absence of nNOS can however not be the only reason for oxidative stress causing muscle degeneration in *mdx* mice as mice lacking nNOS present normal muscle architecture (reviewed in [9]). The series of degeneration-regeneration events in DMD is presumably described the following way: rupture of the myofiber plasmalemma leads to the influx of extracellular calcium (probably causing hypercontraction) causing the myofiber to undergo necrosis (and autodigestion by proteases). The endomysial tube composed of the basal and reticular laminae often survives injury. After macrophages removed the cell debris satellite cells enter the cell cycle, start to proliferate, and form a “seal” of tissue at the inner surface of the basal lamina. When the satellite cells withdraw from the cell cycle they fuse to multinucleated myotubes (partly with the remaining myotubes from before the injury) and the original pool of satellite cells is restored [10]. An altered distribution of the dysferlin protein which is not an integral component of the DGC has been shown in DMD patients suggesting the dysferlin function that is crucial for membrane repair in muscle cells is affected in DMD [11].

1.1.6.4. Therapeutic approaches

Even though the genes and proteins involved in DMD have been known more than 20 years, no effective and lasting cure has been found that is applied routinely in humans. The large size of the gene and its expression in all muscles except brain have so far obstructed the development of an effective treatment [60]. Therefore, current therapeutic approaches focus on symptomatic therapies such as the administration of glucocorticoids in order to slow down muscle wasting, the administration of β-blockers in order to prevent heart failure, physical therapies for the improvement of muscular function, and non-invasive ventilation [54]. Current research activities include gene-replacement strategies using adeno-associated viral vectors, antisense-oligonucleotides to induce exon skipping for the restoration of a milder

phenotype, and read-through stop codon agents such as PTC124 are promising approaches (reviewed in [60]). Antisense-oligonucleotides have been shown to restore dystrophin expression to levels from 3-12% [61] to >25% in humans [62] as well as to ameliorate secondary pathobiochemical abnormalities [63] and clinical trials are currently going on [60].

1.1.6.5. Current Diagnosis

For most of the muscular dystrophies the affected genes and their protein products are known [64, 65]. Current methods for differential diagnosis of muscular dystrophies include clinical examinations, genetic analyses, the measurement of serum CK, electromyography, the histological analysis of variations in muscle fiber size, necrosis and increased amounts of fat and connective tissue as well as the IHC analysis of muscle using a wide range of antibodies [64, 65]. Besides CK, other muscle-specific enzymes such as pyruvate kinase, aldolase, alanine aminotransferase, aspartate aminotransferase, and l-lactate dehydrogenase are found in serum in higher concentrations compared to controls [1]. The increases in CK and myoglobin in serum are more marked in DMD patients than in other forms of muscular dystrophies [1].

In DMD patients, besides the considerable variation in muscle fiber size, degeneration of fibers, hypertrophic and atrophic fibers, decentralized nuclei, connective tissue and fat deposits are seen in muscle histology [1]. In immunolabelings of proteins it is of importance to distinguish primary deficiencies from secondary deficiencies as generalized membrane damage and the resulting loss in membrane proteins is a common feature of dystrophic muscle [48]. Regenerating fibers seen in dystrophic muscle in immunocytochemical analyses often show low levels of β-spectrin and α7-integrin but increased expression of utrophin, laminin-α5 and MHC class I antigens [15]. These regenerating fibers can be visualized by labelling with an antibody against fetal myosin. Moreover, in more than 50% of all DMD patients, single dystrophin-positive fibers are found in IHC [1, 66], referred to as revertant fibers where probably the reading frame has been restored [67]. In DMD carriers even though immunocytochemistry is more sensitive than Western blot analysis, it may not be diagnostic in some cases (reviewed in [8]).

A reliable diagnosis of DMD or BMD is not always possible based on clinical examination and genetic analysis. The detection of deletions and duplications in the large dystrophin gene is comparatively straightforward using direct DNA testing (multiplex PCR, MLPA), however, about one third of all mutations in the dystrophin gene are small mutations, which are more challenging to identify. Sequencing of the large dystrophin gene (79 exons) is time- and cost-intensive. Even with today's methods for the automated detection of point mutations which are being established [68, 69], the percentage of identified mutations in all patients remains around 90% [53, 70, 71]. Genotype-phenotype correlation predictions in DMD/BMD patients are challenging [53, 71]. The reading frame hypothesis predicting severe DMD phenotypes

for mutations which disrupt the reading frame and milder BMD phenotypes for mutations which maintain it [72] holds true in about 90% of the cases, but even in patients with the same mutation phenotypic variability was found [53]. Due to these ranges in variability, in cases of suspected DMD/BMD muscular dystrophy, a muscle biopsy is often taken for diagnostic purposes for subsequent molecular analysis using Western blot techniques and/or IHC. With an informed consent of the patient to participate in a research project muscle biopsies are sometimes taken after a definitive diagnosis for research purposes. The same approach is used for LGMDs. Even though most of the genes affected in the diseases are known, a diagnosis based exclusively on genetic testing is usually not suitable due to low efficiency as well as high costs, and a muscle biopsy remains the gold standard method for LGMD testing [73].

Even though the risk associated with a muscle biopsy is generally minimal, it causes discomfort to the patient and therefore has to be carried out in a way to optimize the usefulness while minimizing pain and inconveniences. Various muscles can be chosen for the muscle biopsy. Gastrocnemius muscle is subject to a heavy workload and can therefore show myopathic alterations due to denervation atrophy [74]. Severely affected muscles are usually not biopsied because of the replacement of muscle tissue by fibrous and fatty connective tissue. Also the muscle should be free from previous trauma (such as a precedent muscle biopsy) that could alter histological findings. If they are not too severely affected, triceps or biceps muscle of the upper extremity or vastus lateralis are often suitable for diagnostic muscle biopsies. In any case, it must always be kept in mind that muscle fibers may have very distinct histochemical profiles according to their innervation and fiber type distributions that vary considerably between muscles. The four fiber types in muscle can be determined by the pH-sensitive ATP reactions at different pHs on cryostat sections (unfixed frozen muscle). Type 1 fibers are base-labile and acid-stabile with the opposite being true in type-2 fibers. Type 2B and type C (infrequent in human muscle) can further be distinguished by their activity over a wider pH range than type 2A fibers [8].

All muscle fibers of one motor unit are of the same fiber type and the typical mosaic “checkerboard” pattern is the result of the intermingling assembly of fibers of different types. As differentiation into the mosaic pattern starts step by step after the 22nd week of fetal life, before the 30th week, the myofibrillar ATPase reactions stain all fibers equally dark regardless of pH or incubation time because the fibers are still undifferentiated or type 2C fibers. In humans, in anterior tibial and deltoid muscles, type 1 fibers are more abundant whereas in vastus medialis or soleus muscles, type 2 fibers can be more abundant in superficial than in deeper muscle regions [74]. These natural predominances of fiber types always have to be taken into consideration when assessing fiber types in muscle and protein alterations that could be altered depending on the analyzed fiber type.

Another complicating feature of muscular dystrophy protein diagnostics are secondary protein deficiencies [65, 73]. In DMD/BMD patients, the absence or reduction of dystrophin is often coupled with secondary deficiencies in proteins of the DGC [55]. Primary absence of one of the sarcoglycans can be coupled with secondary reductions in dystrophin and/or in the other sarcoglycans of such variable extent that the application of one sarcoglycan antibody is not sufficient to discriminate sarcoglycanopathies from other muscular dystrophies [75]. In some cases primary dysferlinopathies (LGMD2B) have been reported to be associated with secondary calpain-3 deficiencies [76], the muscle-specific protease that is reduced in LGMD2A.

In conclusion, when diagnosing muscular dystrophies and when assessing protein levels in muscle biopsies, antibodies to a large panel of proteins are routinely used making biopsy sample size critical also in terms of discomfort for the patient.

1.1.7. Satellite cells and muscle cell culture

Satellite cells are quiescent myoblastic stem cells that are localized at muscle fiber surface inside the basal lamina [10]. During their early development they proliferate and then withdraw from the cell cycle. Satellite cells contain all organelles but no myofibrils and are delimited by a plasma membrane. About 5% of all nuclei in adult muscle depending on the muscle type, age, and species account for satellite cells, postnatally about 30%, while at the NMJ, these numbers are markedly higher [10]. Moreover, slow-twitch muscles contain more satellite cells than fast-twitch muscles. Satellite cells play an important role in muscle growth after exercise, hypertrophy, and regeneration after injury. Resting satellite cells in the muscle are activated upon muscle fiber damage, exercise, denervation, stretching, and overuse. The degeneration-regeneration cycles in DMD include extensive satellite cell proliferation [10]. They are a heterogenous population with a small fraction of cells possessing stem cell properties [8, 10]. Early myogenic cell populations can be distinguished by their expression of muscle-specific proteins such as H36 or desmin. In addition to the satellite cells, mononucleated stem cells with a higher plasticity that are capable of proliferation and differentiation are found at lower numbers in muscle. The restricted lineage of these cells includes myoblast, fibroblast, chondroblast, osteoblast and adipocytes and interconversions can occur. In addition, stem cells originating from other tissue (particularly bone marrow) can have myogenic potential [10]. This effect is only seen after muscle damage though (and the cells having myogenic potential share the surface marker CD34 with satellite cells). Although the basal lamina is often considered a barrier for cell migration satellite cells are probably capable of crossing it in both directions e.g. upon muscle injury (probably in young tissue rather than in adult tissue as the basal lamina thickens with age), which makes myoblast transfer another interesting approach for therapies in various muscle diseases [10], however, there have been numerous failures and limitations to its application (reviewed in [77]). In

order to get activated for proliferation the quiescent satellite cells need at least a competence factor to enter the G_1 phase of the cell cycle and a progression factor to stimulate the cells to undergo the rest of the cell cycle including mitosis. Fibroblast growth factors (FGF) stimulate the proliferation of fibroblasts and in serum-free media, the proliferation of satellite cells, but inhibit the differentiation of satellite cells. Interestingly, the levels of FGF have been found to be elevated in *mdx* muscle and after injury, indicating that FGF might be released from the basal lamina in mature muscle upon muscle damage [10]. Insulin-like growth factors (IGF), on the other hand, have been suggested to act as progression factors stimulating cell proliferation during development (enhanced by dexamethasone which suppresses the production of IGF-binding protein and elevates IGF-receptors in myogenic cell lines), but only when the cells have already entered the cell cycle. The combination IGF/FGF stimulates the proliferation of myoblasts in cell culture. Other factors are known to inhibit satellite cell differentiation such as transforming growth factor β (TGFβ). During the process of myogenesis large rearrangements of the proteome in muscle cells take place [78].
As skeletal muscle tissue is difficult to obtain for research purposes primary human muscle cell cultures could provide a (limited) renewable source of samples. Primary human muscle cells can be cultivated as myoblasts and differentiated *in vitro* into myotubes. Satellite cells are extracted from human muscle biopsies by enzymes (trypsin, pronase) dissolving the basal lamina and stimulated to proliferate using a range of growth factors [10]. In contrast to cell lines they have no unlimited lifespan as the ability of myoblasts to divide declines with every passage [79]. About 25-30 cell doublings can be reached in culture from adult muscle and around 60-70 doublings in cell cultures obtained from fetal muscle [10]. Satellite cells extracted from DMD muscle tissue do not have the same potential of *in vitro* doubling as those from healthy subjects indicating that satellite cells in the patients may be in a more senescent proliferative stage [9, 10]. Generally, cells extracted from neonatal muscle proliferate much earlier in culture than those extracted from human muscle which undergoes a long lag phase [10]. In the absence of mitogenic stimuli that come from serum in tissue culture myoblasts withdraw from the cell cycle elongate and fuse to multinucleated myotubes appearing morphologically very different from myoblasts (see see Figure 3 for an example of C2C12 mouse myoblast cell line). As myoblasts in tissue culture start to differentiate into multinucleated myotubes, dystrophin transcription is initiated [22] and other muscle-specific genes are expressed.

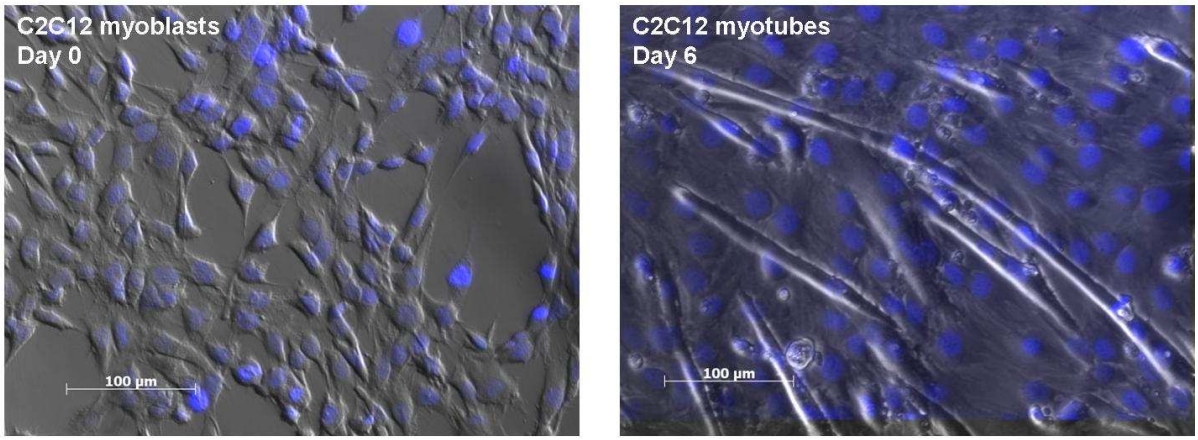

Figure 3: Differentiation of C2C12 mouse myoblasts in culture. After six days of differentiation, multinucleated myotubes are formed. The nuclei are stained with DAPI.

1.1.8. Animal models

There are several animal models for muscular dystrophies. The *mdx* mouse was a spontaneous point mutation in the dystrophin exon 23 from C57BL/10ScSn inbred mice [23, 80] and is widely accepted as animal model for DMD even though the mice' pathology does not perfectly reflect the progression of the disease in human patients. Disease progression in the mouse is milder than in humans, and *mdx* mice undergo a phase of recovery at about 2-3 months of age that is not seen in humans. The reason for the milder disease phenotype in mice is not entirely clear, it has been hypothesized that other proteins compensate for the absence of dystrophin in the mouse or that the animals that are kept in cages in laboratories are not exposed to the same levels of physical stress than humans in everyday life (reviewed in [81]). The symptoms observed in *mdx* limb muscles are relatively mild whereas the *mdx* diaphragm shows severe muscle wasting like human DMD patients (reviewed in [23]). Therefore, a relatively high number of studies are performed on *mdx* diaphragm in order to have a more realistic model of DMD in humans [63, 82, 83]).

1.2. Aim of the Thesis

1.2.1. Proteomic approaches and biomarker discovery

A biomarker is a molecule or characteristic feature that can be measured and therefore represents an indicator of the state of health of an organism [84]. A diagnostic biomarker must be sensitive and specific enough so that it can be applied in a laboratory process [84]. Ideal biomarker properties a) soluble (→ easier access), b) (relatively) abundant (→ favourable signal-to-noise ratio), c) relatively consistent in density between control samples (→ easy statistical evaluation), d) relatively consistent over time in control samples, e) highly disease-specific (so that common pathophysiological pathways between diseases do not lead to misdiagnosis) [85]. At best, the identification of novel biomarkers leads to the optimization of diagnostic processes and the detection of therapeutic targets [85]. To find such biomarkers has turned out to be more challenging than expected and despite the technical development, approvals of biomarkers by the FDA have recently been declining [84]. In contrast to diagnostic biomarkers, disease biomarkers present another group that delivers information underlying molecular mechanisms of the disease itself or its treatment yet do no not meet the same level of sensitivity and/or specificity [84]. Limitations of proteomic approaches to disease or diagnostic biomarker discovery in tissue samples include high sample variability and limited amount of sample [84, 86]. In 2DE, low-concentration proteins are often obscured by highly abundant proteins, protein size range is limited, and there is a relatively high probability of introduction of experimental error due to many manually performed steps. Expression levels of proteins probably vary by several orders of magnitude, therefore a single 2DE experiment is only capable of presenting a limited part of the total proteome present in the sample [85]. In the case of skeletal muscle, the highly abundant proteins actin, tropomyosin, troponin as well as the heavy and light chains of myosin present a challenge in the 2DE separation of the tissue extract as they account for about 50% of a muscle fiber's protein content and might mask other proteins of lower abundance. However, pre-fractionation techniques that are available might by their very nature introduce artefacts such as undesirable modifications to the remaining proteins and are therefore often not recommendable [85]. DIGE reduces gel-to-gel variation, but is extremely costly in terms of fluorophores and software [85].

Despite all these limitations, proteomic profiling using either 2DE or LC methods as separation technique serves as a powerful tool for the fast identification of candidate biomarkers. Based on the data obtained in these screenings, potential novel biomarkers can then be studied by standard biochemical methods (matrix-assisted laser desorption ionisation (MALDI)-ToF MS, electrospray ionization (ESI)-MS/MS, immunoblotting, immunofluorescence) in order to evaluate their usefulness in diagnostic or therapeutic

approaches [85]. We carried out proteomic profiling in human skeletal muscle tissue from DMD patients compared to healthy controls as well as other muscular dystrophies in order to evaluate secondary pathogenic consequences of the absence of dystrophin.

1.2.2. Microarrays

As an increasing number of drug targets is signaling-related and proteomic approaches to molecular network analysis might represent a substantial progress in true patient-tailored therapies [86], reverse protein arrays represent an attaractive technology to this approaches because of the possibility of large-scale analyses as they are capable of measuring multiple analytes in parallel while requiring only minute amounts of samples. Protein microarrays can in contrast to gene microarrays monitor post-translational modifications such as for example phosphorylation events in the profiling of cellular signal pathways [86]. Samples are spotted under denaturing or non-denaturing (for the measurement of protein-protein or protein-DNA/RNA interactions) in serial dilutions generating a certain internal standard and demonstrating the linear range of the measurement. If reference standard proteins are available, a direct and quantitative measurement of analyte concentration is possible within the linear dynamic range of the assay. In spotted lysates phosphorylated isoforms of low abundance proteins can still be detected in under 10 cell equivalents [86].

The low sample volume, low antibody consumption and the measurement of quantitative signals make reverse protein arrays a cost efficient and reliable method for all applications where sample size is limited and quantification is required. Downscaling of the gold standard IHC analyses to a reverse protein array format creates the possibility to perform assays for markers of interest in a sample containing about 10 mg of tissue, as it can be obtained from a single needle biopsy or around 10 cryosections. Various assay formats have been established based on antigen-antibody interactions, for an overview see Figure 4. To achieve low limits of detection despite the extremely small sample volumes highly efficient detection techniques are a prerequisite. We have chosen the planar waveguide based evanescent field fluorescence excitation principle as provided by Zeptosens. This surface-confined analyte detection is highly sensitive and precise and does not require any enzymatic amplification steps [87]. The indirect labelling of the patient sample provides a marked improvement in reproducibility, sensitivity, and robustness of reverse protein arrays [86]. We show that the material- and time-saving method using reverse protein arrays can successfully be employed for the quantitative and reproducible measurement of muscle proteins in tissue samples or cultured primary myotubes of patients suffering from muscular dystrophy using a set of antibodies currently in use for the diagnosis of muscular dystrophies.

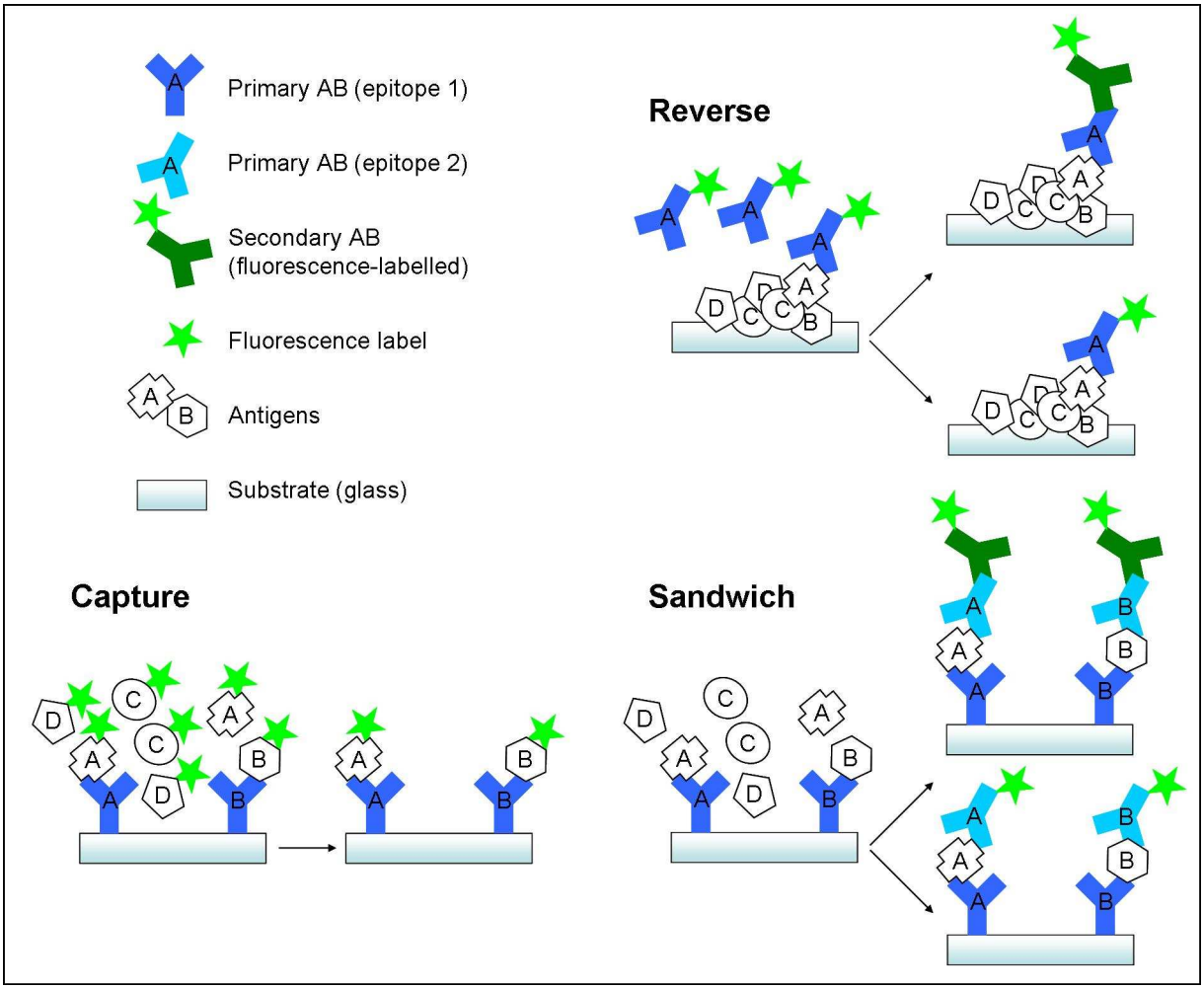

Figure 4: Basic principles of protein microarrays. In capture or sandwich arrays, antibodies are spotted on the chip surface. The arrays are then incubated with sample lysate (labelled in capture assays, unlabelled in sandwich assays). For sandwich assays, a second antibody recognizing the protein of interest is needed (if unlabelled, yet another secondary antibody is applied similar to a minaturized ELISA). In reverse protein arrays, the sample lysate is spotted directly onto the chip surface and the arrays are then incubated with primary antibodies and (if primary antibody is unlabelled) subsequently with a fluorescence-labelled secondary antibody. In all assay formats shown here, readout is fluorescence intensity.

2. MATERIAL AND METHODS

2.1. Preparation of muscle tissue extracts

Muscle biopsies from DMD/BMD/LGMD patients and controls (patients who showed non-specific diagnostic findings) were provided by the muscle tissue culture collection (MTCC) at the Friedrich Baur Institute (FBI) of the Ludwig-Maximilians University in Munich, Germany, the Department of Neurology at the University of Bonn, Germany and the University Hospital Basel, Switzerland. Three control biopsies were a kind gift of Prof. Dr. Eric Kübler (FHNW; Muttenz, Switzerland). Muscle tissue (around 10 mg) was lysed in ten times volume cell lysis buffer (CLB1, Zeptosens) using the Labsonic ultrasonic homogenization system (3x30 sec, 0.6 cycle length and 70% amplitude, cooled down on ice between each homogenization step for 30 sec). Lysates were centrifuged at room temperature at 10,000 g for two minutes and the supernatant was used for further analysis. Samples were stored at -80 ℃ if not processed immediately. A sample list is given in Table 1.

2.2. Cell culture

2.2.1. Primary cell culture

Extraction of satellite cells from human biopsies was carried out in the laboratories of the FBI at the University of Munich according to protocols of the MTCC: Muscle biopsies were stored in solution A (30 mM HEPES pH 7.6, 130 mM NaCl, 3 mM KCl, 10 mM glucose, with a trace of phenol red) at 4 ℃ not exceeding 4 days. Biopsi es were then transferred to solution A with 0.05% trypsin-EDTA and cut in small pieces using sterile scalpel blades. Muscle pieces were stirred in wheaton flasks using magnetic stir bars in solution A with trypsin-EDTA for 15min. Supernatants were poured in Dulbecco's modified eagle medium (DMEM) with 10% fetal calf serum (FCS) and 40 μg/ml gentamicin. Stirring in Wheaton flasks and removal of the supernatant was repeated twice and supernatants were centrifuged at room temperature for 10 minutes at 1200 rpm. The resulting pellets were resuspended and combined in skeletal muscle cell growth medium (SGM, (PromoCell) with 15% FCS, 50 μg/ml fetuin, 1 ng/ml basic fibroblast factor, 10 ng/ml epidermal growth factor, 10 μg/ml insulin, 0.4 μg/ml dexamethasone, 3 mM glutamax, and 0.03 μg/ml gentamicin). Cultures were incubated at 37 ℃ and 5% CO_2. After 24 h, SGM was changed and after 72 h, cultures were rinsed twice with phosphate buffered saline (PBS) in order to remove cell debris. After 48 h, first myoblasts were usually visible.

Myoblast cultures were expanded in SGM at 37 ℃ and 5% CO_2, SGM was replaced every two to three days. Upon reaching about 70% confluence, SGM was removed and myoblasts were differentiated to myotubes in DMEM supplemented with 5% horse serum and

penicillin/streptomycin. Cells were harvested on day four or five of differentiation using ice-cold PBS and a cell scraper. Cell suspensions were centrifuged at 4℃ and 8000 rpm for four minutes, the supernatant was removed and cell pellets were stored at -80℃. Pellets were resuspended in CLB1 and lysates were centrifuged at 10,000 g for 2 minutes at room temperature, then stored at -80 ℃ until spotting. For a sample list, see Table 1.

2.2.2. C2C12 cell culture

The mouse myoblast cell line C2C12 (ATCC Nr. CRL-1772, strain C3H, was obtained at the 6th passage and was a kind gift of Jasmin Althaus (FHNW, Muttenz, Switzerland). Myoblasts were expanded in maintenance medium (DMEM supplemented with GlutaMax (Invitrogen), 10% FCS, and penicillin/streptomycin). Upon reaching ~70% confluence maintenance medium was removed and differentiation of the myoblasts to multinuclear myotubes was induced in DMEM supplemented with GlutaMax, 5% horse serum, and penicillin/streptomycin.

2.3. Antibodies

Mouse monoclonal antibodies against α-sarcoglycan (NCL-a-SARC), β-dystroglycan (NCL-b-DG), β-sarcoglycan (NCL-b-SARC), calpain-3 (NCL-CALP-2C4), δ-sarcoglycan (NCL-d-SARC), dysferlin (NCL-HAMLET), dystrophin (rod-like domain: NCL-DYS1; C-terminus: NCL-DYS2; N-terminus: NCL-DYS3), emerin (NCL-EMERIN), γ-sarcoglycan (NCL-g-SARC), spectrin (NCL-SPEC1), and utrophin (NCL-DRP2) were all purchased from Novocastra Laboratories (Leica Microsystems). The monoclonal mouse antibody against α-dystroglycan antibody (clone VIA4-1) was obtained from Upstate (Millipore),
Monoclonal mouse α-actinin antibody (clone EA-53, skeletal muscle isoform 3, specific for α-skeletal and α-cardiac muscle actinins), monoclonal mouse β-tubulin antibody (clone AA2, reacts with β-tubulin types I, II, III, and IV), and monoclonal mouse MHC fast antibody (clone MY-32, reacts with fast (type II) and neonatal isomyosin molecules in skeletal muscle) were purchased from Sigma-Aldrich.
The desmin antibody was purchased from DAKO and the antibody against an 80kDa fragment of laminin-α2 was from Chemicon (Millipore). Myosin β slow heavy chain antibody was from Alexis Biochemicals. The goat polyclonal FKRP antibody against the C-terminus of the FKRP protein and goat polyclonal heat shock protein (HSP)-β2 antibody were purchased from Santa Cruz Biotechnology (LabForce). The antibodies against voltage-dependent anion channel (VDAC) 2 (goat polyclonal and mouse monoclonal) and against glycerol-3-phosphate dehydrogenase-like protein 1 (GPD1L) were obtained from Abcam.

Table 1: Sample list of muscle tissue and myoblasts spotted on for reverse protein arrays and analyzed in 2DE experiments. Cryosections were all in TissueTek.

Sample	Disease	Mutation	Sample State	Muscle
CONT 1	--	--	Cryosections	quadriceps femoris
CONT 2	--	--	Native Biopsy	tibialis anterior
CONT 3	--	--	Native Biopsy	biceps brachii
CONT 4	--	--	Native Biopsy	deltoideus
CONT 5	--	--	Native Biopsy	tibialis anterior
CONT 6	--	--	Native Biopsy	deltoideus
CONT 7	--	--	Native Biopsy	unknown
CONT 8	--	--	Native Biopsy	unknown
CONT 9	--	--	Native Biopsy	unknown
CONT 10	--	--	Native Biopsy	tibialis anterior
CONT 11	--	--	myoblasts	unknown
CONT 12	--	--	myoblasts	unknown
CONT 13	--	--	myoblasts	unknown
CONT 14	--	--	myoblasts	unknown
CONT 15	--	--	myoblasts	unknown
CONT 16	--		Native Biopsy	unknown
BMD 1	BMD	Duplication (exon 45-49)	Native Biopsy	vastus lateralis
BMD 2	BMD	Deletion (exon 45)	Cryosections	quadriceps femoris
BMD 3	BMD	Deletion (exon 48-50)	Cryosections	quadriceps femoris
BMD 4	BMD	Duplication (exon 45-49)	myoblasts	unknown
BMD 5	BMD	unknown	myoblasts	unknown
DMD 1	DMD	Exon 64 9337C>T	Cryosections	vastus lateralis
DMD 2	DMD	Exon 40 5602-5605del	Cryosections	vastus lateralis
DMD 3	DMD	Duplication (exon 12-21)	Cryosections	vastus lateralis
DMD 4	DMD	Deletion (exon 29-43)	Cryosections	vastus lateralis
DMD 5	DMD	Deletion (exon 4-15)	Cryosections	unknown
DMD 6	DMD*	c357+2T2A, Intron 5	Cryosections	vastus lateralis
DMD 7	DMD	Deletion (exon 45-52)	Cryosections	quadriceps femoris
DMD 8	DMD	Deletion (exon 51)	Cryosections	unknown
DMD 9	DMD	Deletion (exon 3-12)	Native Biopsy	unknown
DMD 10	DMD	Deletion (exon 56-62)	Native Biopsy	quadriceps femoris
DMD 11	DMD	Duplication (exon 8-29)	Cryosections	unknown
DMD 12	DMD	unknown	Native Biopsy	tibialis anterior
DMD 13	DMD	unknown	myoblasts	unknown
DMD 14	DMD	Duplication (exon 8-29)	myoblasts	unknown
DMD 15	DMD	unknown	Cryosections	unknown
DMD 16	DMD	unknown	myoblasts	unknown
DMD Carr 1	DMD Carrier	unknown	myoblasts	unknown
DMD Carr 2	DMD Carrier	unknown	myoblasts	unknown
LGMD2A 1	LGMD2A	unknown	Native Biopsy	unknown
LGMD2A 2	LGMD2A	unknown	Native Biopsy	unknown
LGMD2A 3	LGMD2A	unknown	Native Biopsy	unknown
LGMD2A 4	LGMD2A	unknown	Native Biopsy	unknown
LGMD2C 1	LGMD2C	Deletion (exon 1-4)/Intron 1 -1+5G>A	myoblasts	unknown
LGMD2D 1	LGMD2D	unknown	Native Biopsy	biceps brachii
LGMD2D 1	LGMD2D	Exon 5 402C>G/Exon6 622A>G	myoblasts	unknown
LGMD2D 2	LGMD2D	Exon 3 229C>T/Exon 7 850C>T	Native Biopsy	tibialis anterior
LGMD2D 2	LGMD2D	Exon 2 100C>T/Exon 3 229 C>T	myoblasts	unknown
LGMD2D 3	LGMD2D	Exon 3 229C>T	Native Biopsy	unknown
LGMD2D 4	LGMD2D	Exon 3 229C>T	Native Biopsy	tibialis anterior
LGMD2E	LGMD2E	Exon 4 499G>A	Native Biopsy	unknown
LGMD2I 1	LGMD2I	unknown	Native Biopsy	quadriceps femoris
LGMD2I 2	LGMD2I	unknown	Cryosections	tibialis anterior
LGMD2I 3	LGMD2I	unknown	Cryosections	rectus femoris
LGMD2I 4	LGMD2I	unknown	Native Biopsy	unknown
LGMD2I 5	LGMD2I	unknown	Native Biopsy	unknown
LGMD2I 6	LGMD2I	unknown	Native Biopsy	unknown
LGMD2I 7	LGMD2I	unknown	Native Biopsy	unknown
UKN 1	LGMD2A	unknown	Cryosections	unknown
UKN 1	unknown	unknown	Cryosections	unknown
UKN 2	unknown	unknown	Cryosections	unknown

* intermediate phenotype DMD/BMD

2.4. Microarrays

2.4.1. Sample and array preparation

Tissue or primary cell lysates for microarrays were prepared in CLB1 as described in 2.1 and protein content was determined using the Bradford assay using BSA as standard protein. Total protein concentration in tissue and cell lysates was adjusted to 0.3 mg/ml with CSB 1 (Zeptosens) before spotting onto ZeptoMARK hydrophobic chips in a four-fold serial dilution in duplicate using a contact free NP2.1 spotter (GeSiM). The volume per spot was approximately 400 pl. Reference spots in four equally spaced columns across the array were spotted with Alexa647-labelled BSA. One chip contained six replicate arrays, each array could be probed with a different antibody. After spotting, the chips were blocked for one hour in the ZeptoFOG blocking station with blocking buffer BB1 (Zeptosens).

2.4.2. Western blots

In order to ensure antibody specificity western blotting on control samples was performed for all antibodies applied on ZeptoMARK reverse protein arrays. 30 μg of total protein were diluted in ddH_2O to a final volume of 20 μl. 20 μl 4X sample buffer were added (Laemmli) and the samples were boiled at 95℃ for 5 min. Samples were then loaded on handcast gels of appropriate acrylamide percentage (see Table 2) including a prestained protein marker (peqGold IV from PeqLab with a MW range from 10-170 kDa) and SDS-PAGE was run for 45-50 min at 200 V. Proteins were blotted on nitrocellulose membranes at 1mA/cm^2 using a semi-dry blotting unit from Hoefer Laboratories. The transfer buffer contained 20% methanol. Transfer efficiency and absence of air bubbles in the blotting sandwich was monitored by Ponceau S staining of the membrane. Membranes were then blocked using the blocking solution for nitrocellulose membranes from the WesternBreeze® Western blotting kit from Invitrogen for at least 1h at room temperature and incubated overnight at 4 ℃ in the same blocking solution with the primary antibody at an appropriate dilution (see Table 2). Washing of the membranes, incubation with the alkaline phosphatise-conjugated secondary antibody and chemiluminescence detection of bands was carried out according to Invitrogen's WesternBreeze protocol for all mouse primary antibodies. Images were acquired with a CCD camera from Alpha Innotech and the AlphaEaseFC software. Blots for the FKRP antibody were incubated with 1:2500 rabbit anti-goat horseradish peroxidise-conjugated secondary antibody (Chemicon) and the substrate for chemiluminescence detection was SuperSignal West Pico from Pierce. Images for FKRP blots were acquired using Kodak scientific imaging films on a Curix60 processor and films were scanned using a calibrated densitometer (model GS-800, Bio-Rad).

Quantitation of Western blot bands was carried out using the QuantityOne (version 4.6.1) software package from Bio-Rad. Average band intensities were used in all calculations.

Table 2: Overview of antibodies used on reverse protein arrays and Western blots, Acrylamide percentage and appropriate dilutions for western blots

Protein	Supplier, Product-No. (Clone)	Immunogen	Species	Ig class	MW, predicted*	Acrylamide percentage in SDS-PAGE	Dilution for WB (ECL)	Dilution for MA
α-actinin 2	Sigma, A7811 (EA-53)	Rabbit skeletal α-actinin	Mouse	IgG1	103.9 kDa	7.5%	1:1000	1:1000
α-dystroglycan	Chemicon (Millipore), 05-298 (VIA4-1)	Rabbit skeletal muscle membrane preparation	Mouse	IgG1	(156 kDa)	8%	1:200	1:10
α-sarcoglycan	Novocastra, NCL-a-SARC	Fusion protein containing amino acids 217 to 289 of the rabbit adhalin sequence	Mouse	IgG1	42.9 kDa	10%	1:333	1:10
β-dystroglycan	Novocastra, NCL-b-DG	Synthetic peptide containing 15 of the last 16 amino acids at the extreme C-terminus of the human β-dystroglycan sequence (PKNMTPYRSPPPYVP-PCOOH)	Mouse	IgG2a	(43 kDa)	10%	1:500	1:500
β-sarcoglycan	Novocastra, NCL-b-SARC	Fusion protein RBSG-NT of the human β-sarcoglycan sequence	Mouse	IgG1	34.8 kDa	10%	1:100	1:10
β-tubulin	Sigma, T8328 (AA2)	purified bovine tubulin	Mouse	IgG1	~50kDa	10%	1:2000	1:1000
Calpain-3	Novocastra, NCL-CALP-2C4	Synthetic peptide containing amino acids 1–19 of the human calpain 3 sequence	Mouse	IgG2b	94.3 kDa	10%	1:100	1:10-1:20
δ-sarcoglycan	Novocastra, NCL-d-SARC	Synthetic peptide containing amino acids 1-19 at the N-terminus of the human δ-sarcoglycan sequence	Mouse	IgG2a	32 kDa	10%	1:200	1:10
Desmin	DAKO, M0760 (D33)	Desmin purified from human muscle	Mouse	IgG1, kappa	53.5 kDa	10%	1:125	1:1000
Dysferlin	Novocastra, NCL-HAMLET	Synthetic peptide containing amino acids 1999-2016 of the human dysferlin molecule	Mouse	IgG1	237.3 kDa	7.5%	1:250	1:10
Dystrophin 1	Novocastra, NCL-DYS1	Bacterial fusion protein	Mouse	IgG2a	426.7 kDa	6%	1:100	1:1000
Dystrophin 2	Novocastra, NCL-DYS2	Synthetic polypeptide consisting of the last 17 amino acids at the carboxy terminus of the human dystrophin sequence	Mouse	IgG1	426.7 kDa	6%	1:100	1:100
Dystrophin 3	Novocastra, NCL-DYS3	Fusion protein containing amino acids 67 to 713	Mouse	IgG2a	426.7 kDa	6%	1:100	1:10
Emerin	Novocastra, NCL-EMERIN	Prokaryotic recombinant protein corresponding to a 222 amino acid region near the N-terminus of the emerin protein	Mouse	IgG1	29.0 kDa	10%	1:500	1:10
FKRP	Santa Cruz, sc-48503	Peptide mapping near the C-terminus	Goat	IgG (polyclonal)	54.7 kDa	10%	1:200	1:1000

Table 2**, continued**

Protein	Supplier, Product-No. (Clone)	Immunogen	Species	Ig class	MW, predicted*	Acrylamide percentage in SDS-PAGE	Dilution for WB (ECL)	Dilution for MA
γ-sarcoglycan	Novocastra, NCL-g-SARC	Synthetic peptide containing amino acids 167–178 of the rabbit γ-sarcoglycan sequence	Mouse	IgG2b, kappa	32.4 kDa	10%	1:500	1:250
GPD1L	Abcam, ab68799	Full length human GPD1L protein	Mouse	IgG (polyclonal)	38.4 kDa	10%	1:500	1:500
HSP-β2	Santa Cruz, sc-109284	peptide mapping within an internal region of human HSPβ2	Goat	IgG (polyclonal)	20.2 kDa	12%	1:200	--
Laminin-α2	Chemicon, MAB1922 (5H2)	Purified human merosin	Mouse	IgG1	343.9kDa (80kDa fragment recognized by antibody)	8%	1:1000	1:500
Myosin heavy chain fast	Sigma, M1570 (MY-32)	rabbit muscle myosin	Mouse	IgG1		8%	1:2000	1:2000
Myosin slow heavy chain	Alexis Biochemicals, 805-502-L001 (A4.951)	Purified adult human skeletal muscle myosin (recognizes the N-terminal part (S1) of β slow myosin heavy chain)	Mouse	IgG1	~223kDa	7%	1:500-1:1000	1:5000
Spectrin	Novocastra, NCL-SPEC1	Human red blood cell membrane “ghosts”	Mouse	IgG2b	246.5 kDa (β chain)	7%	--	1:500
Utrophin	Novocastra, NCL-DRP2	Fusion protein containing the first 261 amino acids of the published DMDL gene sequence	Mouse	IgG1	394,5 kDa	6%	1 :100	1 :10
VDAC2 (a)	Abcam, ab77160	GST-tagged recombinant full length human protein	Mouse	IgG2a	31.6 kDa	10%	1 :500	1:1000
VDAC2 (b)	Abcam, ab37985	Synthetic peptide: C-GHKVGLALELEA, corresponding to C terminal amino acids 298/309 of Human VDAC2	Goat	IgG (goat polyclonal)	31.6 kDa	10%	1:333	--

* from Expasy

2.4.3. Reverse protein array assays

Arrays were incubated overnight with the primary antibodies diluted in CAB1 or CAB2 assay buffer (Zeptosens). After two hours incubation with secondary fluorescence-labelled antibodies (Alexa Fluor® 633 goat anti-mouse IgG from Invitrogen) for IgG_1 and fluorescence-labelled Fab fragments (Invitrogen) for IgG_{2a} and IgG_{2b} primary antibodies, fluorescence intensity was measured by using the red excitation/emission channel of the ZeptoReader detection system. In an introductory set of reverse protein array experiments, optimal assay conditions were evaluated for all antibodies (data not shown). Four different antibody dilutions, two assay buffers and fluorescence-labelled detection antibodies or Fab-fragments, respectively, were tested. Optimal assay conditions for each antibody were then chosen according to dose-dependant signal linearity and minimal background fluorescence. The IgG_1-type antibodies from Novocastra applied in this study yielded optimal results at a dilution of 1:10 while for all other antibodies a dilution between 1:250 and 1:5,000 (MHC slow) proved to be adequate (see Table 2).

2.4.4. Image analysis

Images were analyzed using ZeptoView Pro software with automatic spot finding and individual local background subtraction for each spot. The excitation light intensity at each spot position was calculated from the weighted linear least square fits to the reference spot signals of the same row. Referenced fluorescence intensity (RFI) values were calculated using an error weighted linear fit of the four serial dilutions of the samples on the chip. Signals from unspecific binding of secondary antibodies to the samples were subtracted for each sample individually. Serial dilution of the samples on the chip allowed confirmation that all assays were in the linear measurement range.

2.5. Two-dimensional gel electrophoresis

2.5.1. General 2DE

100 μg of total protein in CLB1 were loaded on 17 cm pH 3-10 nonlinear IPG strips (Bio-Rad) in 300 μl rehydration buffer (7 M urea, 2 M thiourea, 60 mM DTT, 2% CHAPS, 0.5% carrier ampholytes with a trace of bromophenol blue). Strips were rehydrated at 50 V for at least 8 h and isoelectric focusing was carried out using the following conditions: 1-200 V in 1min (linear gradient), 1 h at 200 V, 200-500 V in 1 min (linear gradient), 1 h at 500 V, 500-1000 V in 30 min (linear gradient), 1000 V for 1.5 h, 1000-10000 V in 5 h (linear gradient) and 7 h at 10000 V. After focusing the strips were equilibrated in 6 M Urea, 30% glycerol, 5% SDS and 50 mM Tris-HCl pH 8.8 with 1% DTT and subsequently with 260 mM iodoacetamide. Equilibrated strips were either frozen at -20 °C un til further processing or placed directly on top of handcast 10% SDS-PAGE gels. Gels were run at 40 mA for 45 min and at 30 mA to a total of 1 kVh.

For 24 cm pH 3-10 nonlinear IPG strips 120 μg of total protein in CLB1 were loaded in 450 μl rehydration buffer and isoelectric focusing conditions were equal to those applied on 17 cm strips.

Table 3: 2DE experiment list

Number	Genotypes	Members
EXP I (EXP159)	DMD BMD Control	DMD 5 DMD 9 DMD 15 BMD 1 BMD 2 CONT 3 CONT 4 CONT 5 CONT 6 CONT 8 CONT 9
EXP II (EXP162)	DMD Control	DMD 3 DMD 5 DMD 6 DMD 7 DMD 15 CONT 3 CONT 4 CONT 5 CONT 6 CONT 7
EXP III (EXP 161)	LGMD2I Control	LGMD2I 2 LGMD2I 3 LGMD2I 4/6* LGMD2I 7 CONT 5 CONT 6 CONT 9
EXP IV (EXP 167)	LGMD2A LGMD2I Control	LGMD2A 2 LGMD2A 3 LGMD2A 4 LGMD2I 4 LGMD2I 5 LGMD2I 6 CONT 1 (a) CONT 1 (b) CONT 2 (a) CONT 2 (b)
EXP V (EXP 168)	DMD LGMD2A Control	DMD 9 DMD 12 DMD 15 LGMD2A 1 LGMD2A 3 LGMD2A 4 CONT 1 (a) CONT 1 (b) CONT 2 (a) CONT 2 (b)

* pooled

2.5.2. Silver staining

Silver staining was carried out according to Sinha et al. [88]. In brief, gels were fixed in two changes of 30% ethanol/10% acetic acid for 1 h and overnight, sensitized for 45 min in 3 g/L potassium tetrathionate, 0.5 M potassium acetate and 30% ethanol, rinsed 6 times 10 min in water and impregnated for 1 h with 2 g/L silver nitrate. After a brief rinse of the gels in water, development was carried out in 30 g/L potassium carbonate with 300 μl 37% formaldehyde and 125 μl 10% sodium thiosulfate pentahydrate per litre. Development was stopped in 40 g/L Tris base with 5% acetic acid for at least 30 min. After rinsing the gels in water images were acquired using a densitometer.

Gels were stored in closed boxes at 4 ℃ in 5% acet ic acid until spot excision and further processing.

2.5.3. Image analysis

Gel images were acquired using a calibrated densitometer from Bio-Rad (model GS-800). Images were processed using QuantityOne and analyzed using the PDQuest software package from Bio-Rad (Version 8.0). Spots were detected using the advanced spot detection mode with the following parameters: Sensiitivity: 40; Spot size scale: 9; minimum peak: 130. In EXP I sensitivity was 69.7, size scale was 9, and minimum peak was 1451. Horizontal and vertical streaks in the images were removed and the automated speckle filter was applied. After spot finding, spots with a quality below 25 and/or intensity below 10 were cancelled and remaining misinterpreted spots such as air bubbles or gel edges were cancelled manually. Gels were then matched using automated matching and some landmark spots present in all gels in an experiment. In order to compensate for non expression-related differences in spot intensities, the LOESS model included in the PDQuest software was applied for normalization. The model corrects differences in labelling efficiency at different concentration levels in the gels. A curve in the scatter plot (experiment master gel vs. member gel) is calculated that minimizes the distance to all points in the plot and this curve is then used to calculate the normalization factor for each spot. Normalized qualitative and quantitative (OD normalized>4fold differences between groups) analysis sets were evaluated and carefully reviewed spot by spot in the spot review mode. Analysis sets were then created in the spot review mode and exported to Microsoft Excel spreadsheets.

2.5.4. Isoelectric Fractionation (IEF) and narrow-range 2DE

Total muscle protein extracts were separated on the basis of their isoelectric point (pI) into five fractions prior to application to narrow-range IPG strips using the ZOOM® solution phase IEF system (Invitrogen) in order to achieve higher resolving power in 2DE analyses.
Muscle tissue was homogenized in CLB1 as described in the sample preparation in the microarrays section. Protein content was determined using the Bradford assay (Bio-Rad) and four control or patient samples respectively (480 μg from each individual control/patient) were pooled in order to have 1.95 mg total protein for isoelectric fractionation. To these pooled samples in CLB1, 32.5 μl ZOOM® focusing buffer pH 3-7 and pH 7-10 (Invitrogen) respectively, 16.25 μl 2M DTT, a trace of bromophenol blue as tracking dye and protein solubilizer (7 M Urea, 2 M Thiourea, 1% CHAPS) to 3.25 ml were added. This resulted in 650 μl sample containing 0.6 mg/ml protein in each of the five sample chambers. The ZOOM® IEF system was assembled using pH disks 3.0, 4.6, 5.4, 6.2, 7.0, and 10.0. IEF was carried out for 20 min at 100 V, for 1 h 20 min at 200 V and for 2 h at 400 V. The resulting five fractions were then collected and remaining proteins adherent to the sample chamber walls were collected after washing the sample chambers with 293 μl IEF denaturant (7.7 M Urea, 2.2 M Thiourea, 4.4% CHAPS, deonized overnight using mixed bed ion exchanger resin Amberlite NB-150 (Sigma), and filtered trough a 0.2 μm PVDF filter) and 3 μl 2 M DTT on a

shaker for 10min. These solutions were stored separately. Protein concentrations in the fractions were determined using the Bradford assay in order to adjust protein concentrations between control and DMD samples rather than to have an absolute protein concentration.

2.5.5. Protein identification of selected spots from 2D Gels

Spots of interest were cut manually using a sterile syringe or razor blade and washed three times in 50 mM ammonium bicarbonate (pH 8.5)/50% acetonitrile for 30 minutes each. Spots were incubated with 200 µl 0.2 M TCEP in 50mM ammonium bicarbonate at 37 °C for 1 h and subsequently with 200 µl with 10 mg/ml iodocacetamide in 50 mM ammonium bicarbonate at 25 °C for 1 h in the dark. Gel piece s were washed in 50 mM ammonium bicarbonate/50% acetonitrile, overlaid with acetonitrile and dried under vacuum. 200 µl 10 µg/ml sequencing grade porcine trypsin (Promega) were added and left overnight at 37 °C. Peptides were extracted sequentially in 50% acetonitrile/0.1% TFA, 60% acetonitrile/0.1% TFA, and 80% acetonitrile/0.1% TFA in a waterbath with sonication for 10 min each and were pooled with the supernatant from the trypsinisation step. The extracts were dried under vacuum, reconstituted in 10 µl 0.1% TFA, and desalted using C18 peptide cleanup tips (Agilent). Eluates containing peptides were dried under vacuum and then reconstituted in 10 µl 5% acetonitrile/0.1% formic acid.

HPLC-ESI MS/MS analysis of tryptic peptides was performed using an Agilent Ion Trap XCT Plus mass spectrometer (MS) connected to an Agilent Model 1100 Nanoflow HPLC system with an Onyx monolithic C18 capillary column (Phenomenex) and an acetonitrile/0.1% formic acid in H_2O gradient. Capillary voltage was 3500 V and mass spectra were obtained in the positive ion reflector mode. MS/MS acquisitions were performed on precursors over a mass range of 200-2200 Da. Single-charged precursors were excluded and spectra were actively excluded from auto-MS/MS after two spectra for 30 sec.

Protein identification was performed by database searches correlating the tandem mass spectra to entries in the SwissProt database (*Homo sapiens*) using Spectrum Mill protein identification software (Agilent). Three missed cleavages per peptide were allowed and carbamidomethylation of cysteines was assumed. A distinct summed MS/MS search score >12 in Spectrum Mill was considered sufficient for protein identification as suggested by the software manual. Individual selected spots were additionally analyzed at the mass spectrometry facility at the Biozentrum in Basel. Their equipment was a Finnigan LTQ-Orbitrap Mass Spectrometer and the protein identification software was MASCOT.

2.6. Immunofluorescence

C2C12 cells and primary human muscle cells were grown and differentiated (as described before) on 12 mm glass coverslips that have been sterilized by dipping in ethanol and flaming in a sterile bench. Coverslips were washed in PBS before the cells were fixed in 4%

paraformaldehyde for 10 min at room temperature. Coverslips were washed twice in PBS and cells were then permeabilized for 10 minutes in 0.2% Triton X-100. Coverslips were rinsed in four changes of PBS prior to blocking in 5% of either horse or goat serum depending on the host species of the primary antibodies.

Mouse and rabbit primary antibodies were diluted in 5% goat serum while goat primary antibodies were diluted in 5% horse serum and coverslips were incubated sample side down on 25 μl of antibody solution on Parafilm at 4℃ in the da rk overnight. After three washes in PBS coverslips were incubated sample side down on 25 μl of secondary antibody solution (Alexa Fluor 488 goat anti-mouse, Alexa Fluor 488 chicken anti-goat, actin-phalloidin all diluted 1:1000 in the appropriate 5% serum). After additional three washes in PBS coverslips were either rinsed twice in Nanopur H_2O before mounting or incubated sample side down in DAPI (diluted 1:1000 in PBS), then rinsed three times in PBS and twice in Nanopur H_2O. Coverslips were mounted on microscopy slides in Mowiol with 2.5% DABCO and allowed to set overnight at 4 ℃ in the dark before image acqu isition. Images were acquired with a Zeiss Axiovert 40 CFL inverted microscope and the AxioVision software package.

For immunofluorescence experiments, primary antibodies were diluted as follows: desmin 1:100, HSPβ2 1:25, VDAC2 1:25.

2.7. Statistical analyses

Statistical analyses were carried out and all bar- and boxplots were created using the R software environment [89]. Welch two-sided t-tests (p=0.05) were performed to compare mean signal intensities in reverse protein arrays.

3. RESULTS

3.1. Reverse protein arrays for quantitation of protein patterns in mucular dystrophies

3.1.1. Validation of antibody specificity

Western blot analysis was performed on healthy human muscle lysates to give further evidence for the specificity of the antibodies applied on the reverse protein arrays, because unspecific binding to other proteins in the lysates cannot be identified on the array and might therefore lead to false-positive results. Strong single or double (calpain-3, DYS1, and DYS2 as stated by the manufacturer) bands were seen for 14 out of 25 tested antibodies (see Figure 5). Band sizes in Figure 5 are calculated relative to the molecular weight marker (10-170 kDa) and band sizes larger than 170 kDa are therefore estimations. Some bands appeared slightly higher or lower than expected, which can be caused by glycosylation of the protein that causes altered migration in SDS-PAGE. The anti-merosin antibody produced 3 bands on commercially available purified human merosin, but not on the muscle lysates. α-actinin, GPD1L, VDAC2 (a), as well as the MHC slow antibodies yielded multiple bands. The dysferlin antibody (mouse monoclonal) was tested on mouse muscle lysates and therefore produced two bands corresponding to mouse IgGs. α-dystroglycan, NCL-DYS3, HSPβ2, spectrin and utrophin antibodies did not show clear bands on the Western blots.

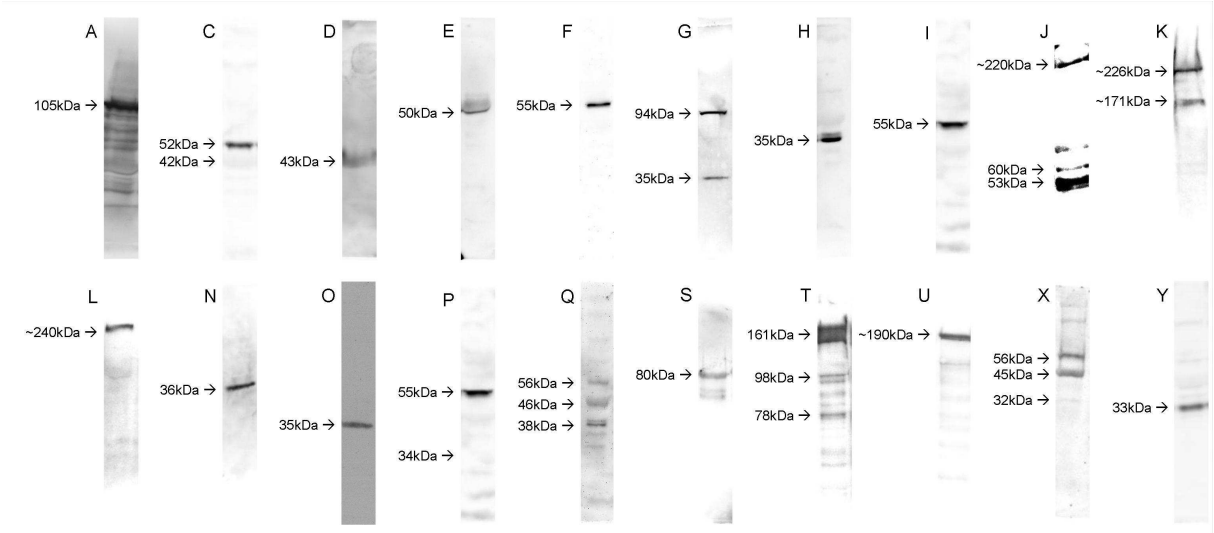

Figure 5: Western blots of antibodies applied on reverse arrays (except for VDAC2 (b) that was not included in the reverse protein array study). A: α-actinin; B: α-sarcoglycan; C: β-dystroglycan; D: β-sarcoglycan; E: β-tubulin; F: calpain-3; G: δ-sarcoglycan; H: desmin; I: dysferlin; J: dystrophin (NCL-DYS1); K: dystrophin (NCL-DYS2); L: emerin; M: FKRP; N: γ-sarcoglycan; O: GPD1L; P: merosin; Q: MHC fast; R: MHC slow; S: VDAC2 (a); T: VDAC2 (b). All western blots were carried out on healthy human muscle except for dysferlin (I, carried out on mouse muscle), and merosin (P, carried out on purified human merosin protein). Band sizes do not exactly match the protein sizes indicated in **Table 2**, because they are measured on the membrane relative to the protein MW marker. Band sizes that are larger than 170 kDa are estimations.

3.1.2. Muscle tissue lysate arrays

Assays on muscle tissue were carried out for all 19 antibodies that were evaluated in the preliminary antibody tests. An example array layout is given in Figure 6.

As shown in Figure 7 (left panel) and in Figure 6, the DYS1 antibody yielded particularly significant results. DMD samples showed almost no signal after background subtraction whereas the control samples showed distinct high fluorescence signals. BMD samples showed an intermediate mean signal indicating that these patients express lower levels of dystrophin compared to healthy controls. However, the range of residual dystrophin in BMD patients was highly variable and as only three BMD samples were analyzed, the difference between DMD and BMD samples was not significant in this study. DMD and BMD patients showed significantly lower DYS1 levels than LGMD patients even though DYS1 levels appeared to be slightly reduced in LGMD2A patients. The DYS2 antibody could only differentiate DMD patients from controls or LGMD2A patients who showed higher DYS2 signals (Figure 7; middle panel). BMD samples did not significantly differ from controls. For both DMD and BMD samples the difference to LGMD2A patients was significant but not those to LGMD2D.

A similar but less pronounced pattern than for DYS1 was observed for the DYS3 antibody (Figure 7; right panel). Although the overall signal intensities (RFI values) were much lower and the DMD samples still showed some fluorescence signals they could be clearly distinguished from the control samples. DYS3 signals BMD samples were again (as for DYS2) not significantly lower compared to controls. For DMD samples the mean difference to LGMD2A and LGMD2D was significant, which was not true for BMD samples.

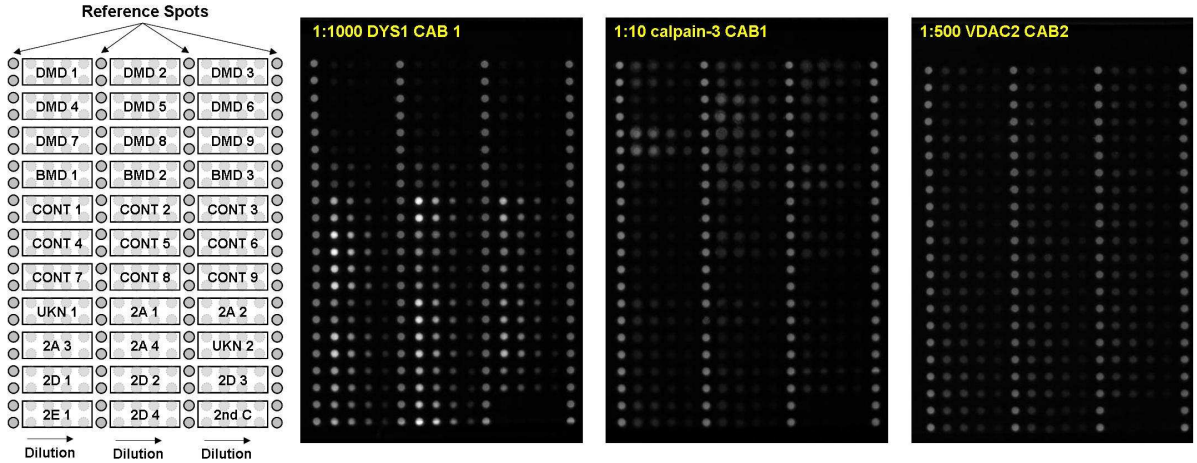

Figure 6: Left panel: Array layout, all samples were spotted in duplicate in a fourfold dilution series. Right panels: Arrays probed with DYS1, calpain-3, and VDAC2 (from left).

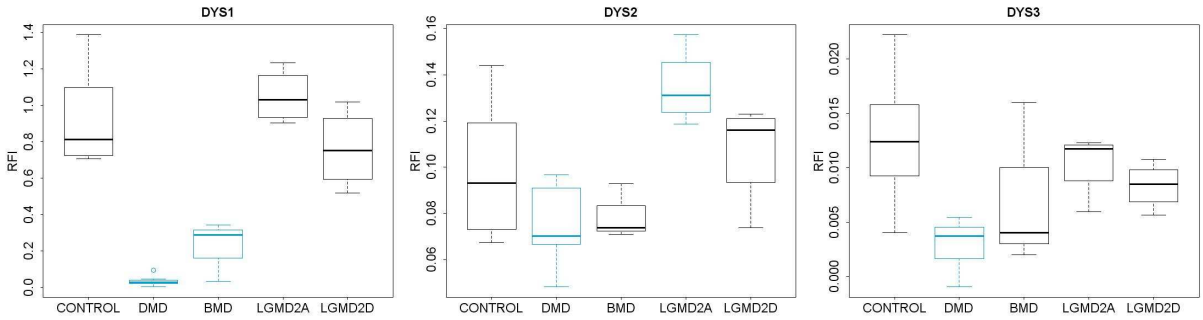

Figure 7: Boxplots for dystrophin signals on reverse protein arrays. Blue boxes represent significant mean differences from control group (t-test, two sided, $p<0.05$). Sample sizes were n=9 for controls and DMD patients, n=3 for BMD patients and n=4 for LGMD2A and LGMD2D patients.

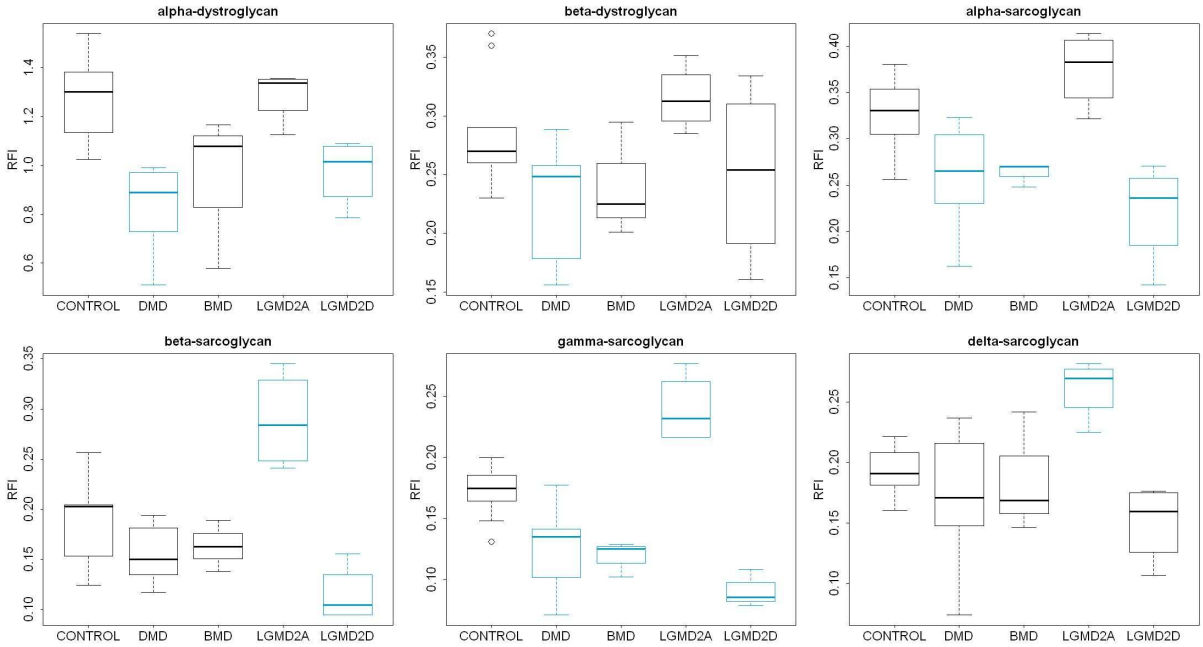

Figure 8: Boxplots for dystroglycan, α-, β-, γ-, and δ-sarcoglycan RFI signals on reverse protein arrays. Blue boxes represent mean RFI values that differ significantly from the control group (t-test, two sided, $p<0.05$). Sample sizes were n=9 for controls and DMD patients, n=3 for BMD patients and n=4 for LGMD2A and LGMD2D patients.

Secondary reductions in dystroglycans and sarcoglycans in DMD/BMD patients could be monitored on the reverse protein arrays (see Figure 8). DMD patients showed significant reductions in both dystroglycans, α-, and γ-sarcoglycan. Significant α- and γ-sarcoglycan reductions could be detected as well in BMD patients. Overall, secondary reductions in sarcoglycans in DMD patients resulted in 77%, 83%, 71%, and 89% remaining protein compared to controls in this study for α-, β-, γ- and δ-sarcoglycan, respectively. LGMD2D patients showed significantly lower α-sarcoglycan RFI values than controls as well as (secondary) reductions in α-dystroglycan, β-, and γ-sarcoglycan. In order to distinguish between secondary reductions in DMD patients and LGMD2D patients only β- and γ-sarcoglycan can be applied as they show a significant difference between mean RFI values. The measurement of α-sarcoglycan on the reverse protein arrays is not sufficient to

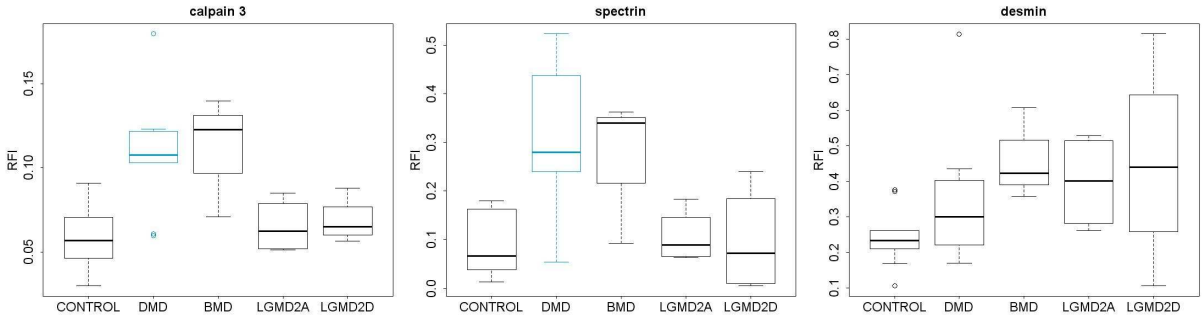

Figure 9: Boxplots for calpain-3, spectrin and desmin RFI signals on reverse protein arrays. Blue boxes represent mean RFI values that differ significantly from the control group (t-test, two sided, $p<0.05$). Sample sizes were n=9 for controls and DMD patients, n=3 for BMD patients and n=4 for LGMD2A and LGMD2D patients.

discriminate between the primary (in LGMD2D) and secondary (in DMD/BMD) reductions. In LGMD2A patients all sarcoglycans showed slightly higher RFI values than controls and other groups, for β- and δ-sarcoglycan this difference was significant.

Calpain-3 levels could also be measured on reverse protein arrays (see Figure 9, left panel) but RFI values between LGMD2A patients and controls (as well as LGMD2D patients) did not allow a separation of LGMD2A patients from controls and other dystrophies. Interestingly, DMD and BMD samples had higher RFI values for calpain-3 compared to LGMD2A/2D and controls (significant for DMD, but not for BMD). The outliers in the DMD groups seen for calpain-3 and for desmin levels do not come from the same samples giving further evidence that extreme high or low signals do not represent artefacts of total protein differences in samples. Spectrin levels were significantly higher in DMD patients than in controls (Figure 9, middle panel), and no significant differences for desmin could be demonstrated on reverse protein arrays even though a general tendendy of higher desmin levels in muscular dystrophies was seen (Figure 9, right panel). Out of the other tested antibodies (dysferlin, emerin, merosin, utrophin) no significant differences between groups were found (see Figure 10). Utrophin upregulation in DMD patients was not observed on reverse protein arrays even though the mean utrophin level in DMD patients was slightly higher than in controls. MHC slow and MHC fast did not show any significant differences (see Figure 11), and α-actinin II levels were only slightly higher in LGMD2D patients than in DMD patients.

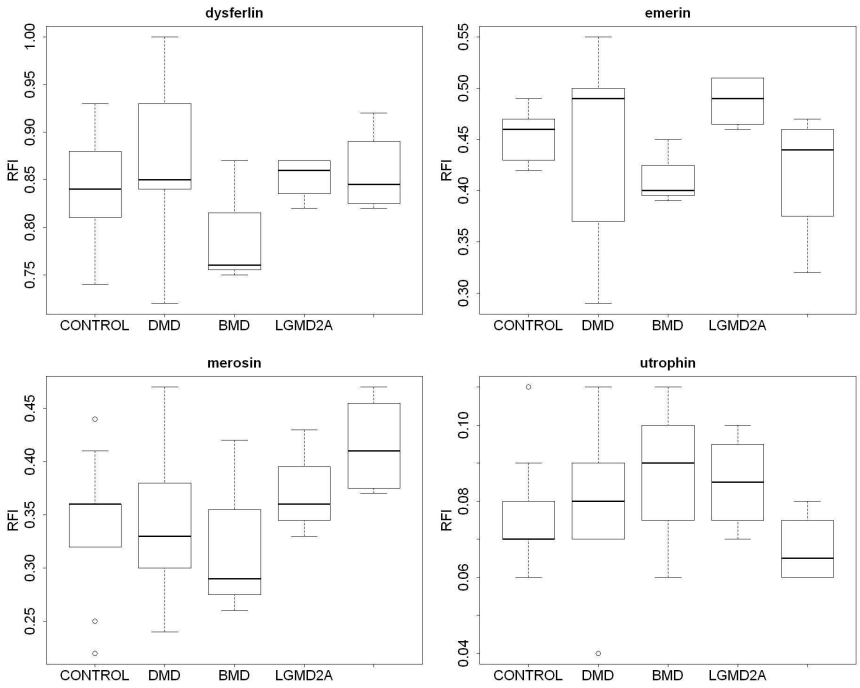

Figure 10: Boxplots for dysferlin, emerin, merosin and utrophin RFI signals on reverse protein arrays. No significant differences were observed any patient group compared to controls. Sample sizes were n=9 for controls and DMD patients, n=3 for BMD patients and n=4 for LGMD2A and LGMD2D patients.

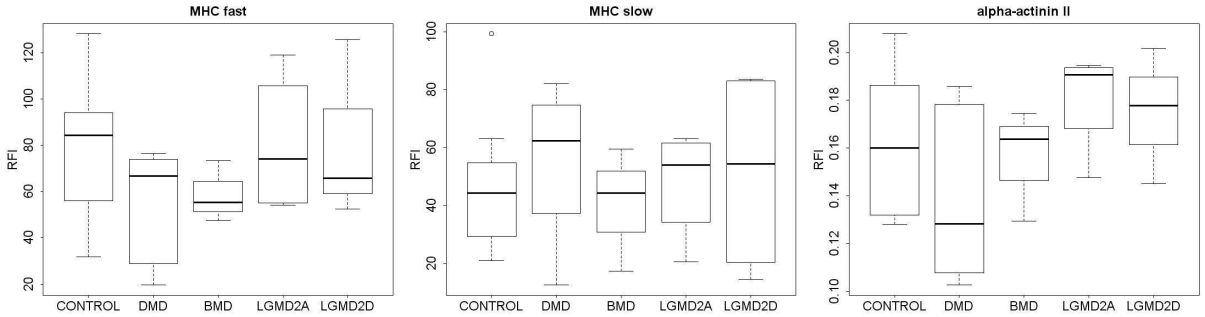

Figure 11: Boxplots for MHC and α-actinin II RFI signals on reverse protein arrays. No significant differences were found between any patient group compared to control groups. Sample sizes were n=9 for controls and DMD patients, n=3 for BMD patients and n=4 for LGMD2A and LGMD2D patients.

A protein that is probably the voltage-dependent anion channel (VDAC) 2 was found to be reduced in DMD and BMD patients in 2DE experiments. Using a mouse monoclonal antibody against this protein on reverse protein arrays a significant difference between DMD and BMD patients and controls could indeed be demonstrated, however, this antibody yielded multiple bands in Western blots and only a very weak band at the predicted MW for VDAC2 (see Figure 12, upper right panel). Therefore, a goat polyclonal antibody was evaluated that appeared more specific in Western blots, and the pattern that was obtained using the mouse monoclonal antibody could not be confirmed (see Figure 12, lower right and upper left panel). Even though the levels in DMD patients seemed slightly lower also when using the goat polyclonal antibody, a significant difference was not seen. In a Western blot including four

DMD and control samples, higher VDAC2 levels could not be seen using this antibody and, moreover, the band intensities from Western blot analyses did not correspond to the RFI signals from the reverse protein array using the same antibody and samples (see Figure 12, lower left panel)

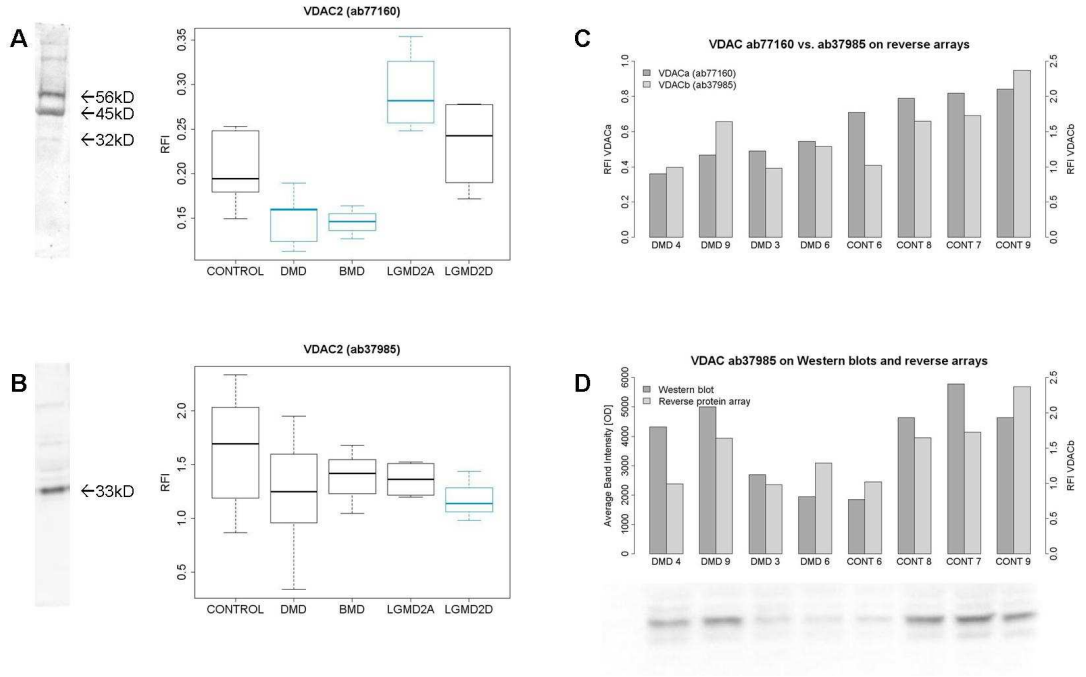

Figure 12: VDAC2 on reverse protein arrays and in Western blots. A: VDAC2a (mouse monoclonal) antibody yields multiple band in a Western blot with a very weak band at the predicted protein size. DMD patients show significantly lower RFI values using this antibody. B: Lower RFI values can no longer be seen using VDAC2b (goat polyclonal) antibody showing only one band at the predicted MW. C: RFI signals for VDACa and VDACb do not show a strong correlation. D: Band intensities on Western blot for VDAC2b and corresponding RFI signals do not correspond to a large extent.

3.1.3. Correlation with Western blot data

Data from muscle tissue lysate arrays showed a strong correlation with the Western blot analyses performed on the same samples (see two examples in Figure 13). In general, strong bands in Western blots corresponded to high RFI values on the reverse protein arrays and faint bands corresponded to low RFI values.

For example, the values for dystrophin of patient DMD6 using DYS1 were between those of the DMD and BMD samples, which is consistent with the clinical presentation of patient who as an intermediate DMD/BMD phenotype (data not shown) and is seen as the outlier in the DMD group of the DYS1 boxplot in Figure 2.

Calpain-3 expression levels could be monitored using reverse protein arrays, the RFI values correlated mostly with Western blot data where patient LGMD2A 2 showed normal calpain-3 bands (see Figure 15). CONT2 showed an intermediate RFI signal, CONT 16 that appeared normal on the western blot was however indistinguishable from patients LGMD2A 3 and 4. Samples with unknown genotype (suspected LGMD2A) had

particularly high calpain-3 levels both on Western blots and on reverse protein arrays. In DMD samples, calpain-3 levels wfere found to be very variable on microarrays (see Figure 9) but also on Western blots (see Figure 15).

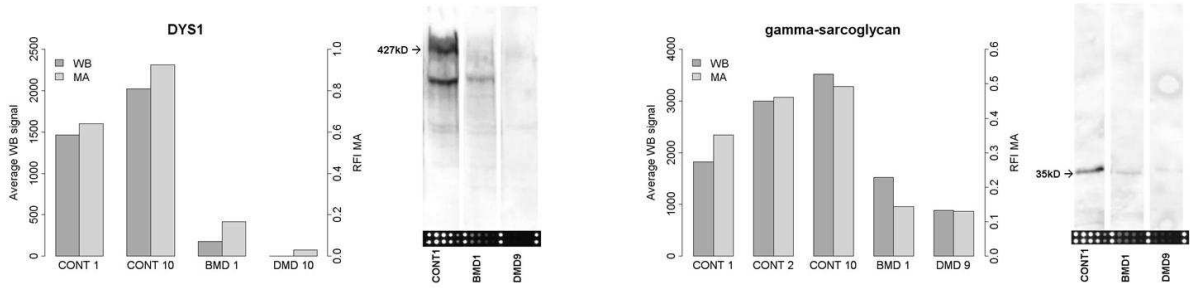

Figure 13: Correlation of Western blot data with microarray signals. Left panels: Average band intensities in Western blots are dark grey, respective microarray signals of the same samples are light grey. WB: Western blot; MA: Microarray. Right panels: Western blot sections with corresponding microarray sections. Sample DMD 9 was not analyzed on Western blot because no sample was left.

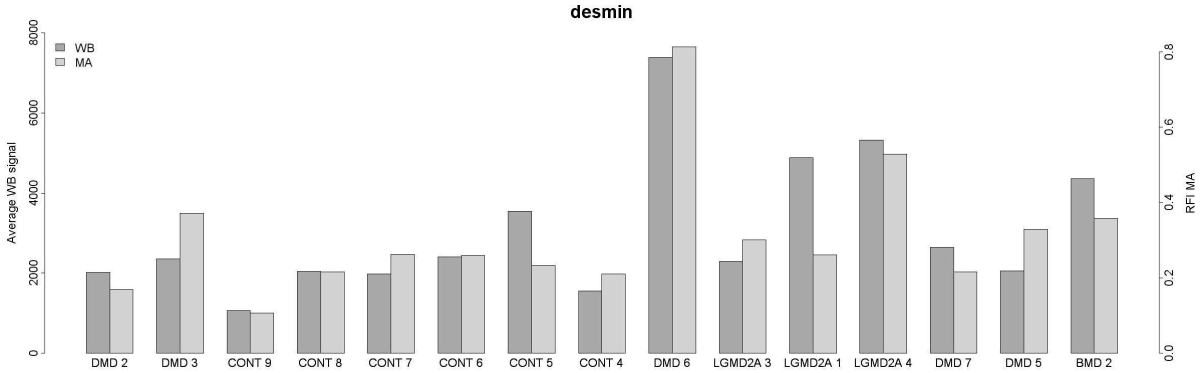

Figure 14: Comparison of Western blot and reverse array data for desmin. Overall good correlation with some exceptions such as LGMD2A 1. WB: Western blot; MA: microarray.

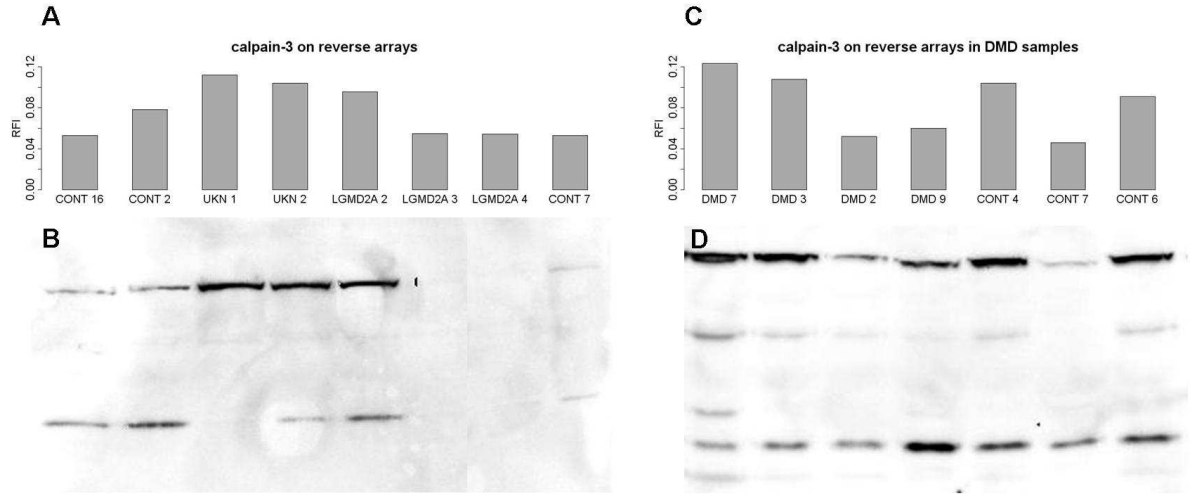

Figure 15: Calpain-3 signals on reverse protein arrays (upper panel, A and C) and corresponding bands in Western blots (on independent gels, lower panel, B and D). Patient LGMD2A 2 shows persistent calpain-3 expression on reverse arrays as well as in Western blot. DMD patients show higher calpain-3 expression than controls in some cases.

3.1.4. Microarrays from cultured primary human muscle cells

Assays for lysates of cultured primary muscle cells were carried out using 13 antibodies. DMD cells showed generally lower RFI signals using the antibodies against proteins of the DGC complex than control cells. Due to very small sample sizes (n=3 for controls and LGMD2D, n=2 for DMD, BMD and carriers), most of those differences reached no statistical significance. As in the muscle tissue samples the signals obtained with the DYS1 antibody were significantly lower in cell lysates from DMD patients compared to those from BMD patients and both DMD and BMD cells had a significantly reduced dystrophin expression compared to control cells (in DMD 1%, in BMD 9%; see Figure 6; left panel). The difference between the DMD and the BMD samples using the DYS2 antibody was more pronounced than in tissue lysates. Cells from the LGMD2C patient showed a very similar protein expression pattern to the cells from LGMD2D patients. The RFI value for α-sarcoglycan was slightly higher in cells from LGMD2C than in LGMD2D. A stronger reduction of γ-sarcoglycan in the cells from the LGMD2C patient compared to LGMD2D cells could not be observed (data not shown). Female DMD Carriers showed an intermediate signal between controls and DMD/BMD cells for dystrophin using all three dystrophin antibodies (see Figure 16), but no significant differences between the control group and the female DMD carriers could be observed. Sarcoglycans and dystroglycans, on the other hand, did not seem to be reduced in the female DMD carriers (see Figure 17). Desmin levels that could be regarded as an indicator of myogenicity in the muscle cell cultures varied considerably between and within the sample groups (data not shown).

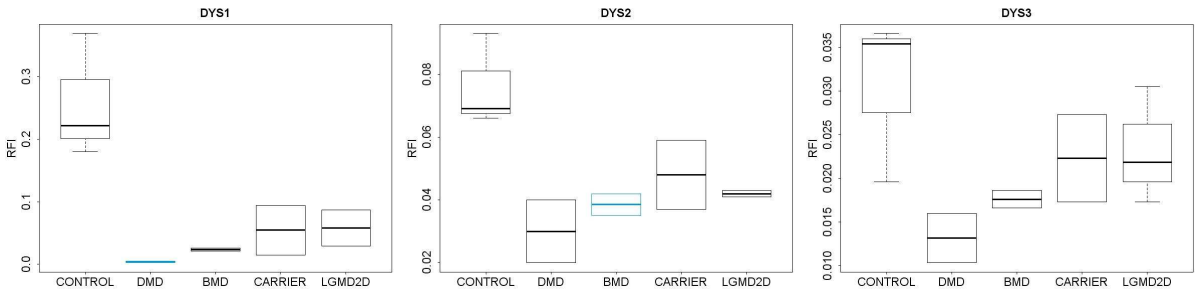

Figure 16: Boxplots for dystrophin signals in myotubes on reverse protein arrays. Sample sizes were n=3 for controls and n=2 for all patient groups.

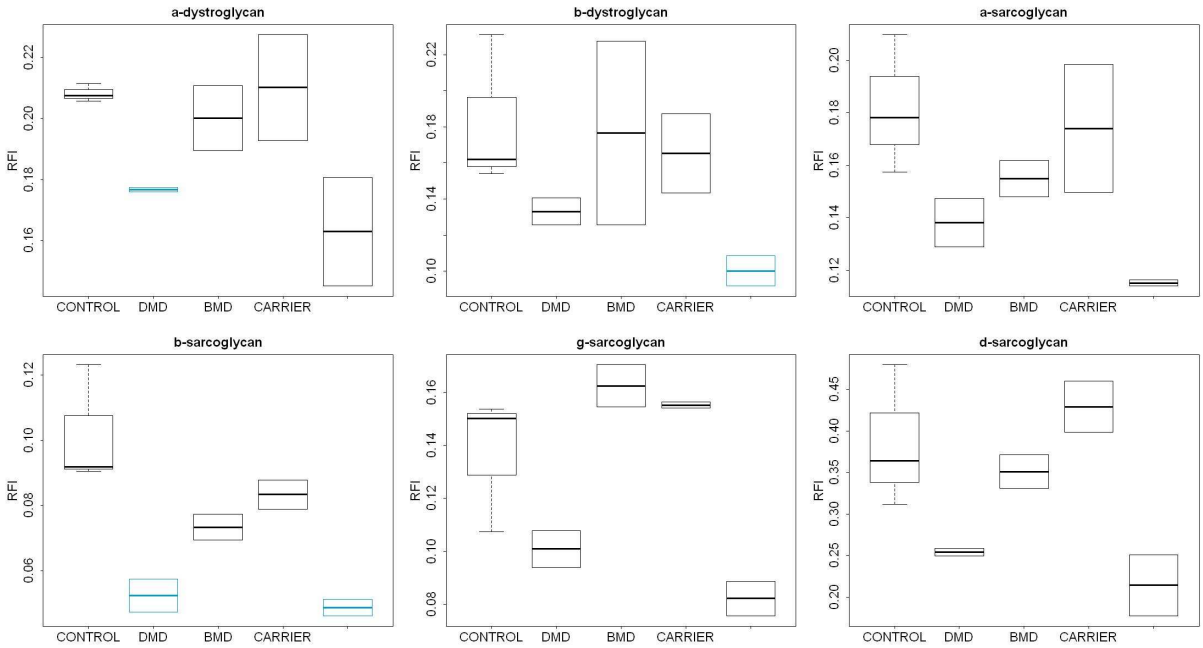

Figure 17: Boxplots for the dystroglycan and sarcoglycan signals in myotubes on reverse protein arrays. Sample sizes were n=3 for controls and n=2 for all patient groups

3.1.5. Reproducibility of microarray results

A reproducible sample preparation is crucial for reliable assay performance. Reproducibility of the sample preparation was assessed in a first series of microarray assays by multiple sample preparation and calculation of coefficients of variation (CV) for each sample and antibody. The average CV of 18.3% shows a good overall assay reproducibility including sample preparation even without normalization. Out of 72 samples with respective antibodies, 46 had a CV below 20%, 18 were between 20% and 30% and only 8 were above 30% (see Table 4).

Table 4: CV overview for selected samples prepared repeatedly (n=2 for DMD10, CONT 10, and CONT 1; n=3 for DMD 9, BMD 1, and CONT2) for reverse protein arrays

Sample	α-SG	α-DG	β-SG	β-DG	δ-SG	DYS1
DMD 9	9.5%	16.9%	7.6%	13.3%	12.1%	7.0%
DMD 10	10.2%	17.9%	18.1%	19.3%	38.9%	30.4%
BMD 1	12.4%	9.3%	19.8%	18.3%	23.9%	16.0%
CONT 2	16.9%	15.4%	20.1%	19.7%	17.1%	24.3%
CONT 10	33.3%	27.3%	34.6%	34.7%	21.5%	25.1%
CONT 1	19.2%	12.6%	14.1%	17.1%	0.8%	23.6%

Sample	DYS2	emerin	γ-SG	merosin	myosin	utrophin
DMD 9	19.2%	7.9%	13.3%	30.7%	28.7%	18.7%
DMD 10	25.6%	12.5%	20.7%	9.3%	15.1%	24.6%
BMD 1	14.5%	8.2%	4.4%	20.0%	25.9%	1.5%
CONT 2	22.8%	4.0%	11.8%	26.5%	23.1%	29.4%
CONT 10	30.3%	28.3%	4.1%	46.9%	14.9%	7.5%
CONT 1	11.4%	16.2%	19.1%	20.9%	5.6%	6.3%

Similar to Western blotting, reverse protein arrays provide relative information of measures. The name “RFI” indicates that results are quantified according to the fluorescence intensity of the control spots consisting of Cy5-labelled BSA on the array. Therefore, RFI values from different experiments cannot be compared in absolute values. In two independent runs four identical samples were spotted on reverse protein arrays and RFIs were compared. R^2 as an indication of linear regression was 0.93 on average for DYS1, DYS2, the dystroglycans as well as α-, β-, γ-, and δ-sarcoglycan respectively (see Figure 18). Best correlations were seen for DYS2 and γ-sarcoglycan (both 0.99), and α-dystroglycan showed the lowest R^2 of 0.56. Possible sources of variation in replicates on reverse protein arrays from different experiment runs include (possibly among others): sample preparation, determination of total protein concentration, spotting, antibody concentrations/performance, laser intensity, and array quality. In order to assess the reproducibility of the overall method twelve biopsies were divided in two pieces and assessed independently in two different experiment runs (see Figure 19). The average R^2 was 0.71 and therefore markedly lower compared to the comparisons between two experiment runs and identical samples. RFI values for DYS1 and DYS2 showed both a high correlation of 0.92 between run 3 and run 4. Again, α-dystroglycan showed the lowest R^2-value of in this case only 0.21.

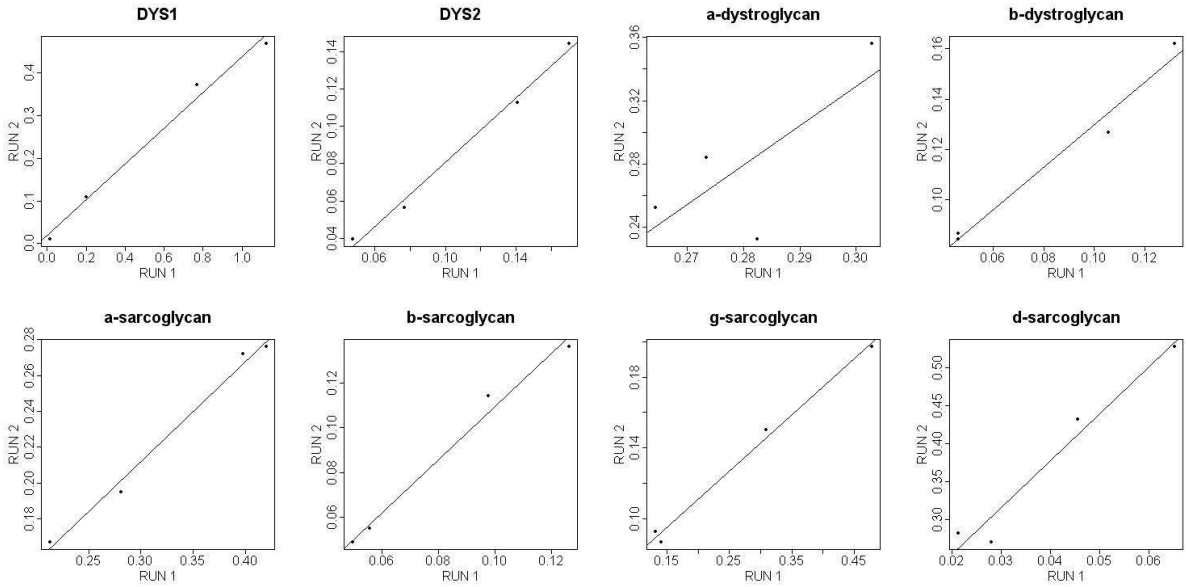

Figure 18: Linear regression for reproducibility of results between runs (run 1 vs. run 2, n=4). Identical sample preparations were spotted twice on reverse protein arrays. R^2 as an indication of linear regression was 0.93 on average with the lowest value for a-dystroglycan (R^2=0.56).

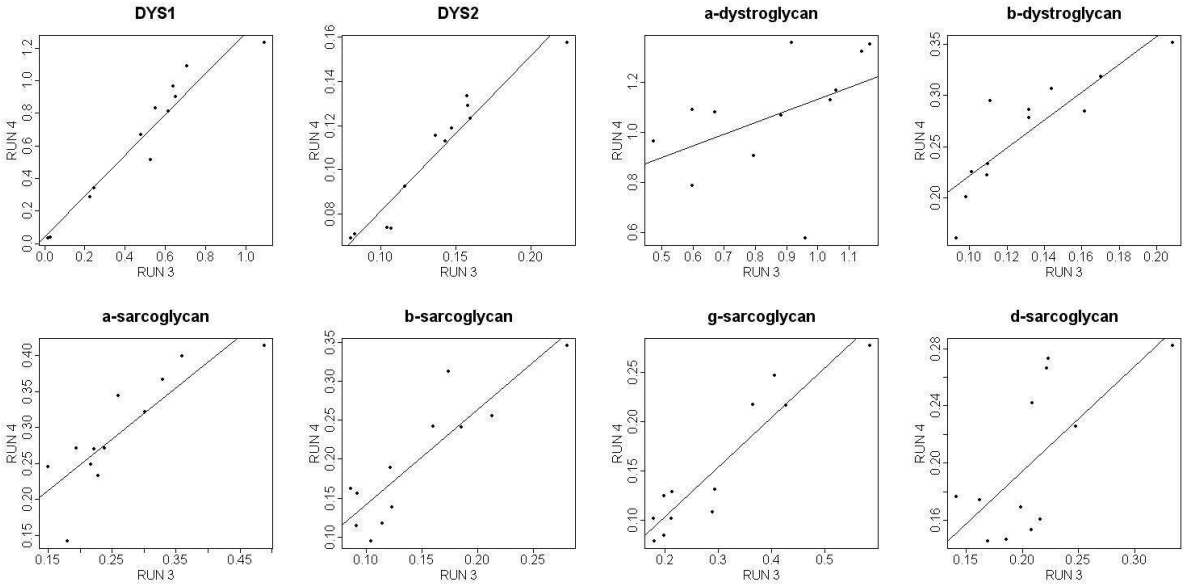

Figure 19: Linear regression for reproducibility of results between runs (run 3 vs. run 4, n=12). Sample preparation and determination of total protein concentration for spotting was completely independent in both runs. R^2 as an indication of linear regression was 0.71 on average with the lowest value for a-dystroglycan (R^2=0.21).

3.1.6. Normalization to muscle "housekeeping" proteins

In a preliminary study normalization of RFI signals to α-actinin led to a slight decrease of the overall CV in all sample groups. Therefore, it was assumed that normalization of the signals to muscle "housekeeping" proteins could compensate for the various amounts of actual muscle tissue in the biopsies.

Average CVs in sample groups of the microarray containing nine control, nine DMD, three BMD, and each four LGMD2A and LGMD2D samples were 23% without normalization for all antibodies except candidate normalizing proteins. Here, normalization to α-actinin and β-tubulin (in CAB1) increased the average CV to 30% and 34% respectively. Normalization to myosin fast heavy chain, myosin slow heavy chain, β-tubulin in CAB2 led to dramatic increases of CVs (>50%) over all sample groups indicating that normalization of signals to these proteins is not feasible on reverse protein arrays.

Normalization to α-actinin and β-tubulin did not have an impact on statistical decisions in most cases indicating good assay stability. DMD patients showed still significantly lower DYS1 and DYS3 signals after normalization, only with DYS2 this was not the case (see Figure 20). α-sarcoglycan levels in LGMD2D were significantly lower compared to control samples after normalization to α-actinin or β-tubulin. For the other sarcoglycans and dystroglycans as well as calpain and spectrin, statistical decisions remained mainly unchanged however some sample groups differed no longer after normalization. The only case where a sample group differed significantly from the control group only after normalization was the increased signal for α-sarcoglycan in LGMD2A patients. Desmin

normalization increased markedly the overall CVs in the tissue as well as in the myotube arrays.

If muscle proteins in myotubes should be assessed, myogenicity of the myoblast cultures has to be carefully monitored. As seen in Western blots of total cell lysates from developing myotubes (in Figure 21), the contents of α-actinin and desmin as muscle-specific proteins vary dramatically between cultures. While sample CONT 14 shows the typical increase of α-actinin over differentiation time and the developmental pattern of desmin expression, in CONT 15 α-actinin levels increase slower and desmin expression is seen only at very low level. The same was found in immunofluorescence analysis (see Figure 22), where in the culture of CONT 15 at day 0 indeed only single desmin-positive cells were found and after 5 days of differentiation myotube formation was negligible.

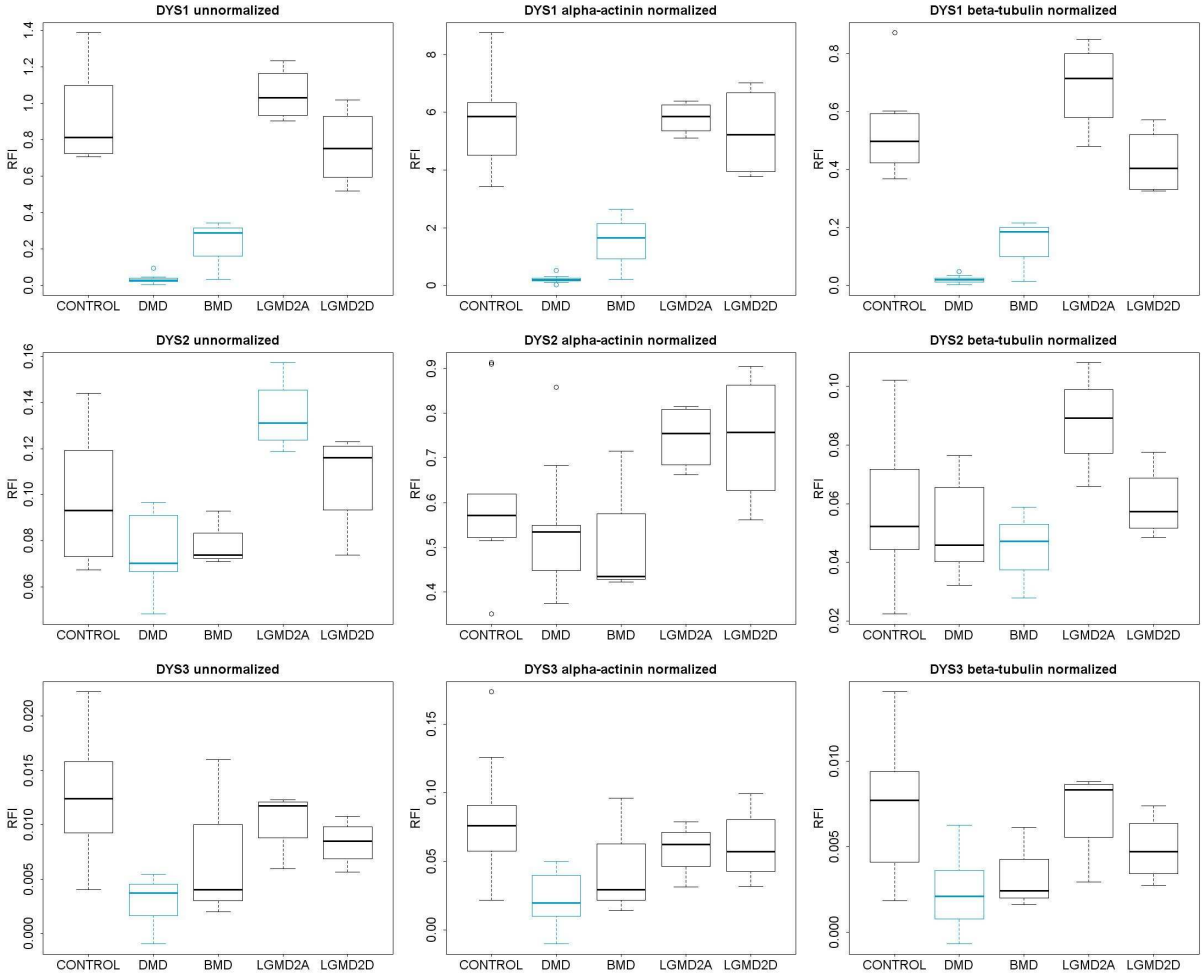

Figure 20: Normalization of RFI signals to candidate „housekeeping“ proteins. For DYS1 and DYS3, normalization to α-actinin levels or β-tubulin levels do not have an impact on statistical decisions. In contrast, DYS2 signals in DMD patients do not differ significantly from controls after normalization.

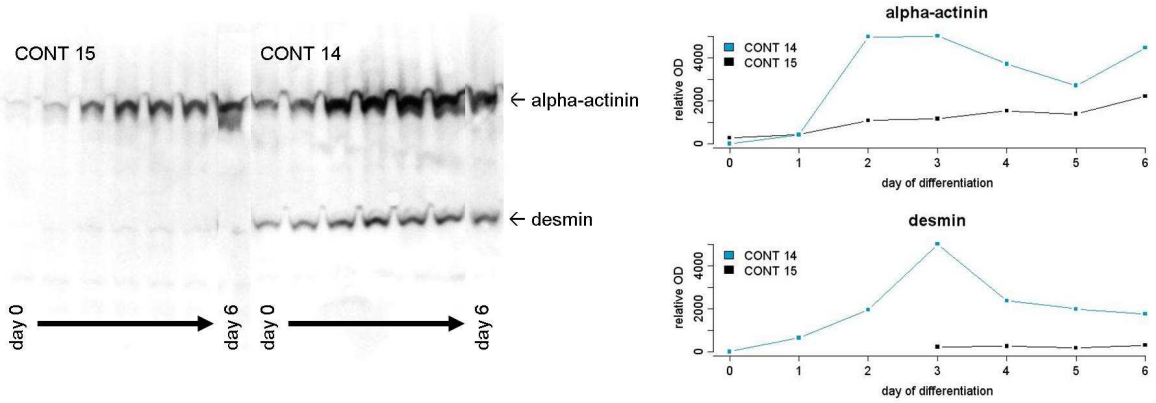

Figure 21: Desmin and α-actinin in differentiating control myoblasts from primary culture. Myogenicity can vary dramatically between cultures as seen in the amounts of desmin and α-actinin. CONT 15 shows considerably lower desmin levels compared to CONT 14. Right panel: Densitometric analysis of bands on western blots (average intensity).

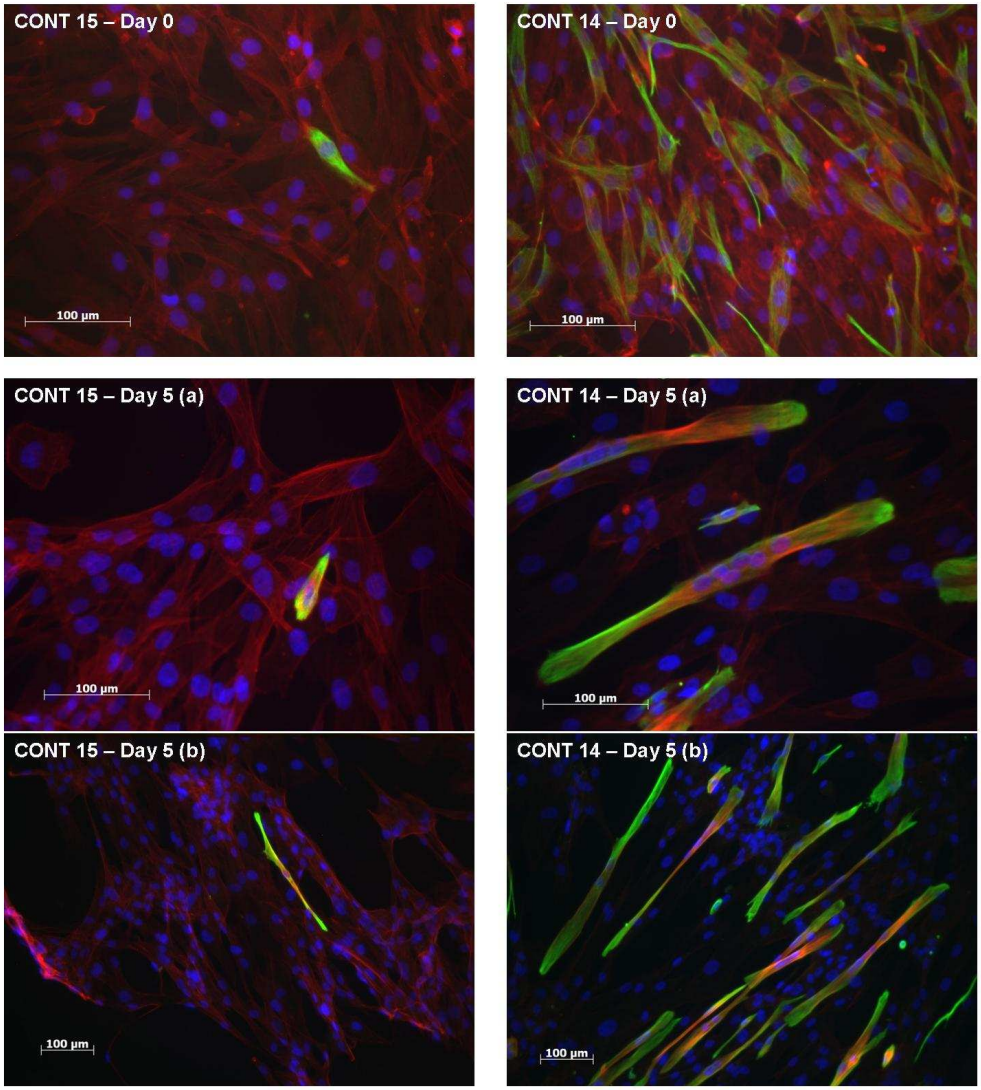

Figure 22: Desmin in myoblasts and myotubes in two control muscle cell cultures. Green cells are desmin-positive, red is actin-phalloidin and blue is DAPI staining. CONT 14 shows considerably more desmin-positive cells (higher myogenicity) on day 0 than CONT 15 where only single desmin-positive cells are seen. On day 5 of differentiation, multinucleated myotubes are formed in CONT 14 culture while in CONT 15 only one myotube-like cell was found in the culture.

3.2. Two-dimensional gel electrophoresis

Figure 23 shows representative 2DE gels for DMD and control muscle tissue obtained with either 17cm nonlinear IPG strips for isoelectric focusing (left panels) or 24cm nonlinear IPG strips (right panels). After manually cancelling misinterpreted spots the average number of spots found on large gels was slightly higher than on smaller gels but the most striking advantage of the larger gels is the considerably higher resolution in extreme pH ranges. Average number of spots found in the experiments was lowest in EXPV (504 spots) and highest in EXPIII (869) and probably depended on the moment of the stopping of the silver staining.

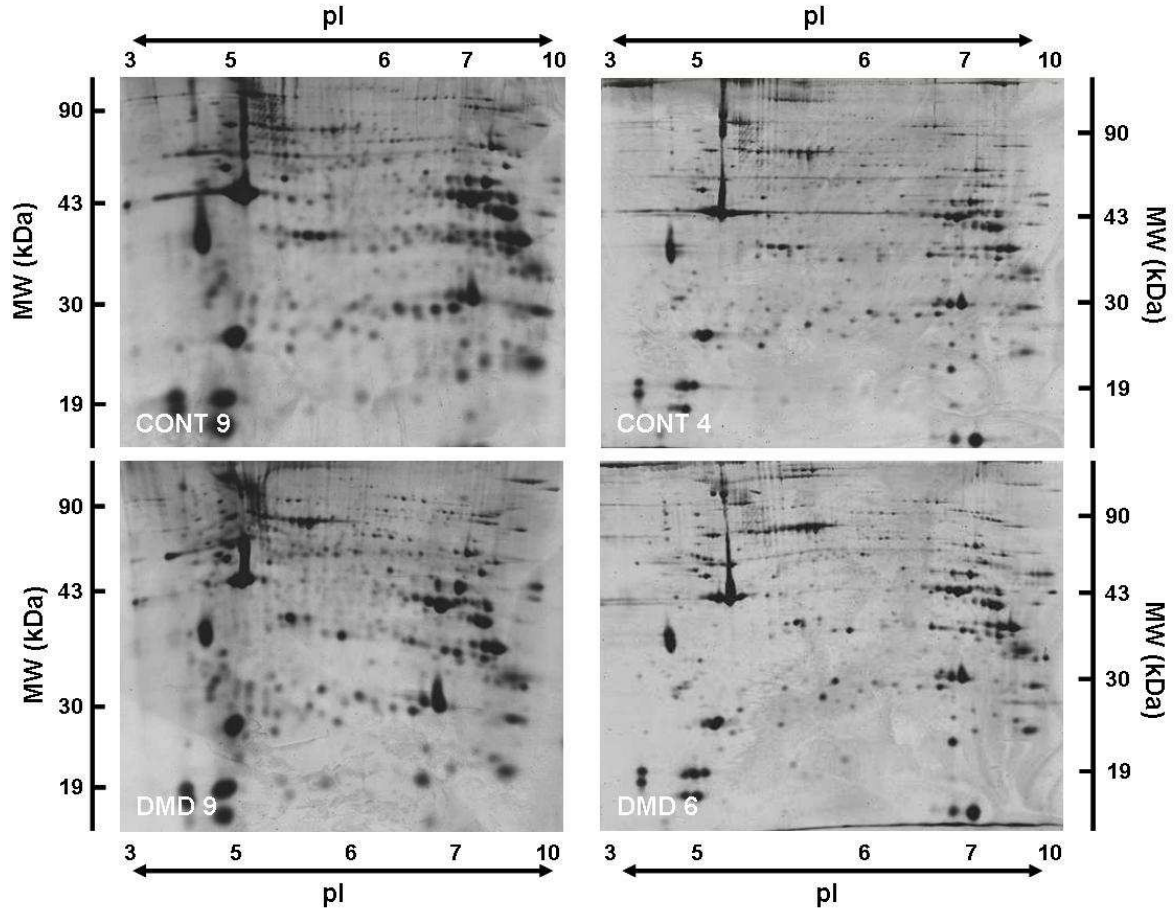

Figure 23: Total muscle tissue protein extracts from control and DMD muscle on 17cm nonlinear IEF strips/10% acrylamide gel (left, 90μg total protein, from EXPI) and 24cm nonlinear IEF strips/10%acrylamide gel (right, 120μg total protein, from EXP II); silver stained. Higher resolution especially in extreme pH range is reached on 24cm strips.

3.2.1. HPLC-MS/MS analysis of selected spots

Landmark spots were identified by HPLC-MS/MS in order to compare the gels from human muscle tissue with gels from databases or literature. 61 spots were analyzed and the corresponding proteins identified. Out of 47 proteins that were identified ten were found in more than one spot indicating that isoforms of the corresponding proteins are present in skeletal muscle. An example gel showing all the identified proteins is shown in Figure 24 and

the list of corresponding proteins is given in Table 5. The complete list of all peptides found in the HPLC-MS/MS analysis is given in Appendix I. Eight proteins (β-enolase (spot No. 3), HSP-β1 (No.5), L-lactate dehydrogenase A chain (No. 9), triosephosphate isomerase (No. 11), myosin regulatory light chain 2 (ventricular/cardiac muscle isoform, No. 14), fructose-bisphosphate aldolase A (No. 20), α-1 antitrypsin (No. 22), and peroxiredoxin-2 (No. 47) were identified in two spots while troponin C from slow skeletal muscle (spot No. 35-35c) and troponin C from fast skeletal muscle (spot No. 39-39c) were found in four different spots on the gel, some of them identified with only one peptide, though. Muscle proteins with a MW range from 83.3 kDa (HSP-90β) to 17.2 (myoglobin) and a pI range from 4.04 (Troponin C, slow skeletal and cardiac muscles) to 9.31 (zinc finger protein 705F) were identified on the gel. Zinc finger protein 705F (No. 42) was identified by only one peptide as well, but the position at the very basic edge of the gel indicates a high probability that spot No. 42 might indeed represent this protein with a MW of 34.9 kDa and a pI of 9.31. The general spot pattern on the gel based on MW/pI of the identified proteins (see Figure 24) was plausible with some exceptions such as spots No. 22, 24, 26, 29, 39, and 44 that appeared at positions on the gel not fully compliant with the spots in their close environment. Spot 16, in addition to tubulin β-2 chain (spot No. 16, UniProt No. P68371) was identified as tubulin β-3 chain (UniProt No. Q13509) and twice as tubulin-β chain (P07437).

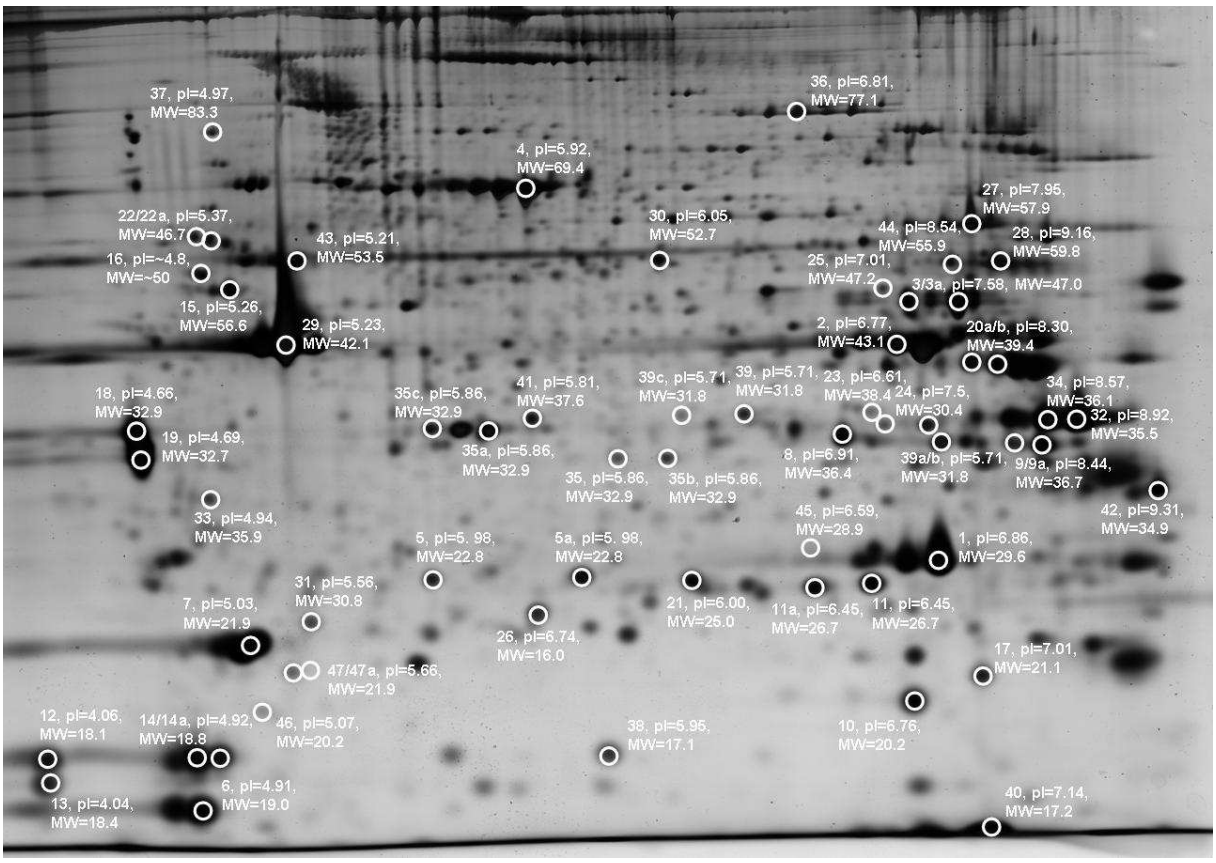

Figure 24: All proteins identified after 2DE and HPLC-MS/MS on their position on a representative gel from human muscle tissue. The sample shown is LGMD2I 3.

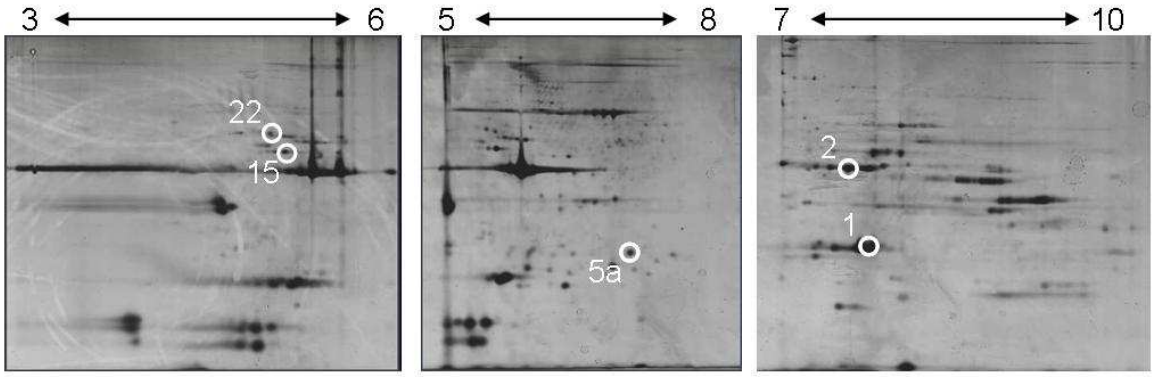

Figure 25: Control muscle (pooled) on narrow-range-pI IEF/2DE (after ZOOM prefractionation). Numbers on top are pI ranges, numbers on gels are identified proteins from ZOOM gels. Overall resolution was not enhanced due to introduction of artefacts such as horizontal streaking.

Table 5: List of identified proteins in human skeletal muscle tissue on 2DE gels

Nr	Unique Peptides	Percent Coverage	MW [kDa]	pI	Uniprot Nr	Name	Remarks
1	12	48	29.6	6.86	P07451	Carbonic anhydrase 3	*******
2	11	30	43.1	6.77	P06732	Creatine kinase M-type	****, ******
3	12	32	47.0	7.58	P13929	B-enolase	***
3a	2	5	47.0	7.58	P13929	B-enolase	
4	32	54	69.4	5.92	P02768	Serum Albumin	
5	3	20	22.8	5.98	P04792	Heat shock protein β-1	
5a	5	34	22.8	5.98	P04792	Heat shock protein β-1	****, ******
6	11	72	19.0	4.91	Q96A32	Myosin regulatory light chain 2, skeletal muscle isoform	***
7	9	48	21.9	5.03	P08590	Myosin light chain 3	
8	4	16	36.4	6.91	P40925	Malate dehydrogenase, cytoplasmic	***
9	5	15	36.7	8.44	P00338	L-lactate dehydrogenase A chain	****
9a	6	17	36.7	8.44	P00338	L-lactate dehydrogenase A chain	
10	4	32	20.2	6.76	P02511	A-crystallin β chain	
11	6	32	26.7	6.45	P60174	Triosephosphate isomerase	
11a	2	12	26.7	6.45	P60174	Triosephosphate isomerase	
12	1	6	18.1	4.06	P02585	Troponin C, skeletal muscle	
13	2	13	18.4	4.04	P63316	Troponin C, slow skeletal and cardiac muscles	
14	4	21	18.8	4.92	P10916	Myosin regulatory light chain 2, ventricular/cardiac muscle isoform	***
14a	3	15	18.8	4.92	P10916	Myosin regulatory light chain 2, ventricular/cardiac muscle isoform	
15	12	30	56.6	5.26	P06576	ATP synthase subunit β, mitochondrial	***, ******
16	3	8	49.8	4.79	P68371	Tubulin β-2 chain	***
17	5	35	21.1	7.01	P30086	Phosphatidylethanolamine-binding protein 1	****
18	6	19	32.9	4.66	P07951	Tropomyosin β chain	
19	4	15	32.7	4.69	P09493	Tropomyosin α-1 chain	
20	8	26	39.4	8.3	P04075	Fructose-bisphosphate aldolase A	****

Table 5**, continued**

Nr	Unique Peptides	Percent Coverage	MW [kDa]	pI	Uniprot Nr	Name	Remarks
20a	3	10	39.4	8.3	P04075	Fructose-bisphosphate aldolase A	
21	2	8	25.0	6	P30041	Peroxiredoxin-6	
22	3	6	46.7	5.4	P01009	A-1 antitrypsin	******
22a	5	12	46.7	5.4	P01010	A-1 antitrypsin	******
23	15	nd	38.4	6.61	Q8N335	Glycerol-3-phosphate dehydrogenase 1-like protein	*****
24	3	nd	30.4	7.5	P45880	VDAC2	*****
	3	nd	36.4	6.91	P40925	Malate dehydrogenase, cytoplasmic	*****
	2	nd	36.1	8.57	P04406	Glyeraldehyde-3-phosphate dehydrogenase	*****
25	2	4	47.2	7.01	P06733	A-enolase	**
26	2	15	16.0	6.74	P68871	Hemoglobin subunit β	
27	7	13	57.9	7.95	P14618	Pyruvate kinase isozymes M1/M2	
	4	8	59.8	9.16	P25705	ATP synthase subunit α, mitochondrial	
29	19	46	42.1	5.23	P68133	Actin, α skeletal muscle	*******
30	3	8	52.7	6.05	Q6ZMU5	Tripartite motif-containing protein 72	
31	2	8	30.8	5.56	P02647	Apolipoprotein A-I	***
32	10	39	35.5	8.92	P40926	Malate dehydrogenase, mitochondrial	
33	1	3	35.9	4.94	P08758	Annexin A5	***
34	5	22	36.1	8.57	P04406	Glyceraldehyde-3-phosphate dehydrogenase	
35	2	7	32.9	5.86	P13805	Troponin T, slow skeletal muscle	
35a	4	10	32.9	5.86	P13805	Troponin T, slow skeletal muscle	
	2	7	36.6	5.71	P07195	L-lactate dehydrogenase B chain	
35b	1	3	32.9	5.86	P13805	Troponin T, slow skeletal muscle	
35c	2	7	32.9	6.86	P13806	Troponin T, slow skeletal muscle	******
36	11	19	77.1	6.81	P02787	Serotransferrin	
37	2	3	83.3	4.97	P08238	Heat shock protein HSP 90-β	***
38	2	14	17.1	5.95	O14558	Heat shock protein β-6	
39	2	10	31.8	5.71	P45378	Troponin T, fast skeletal muscle	
39a	5	17	31.8	5.71	P45378	Troponin T, fast skeletal muscle	
39b	3	16	31.8	5.71	P45378	Troponin T, fast skeletal muscle	
39c	1	2	31.8	5.71	P45378	Troponin T, fast skeletal muscle	
40	8	57	17.2	7.14	P02144	Myoglobin	
41	4	14	37.6	5.81	P21695	Glycerol-3-phosphate dehydrogenase [NAD+], cytoplasmic	
42	1	7	34.9	9.31	A8MVS1	Zinc finger protein 705F	
43	19	41	53.5	5.21	P17661	Desmin	*******
44	3	7	55.9	8.54	P02675	Fibrinogen β chain	****
45	3	10	28.9	6.59	P00915	Carbonic anhydrase 1	
48	1	8	20.2	5.07	Q16082	Heat shock protein β-2	**, ***
47	2	10	21.9	5.66	P32119	Peroxiredoxin-2	
47a	2	10	21.9	5.66	P32119	Peroxiredoxin-2	****

* different parent charges; ** confirmed by experiments at the Biozentrum, Basel (Suzette Moes); *** confirmed by an additional experiment (at least one more unique peptide; **** confirmed by an additional experiment (at least one unique peptide), ***** identified the Biozentrum, Basel (Suzette Moes); ****** data from ZOOM experiment; ******* confirmed in ZOOM experiment

In order to enhance resolution in the first dimension of 2D-PAGE a prefractionation of the sample was carried out using Invitrogen's ZOOM system for fractionation of protein samples according to pI in solution. Sample fractions were then applied to narrow-range matching IEF strips resulting in three gels per sample with an overlapping pH range. Running all three gels in the same gel run resulted in comparable separation according to MW over all three tells. As shown in Figure 25, this additional sample step introduced considerable experimental artefacts such as horizontal streaking and a smaller number of total protein spots rather than higher resolution. As a consequence, comparisons between muscle tissue lysates from patients and controls were all carried out on single pH 3-10 nonlinear IEF strips in the first dimension.

3.2.2. Differentially expressed proteins between in DMD muscle tissue

Eight spots were reproducibly found to be differentially expressed between DMD muscle tissue and healthy control tissue in the present sample set in EXP I and EXP II. HSP β-2 (HSPβ2), α-enolase, annexin-A5 as well as two unknown proteins were found to be increased in DMD muscle tissue compared to controls while a protein that was identified as VDAC2 at the Biozentrum, GPD1L, and an isoform of troponin T fast skeletal muscle isoform were found to be decreased in patient tissue. The most prominent increases were those of HSPβ2 (not detectable in controls in EXP I and 8.51-fold increased in EXP II) and unknown protein II (not detectable in controls in EXP I and 8.46-fold increased in EXP II). VDAC2 (likely) and GPD1L were decreased dramatically with VDAC2 being non-detectable in controls in both experiments and GPD1L detected only in EXP II. An overview on fold-changes and p-values between DMD patient samples and controls is given in Table 6 and images of the spots representing the differentially expressed proteins are shown in Figure 26. In EXP I the two BMD samples showed intermediate mean values between DMD and control samples in all cases except for GPD1L (see Figure 26). Figure 27 shows comparisons of EXP I and EXP II for the differentially expressed proteins. Even though the experiments were carried out using different samples the results seem highly reproducible. In EXP I α-enolase, HSPβ2 and unknown protein II were not detectable in control samples using the given experiment parameters while they were found at low levels in EXP II (in four out of five, one out of five, and two out of five for α-enolase, HSPβ2, and unknown protein II respectively). GPD1L was in contrast not detected in DMD samples in EXP II but it was found at low levels in two DMD samples in EXP I. Expression of HSPβ2 and α-enolase was significantly higher in DMD patients than in control samples in all three experiments, and levels of GPD1L and an isoform of troponin T (fast) were significantly lower in DMD patients in all experiments.

Table 6: Fold-changes and p-values for differentially expressed proteins in DMD

	Fold Change EXPI	Fold Change EXP II	Fold Change EXP V	p-value EXP I	p-value EXP II	p-value EXP V	Average Fold Change
HSPβ2	100	8.51	100	8.65E-04	7.31E-04	0.04	8.51*
unknown protein II	100	8.46	2.00	0.20	0.01	0.37	5.23*
α-Enolase	100	3.73	3.55	0.03	0.03	0.03	3.64*
Annexin-A5	2.90	3.57	4.03	0.11	0.02	0.05	3.50
unknown protein I	3.79	3.35	1.40	0.10	0.01	0.34	2.85
VDAC2	0	0	0	0.09	0.01	0.33	0
GPD1L	0.29	0	0	0.04	0.01	0.03	0.11
Troponin T, fast skeletal muscle (isoform)	0.11	0.19	0.40	0.01	0.01	0.03	0.23

* Fold Change 100 in EXP I and EXP V are imaginary values, therefore the average Fold Change was not calculated using this value

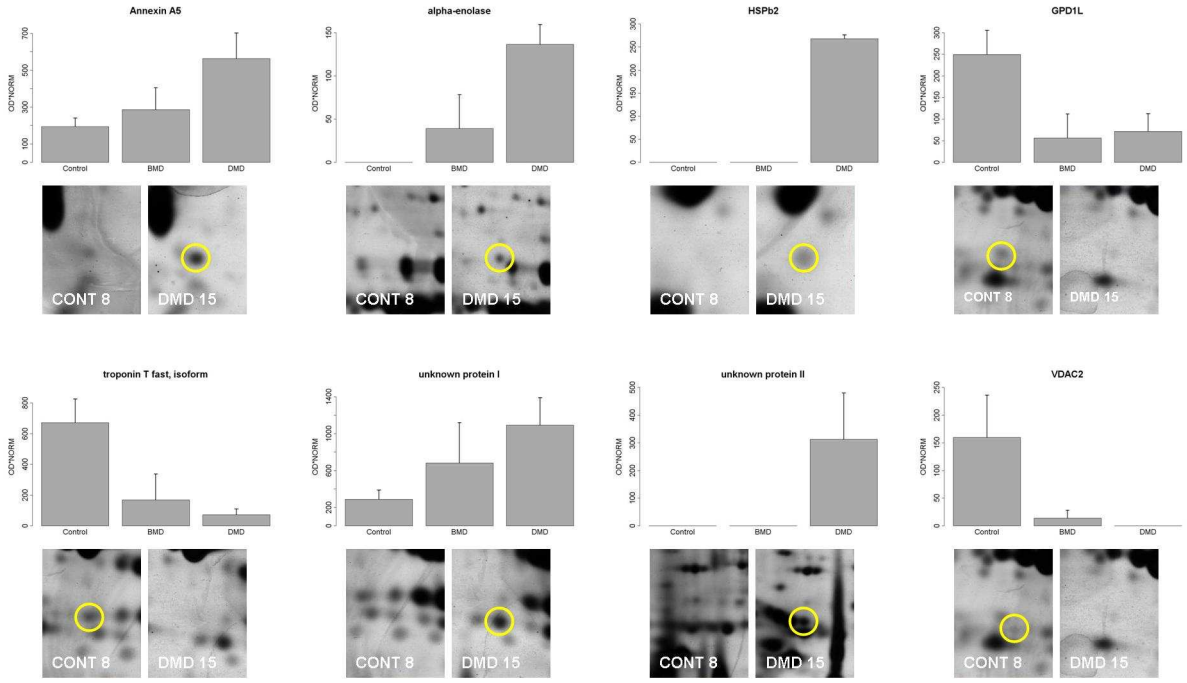

Figure 26: Proteins found to be differentially expressed in DMD. Sample sizes are n=6 for controls, n=2 for BMD and n=3 for DMD. Error bars are SEM.

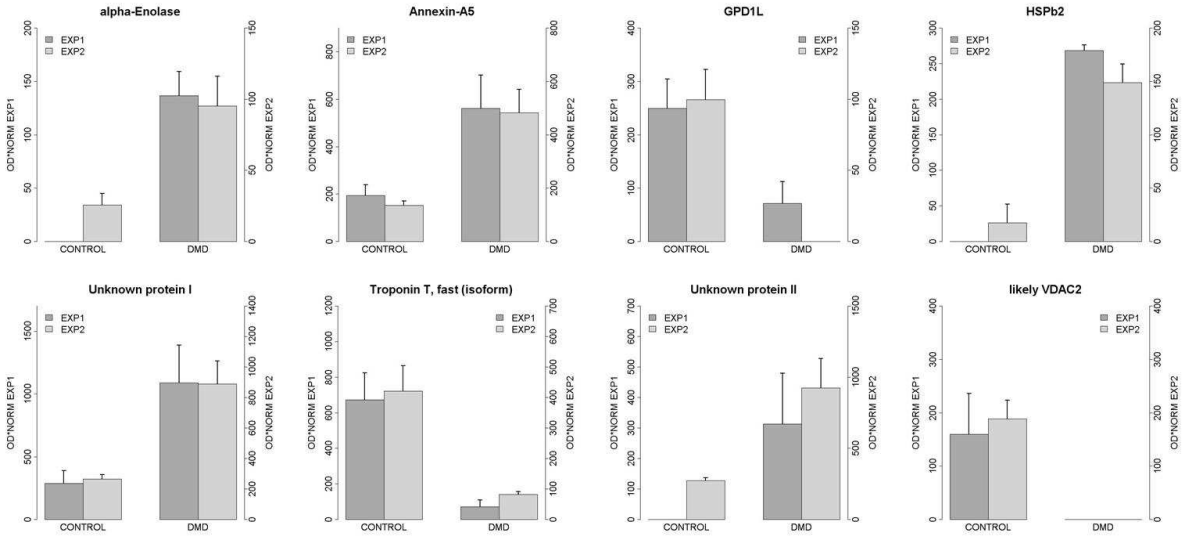

Figure 27: Comparison of two 2DE experiments for differentially expressed proteins between DMD and control muscle tissue. Error bars are SEM.

3.2.3. Expression of candidate DMD markers in LGMD2A and LGMD2I patients

In order to find out whether the proteins found to be differentially expressed in DMD muscle tissue are specifically increased or reduced in dystrophinopathies or rather general features of muscle disease the same spots were analyzed in LGMD2A and LGMD2I. An overview on fold changes and p-values between control samples and LGMD2A and LGMD2I respectively is given in Table 7. For HSPβ2 the differences between control muscle and other MD muscle was not significant. In EXP III, the p-value between control and LGMD2I samples was 0.051 indicating a slightly higher HSPβ2 expression in LGMD2I patients. This could not be confirmed in a second experiment using different LGMD2I patient samples (see Figure 28, HSPβ2 section). In EXP V combining LGMD2A and DMD patient samples in one experiment the difference between DMD patients and controls as well as between DMD patients and LGMD2A patients was significant with an over 15-fold higher average HSPβ2 expression in DMD than in LGMD2A patients in this experiment (p=0.037 and p=0.040, respectively; Figure 28). α-enolase is found at higher levels also in LGMD2A and LGMD2I patients, but the mean overall differences to control muscle tissue are not significant. The proteins that are found at lower levels in DMD patients (VDAC2, GPD1L, the isoform of troponin T (fast), and PEPB1 do not seem show any up- or downregulation in LGMD2A or LGMD2I patients. Out of the four proteins that were consistently and significantly differentially expressed in DMD patients only HSPβ2 and GPD1L were significantly higher (for HSPβ2) or lower (for GPD1L) in DMD patients compared to LGMD2A in the same experiment run (EXP IV, see Table 7). α-enolase and the isoform of troponin T (fast skeletal muscle) were not differently expressed in DMD patients compared to LGMD2A.

3.2.4. HSPβ2

The goat polyclonal antibody against HSPβ2 was not specific on Western blots and produced multiple bands on muscle tissue lysates and also on cell lysates. It was therefore not applied on microarrays. Immunofluorescence on C2C12 cells and primary human muscle cells (myoblasts and myotubes) resulted in unspecific staining with high background (data not shown).

Table 7: Fold-changes and p-values of candidate DMD markers in other muscular dystrophies (LGMD2A and LGMD2I). nd: Spot was not analyzeable in the respective experiment.

	Fold Change CONT vs LGMD2A EXP IV	Fold Change CONT vs LGMD2A EXP V	Fold Change DMD vs LGMD2A EXP V	Fold Change CONT vs LGMD2I EXP III	Fold Change CONT vs LGMD2I EXP IV	p-value CONT vs LGMD2A EXP IV	p-value CONT vs LGMD2A EXP V	p-value DMD vs LGMD2A EXP IV	p-value CONT vs LGMD2I EXP III	p-value CONT vs LGMD2I EXP IV
HSPβ2	2.29	100.00*	15.46	4.43	0.00	0.64	0.42	0.04	0.05	0.42
unknown protein II	nd	0.50	3.98	nd	nd	nd	0.57	0.12	nd	nd
α-Enolase	2.53	1.25	2.85	1.02	3.79	0.41	0.87	0.20	0.96	0.10
Annexin-A5	0.82	3.08	1.31	1.24	0.88	0.74	0.42	0.68	1.86E-03	0.26
unknown protein I	1.84	0.86	1.63	1.12	2.85	0.33	0.67	0.25	0.71	0.11
likely VDAC2	1.04	1.04	0.00	0.30	0.89	0.91	0.98	0.42	0.09	0.79
GPD1L	1.06	1.56	0.02	1.09	0.78	0.84	0.15	0.02	0.78	0.58
Troponin T, fast skeletal muscle (isoform)	1.01	0.68	0.58	0.63	0.79	0.98	0.63	0.66	0.35	0.48

* Fold Change 100 is an imaginary value as in the controls, no **HSPβ2 was detected.**

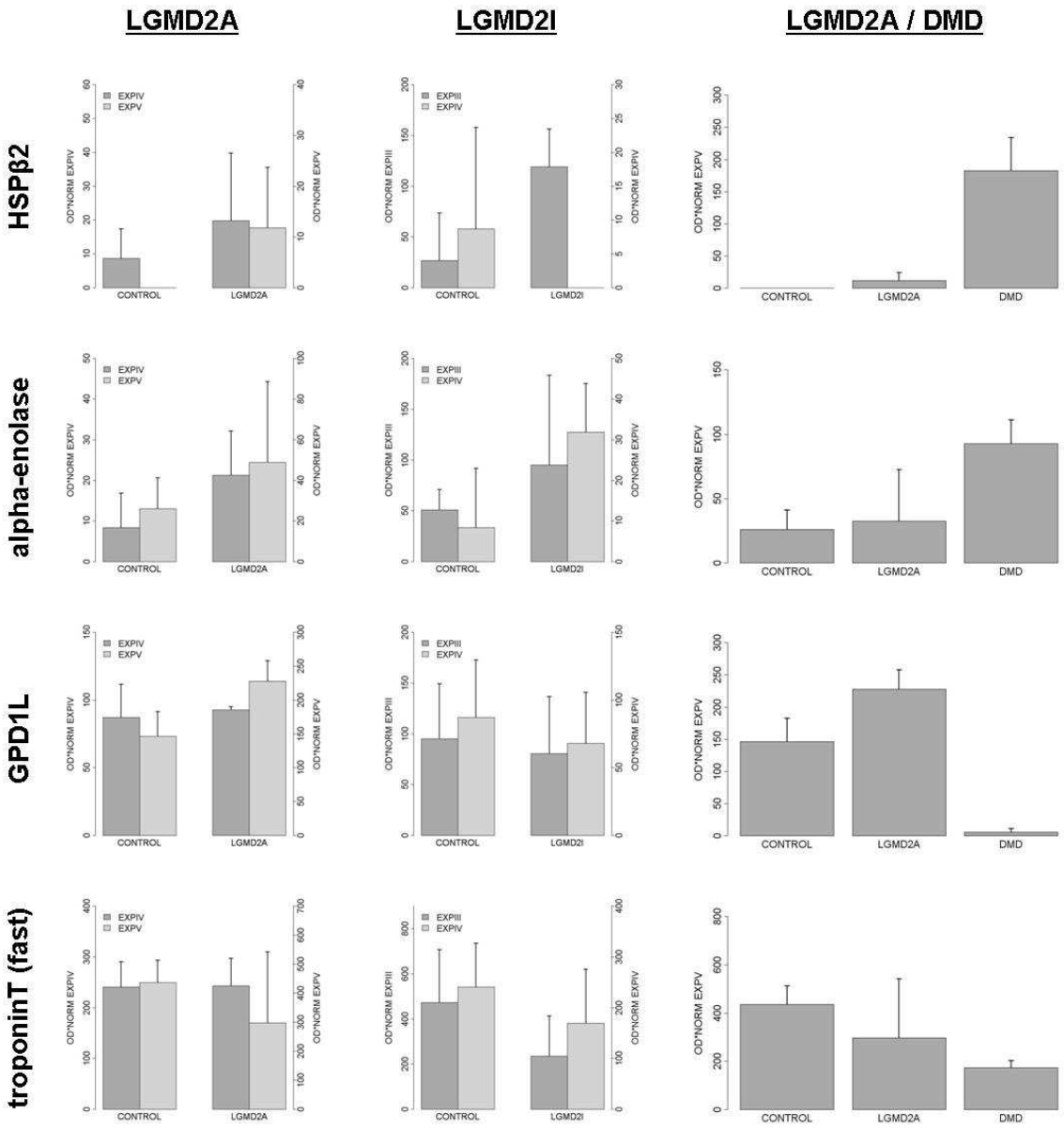

Figure 28: HSPβ2, α-enolase, GPD1L, and troponin T (fast skeletal muscle, isoform) in LGMD2A and LGMD2I (left and middle panels). Right panels are comparisons between controls, LGMD2A and DMD patients from the same experiment run. Error bars are SEM.

4. Discussion

4.1. Reverse protein Arrays for Quantification of Muscle Proteins in Muscular Dystrophy

4.1.1. Dystrophin and DGC proteins quantification on reverse protein arrays

In the present work we assessed a reverse protein array approach for the quantification of muscle proteins used in the diagnosis of muscular dystrophies. Tissue lysate reverse protein arrays provide a tool to screen for diagnostically relevant marker proteins in a very small amount of patient tissue and deliver valuable information for an optional later mutation analysis as suggested by Pogue et al. [75].

In the muscle tissue lysates used in this study dystrophinopathies were easily and reliably detected by the low levels of dystrophin on reverse protein arrays. Similar results were obtained in sarcoglycanopathies where a significantly reduced sarcoglycan expression on the arrays was seen. Secondary reductions of other DGC associated proteins could be measured and quantified with high sensitivity. The three BMD samples in this study showed considerable differences in dystrophin expression. For the DYS1 antibody, RFI values differed from a DMD-like 0.03 to for the BMD3 sample to an intermediate 0.29 and 0.34 for the BMD 1 and BMD 2 samples respectively (mean DMD value: 0.03; mean control value: 0.93). The BMD 3 patient carried a deletion in exons 48-50 which probably resulted in a more severe BMD phenotype as many patients with the same mutation have been reported to show a DMD or an intermediate DMD/BMD phenotype [90]. On the other hand, the DYS1 value of patient DMD 6 was between those of the DMD and BMD samples, which is consistent with the clinical presentation of patient who had an intermediate DMD/BMD phenotype and is seen as the outlier in the DMD group of the DYS1 boxplot (RFI value 0.09, see Figure 7). The splice site mutation (c357+2T>A in intron 5) in the DMD 6 patient has been reported to result in a BMD phenotype of variable severity [90, 91].

Great care must be taken not to misdiagnose primary and secondary deficiencies of dystrophin and the sarcoglycans [75]. It is often not possible to clinically discriminate between the different LGMD subtypes [92] and even in muscle immunoanalysis, primary deficiency in one of the sarcoglycans often cannot be determined unequivocally [93]. Indeed, a lower RFI signal for β-sarcoglycan in the LGMD2E sample compared to LGMD2D samples was not observed. The LGMD2E sample showed a higher signal for α-sarcoglycan than the LGMD2D samples but this is probably of limited relevance given the fact that only one LGMD2E sample was included in the study.

We also showed that the reverse protein array assays worked well using lysates from cultured myotubes as the levels of expression using the DYS1, DYS2, and DYS3 antibodies were very similar to those from muscle tissue lysates. RFI signals obtained with the DYS1

and DYS2 antibodies on myotubes from LGMD2D patients were lower than those on control myotubes. Dystrophin was originally not expected to be reduced in LGMD2D [94] but also other authors [46, 95] found that dystrophin levels can be reduced in patients with α-sarcoglycanopathy. This effect was also seen on the tissue arrays but was not significant there. As our arrays allow the analysis of any combination of antibodies of interest, it was possible to discriminate between cultured cells from DMD and LGMD2D patients as overall DYS signals were markedly lower and the α-sarcoglycan signals were higher in DMD cells compared to LGMD2D cells even though this was not also significant in our sample set including only two samples from LGMD2D patients. Lower γ-sarcoglycan expression in the LGMD2C 1 cells compared to the LGMD2D samples was not observed giving further evidence that the diagnostic decision on sarcoglycanopathies based on protein analysis remains difficult [93].

To work with myoblast cultures is technically challenging, tedious, and the cell's myogenicity has to be carefully monitored over the entire period of cell culture as we have seen in the immunostainings for desmin (see Figure 22). The samples CONT 14 and CONT 15 in Figure 22 have not been analyzed on reverse protein arrays so a direct comparison of immunofluorescence and reverse protein array results can not be made, however the highly variable amount of desmin-positive cells in the cultures emphasizes the differences in myogenicity that can appear in primary cultures. It is also not clear to which extent myotubes from culture represent the phenotype of the muscle including secondary pathogenic cascades in muscle tissue. For these reasons, *in vitro* differentiated myotubes do probably not constitute a material that can be applied in diagnostic processes but might play a role in preclinical research where many compounds are screened for a possible beneficial effect. Furthermore, if a muscle biopsy should be avoided and muscle proteins should be assessed, skin fibroblasts transfected with MyoD and expressing muscle proteins might provide another interesting amendment of the assay.

4.1.2. Calpain-3 measurement on reverse protein arrays

In contrast to dystrophinopathies and sarcoglycanopathies, diagnosis of LGMD2A caused by mutations in the gene coding for calpain-3 turned out to be more challenging. Calpains are ubiquitous Ca^{2+}-activated proteases (μ-calpain and m-calpain) with calpain-3 as the muscle-specific isoform. A standard IHC diagnosis of LGMD2A using muscle sections is currently not established. Western blot as well as recently evaluated IHC analyses [96] can show normal amounts of calpain-3 in LGMD2A patients as a loss of calpain-3 function is not always accompanied by reduced protein levels [97]. In our study patient LGMD2A 2 showed preserved calpain-3 expression with normal bands in Western blot and a RFI signal on the array that was indistinguishable from controls. We saw increased calpain-3 signals in DMD patients and in BMD patients even though the latter was not significant and an overall good

correlation with Western blots. μ-calpain and m-calpain activity were shown to be increased in *mdx* mice but calpain-3 didn't contribute to this phenomenon in these experiments [98]. The upregulation of μ-calpain and m-calpain is not specific for muscular dystrophy [98, 99]. Ueyama et al. [99] found decreased calpain-3 mRNA expression in biopsies from patients with progressive muscular dystrophy (two DMD patients, one BMD patient and two patients with LGMD) but this effect was not significant. In an earlier study by Spencer et al., increased μ-calpain and m-calpain but decreased calpain-3 protein levels in the peak necrotic phase at two weeks in *mdx* mice were shown using an antibody against an epitope that is conserved among all three isoforms [100]. In human muscle tissue from DMD patients, calpain-3 was found to be reduced only in single cases [76].

Higher calpain-3 in IHC stainings of immature fibers confirmed by labelling of adjacent sections with neonatal MHC have been shown by [97]. As the expression of embryonic and neonatal myosin isoforms is considered a characteristic feature of muscular dystrophies [101] the higher calpain-3 levels in DMD patients in our study might be an effect of the regenerating muscle in DMD patients. General protein degradation in control samples only causing an artefact of reduced calpain-3 staining in the controls on the other hand is very unlikely according to the results from Western blotting and general protein patterns obtained in parallel 2DE experiments. The authors of [97] stated further that the 2C4 antibody yielded better IHC/WB correlation than12A2. Generally, experimental artefacts in immunolabelling of calpain-3 are quite common as for example thawing of the muscle biopsies or remaining mounting medium can lead to false-negative measurements and absence of overall protein degradation has to be carefully monitored [76]. Consequently, even though we were able to measure calpain-3 levels similar to Western blots on the reverse protein arrays our results did not differ significantly between LGMD2A patients and controls or other dystrophies suggesting that reverse protein array analysis is not sufficient for the direct detection of mutations in the calpain-3 encoding gene. However, we found significantly increased sarcoglycan signals (and higher dystrophin expression when using the DYS2 antibody) in LGMD2A compared to controls and to other assessed muscular dystrophies suggesting that increased expression of these proteins might indirectly help to diagnose LGMD2A when using the array.

4.1.3. Increased desmin expression in development and diseased muscle

Desmin are class-III intermediate filaments that form a fibrous three-dimensional scaffold in cardiac, skeletal and smooth muscle cells. They are circularly arranged at the periphery of Z-disks keeping adjacent myofibrils laterally aligned and connecting sarcomeres to nuclei and to the sarcolemma (reviewed in [1, 102]). Desmin filaments are connected by plectin filaments, and the β chain of α-crystallin, a HSP that protects the cytoskeleton from mechanical damage [1]. Desmin has therefore an important role in transferring force that

occurs during muscle contraction to the entire muscle fiber. Desmin is the main intermediate filament protein in adult skeletal and heart muscle with a low concentration in expanding myoblasts and satellite cells and a high concentration in differentiated myotubes [103] and accounts for 0.35% of total protein in mammal skeletal muscle cells [102]. It is especially abundant at the MTJ and at NMJ of skeletal muscle [102].

Abnormal accumulation of desmin in muscle fibers is responsible for desmin-related myopathies (DRMs) caused by either primary mutations in the desmin gene or familial myopathies mapping to the α-B-crystallin gene and other genes (reviewed in [102]). DRMs are very heterogeneous diseases with diverse clinical manifestations [103]. DRMs represent a exceptional disease state where instead of an absence or reduction of the protein encoded by the mutant gene like in other myopathies, an aggregation of the protein is responsible for the phenotype. Initially, we considered desmin a candidate normalizing protein for the quantification of muscle proteins on reverse protein arrays as many studies it was applied to assess the myogenicity of muscle cell cultures [78, 104-106]. Normalization to desmin in muscle biopsies was, however, not applicable on the reverse protein arrays as it increased the CVs in the sample groups dramatically and also because of the existence of DRMs with altered desmin concentrations. In [104], desmin levels at day 0 after seeding were higher in DMD than in control cultures. This suggests that DMD myoblasts were more mature due to the fact that their progenitor satellite cells had to undergo many more cell divisions than their equivalents in normal muscle. However, after equal differentiation time, higher desmin levels in DMD myotubes could no longer be seen.

The mononuclear cells in muscle tissue can undergo repeated cycles of regeneration and are activated in muscular dystrophies to proliferation and differentiation upon muscle damage. On the molecular level this is seen in the overexpression of genes encoding proteins in cytoskeletal microtubules, intermediate filaments (desmin in muscle) and microfilaments, especially myosin and actin isoforms that are normally highly expressed in neonatal or developing muscle [101]. Higher desmin content in biopsies as was measured in on reverse protein arrays is therefore most likely due to regenerating muscle [101] or a natural repair mechanism as compensation for the loss of dystrophin [23]. In narrow-pI-range 2D-PAGE a more intense spot corresponding to desmin was also found in gels from DMD/BMD patients.

4.1.4. Reasons for increased spectrin levels in DMD patients

Spectrin is the major constituent of the cytoskeleton network under the plasma membrane in erythrocytes with muscle-specific β-spectrin isoform that is assumed to be associated to the costamere along the sarcolemma [102, 107]. The antibody against spectrin that was applied in this study recognizes not only the muscle-specific β-chain of spectrin but also the erythroid isoform. Therefore, spectrin RFI signals on reverse protein arrays consisted not only of

muscle spectrin but also of erythroid spectrin, which is highly influenced by the amount of blood in the muscle biopsy. 2D-PAGE actually showed more intense spots for serum albumin as an indicator of blood content in the biopsies of some DMD patients and an overall good correlation with RFI signals for spectrin on the reverse protein arrays (see Figure 29). It is therefore likely that higher spectrin RFI signals in DMD patients are not a consequence of increased spectrin in muscle but of a different amount of blood in the sample. In IHC experiments fibers which show negative labeling for both dystrophin and spectrin are considered damaged or in early stages of regeneration whereas dystrophin-negative but spectrin-positive fibers represent “real” dystrophin abnormalities. In immunohistological studies of the plasma membrane the labelling of β-spectrin is often used to monitor membrane integrity. In immunohistological intensity measurements, spectrin intensity values obtained in control samples using the same antibody as we did on the microarrays were set as standard for the calculation of normalization factors [108]. This is however not suitable on reverse arrays using whole tissue homogenates and the antibody chosen in our study. As the amount of blood in the muscle biopsies cannot be assessed adequately, this normalization would render the results of the microarrays very unreliable and thus useless. Furthermore, β-spectrin levels are higher in slow-twitch muscle (soleus) than in fast-twitch (extensor digitorum longus) [109]. As the muscle used for the biopsy in our samples is unfortunately unknown in many cases such as DMD 5, we cannot make a statement if higher spectrin levels particularly in some DMD samples could be associated tot the higher content of type II fast-twitch fibers in the respective muscle.

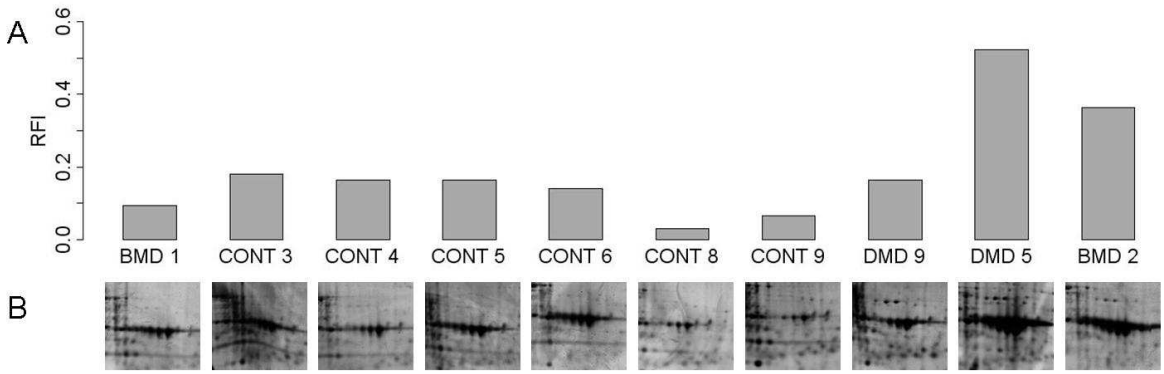

Figure 29: A: Spectrin RFI signals on reverse protein arrays; B: Corresponding albumin spots on 2DE gels. As the SPEC1 antibody applied on the reverse protein array recognizes spectrin in muscle and in blood, high spectrin signals in DMD patients (e.g. DMD 5) are probably an artefact of higher blood content (represented by intensity of albumin spots).

4.1.5. Normalization of muscle protein levels to muscle “housekeeping” proteins

Sample drawing from the patient has been shown to be critical in muscle tissue arrays as differences in the type of muscle used and the actual proportion of muscle tissue in the biopsy can significantly influence the outcome of the assay. Comparisons of protein levels in

muscle tissue based on total protein measurements do not account for the varying amounts of fibrotic and/or adipose tissue in patients and neither for varying amounts of blood that is included while the biopsy is performed. The significantly increased spectrin RFI signals in DMD patients (see Figure 9) might for example represent an artefact of differences in sample drawing where DMD biopsies incidentally contained more blood than control biopsies. Such differences could be accounted for by normalization of tissue from diseased and healthy patients using a muscle “housekeeping” protein. A housekeeping protein in general should be ubiquitously and constitutively expressed so that signals of proteins of interest can be normalized according to it thereby compensating for experimental differences in loading or labelling. The application of such housekeeping proteins for signal normalization has to be carefully monitored as even in matched tissue samples the relative levels of commonly used housekeeping proteins such as GAPDH or β-tubulin [110] and in serum the concentrations of common proteins such as albumin or fibrinogen (3.5-5g/dl and 0.2-0.45g/dl respectively) [84] or the “normal” concentration of serum CK (reviewed in [111]) in the population vary considerably. In our experiments normalization to a muscle-specific protein would be particularly suitable because dystrophic muscle contains more connective tissue and fat than normal muscle. That’s why differences in muscle proteins could come from the fact that the dystrophic biopsies do not contain the same amount of actual muscle tissue. To this end other authors have most commonly used MHC [100], in immunoblots by coomassie-staining [97, 112], which was not applicable in our study due to extremely high MHC signals on the arrays rendering the analysis unreliable. In [61] dystrophin levels are calculated relative to laminin-α2 signals assuming that this protein is not affected in DMD patients. β-dystroglycan staining for the assessment of protein transfer to immunoblots as in [97] is not feasible in the case of DMD/BMD because of secondary reductions that would then lead to false-positive results. In myotubes from primary cell culture the myogenicity of the culture should be carefully monitored. Normalization to actin in cell lysates is common [84], but remains difficult in serum samples, or when biopsies from special tissues are analyzed.

Normalization to skeletal muscle α-actinin or β-tubulin did not have a great influence on the results of the assays and on statistical decisions indicating good overall assay stability. After normalization to MHC, on the other hand, even the very clear differences between DMD patients and controls could no longer be monitored. It is, however, debatable whether a normalization to muscle-specific proteins should be performed at all thereby increasing the overall CVs in the sample groups. The fact that dystrophic tissue contains a higher amount of fatty and connective tissue contributes to the measurement of lower signals for some muscle proteins and might also be regarded as a further hint on the dystrophic processes.

4.1.6. Reverse protein arrays – general considerations

As opposed to gene microarrays, where the probes can be manufactured with a high degree of predictability in terms of specificity and affinity reverse protein microarray are probed with antibodies that very often lack this predictability [86]. The quality of the results obtained from tissue or cell lysate protein arrays depends strongly on the quality of the primary detection antibodies used. Antibodies that show unspecific binding to other proteins on Western blots are prone to cause false-positive results on reverse protein arrays since this method, similar to ELISA, is fully dependent on the specificity of the recognition elements and does not deliver further information such as MW of the protein of interest. Therefore, prior to application on the microarray, and just as in immunocytochemical methods [15], antibodies need to be carefully validated in Western blots (reviewed in [86, 113]). The importance of highly specific antibodies became especially obvious in the case of VDAC2. After the identification of VDAC2 as a candidate marker for DMD in 2D-PAGE gels, a commercially available mouse monoclonal antibody against this protein was applied on reverse protein arrays and a significantly lower expression in DMD patients was indeed confirmed on the arrays (see Figure 12). In Western blots this antibody produced multiple bands indicating that it was not specific for VDAC2 and the results of the reverse arrays were therefore useless. Another commercially available antibody produced in goat yielded one single clear band in Western blots, however, the effect of lower expression in DMD patients was no longer seen on reverse protein arrays. In the case of VDAC2 no confirmation of the results from 2D-PAGE was possible on reverse protein arrays due to the lack of a suitable antibody.

The reverse protein array assay format clearly has big advantages over other assay formats. As opposed to a sandwich-array depending on two detection antibodies recognizing different epitopes it requires only one detection antibody, which is obviously an important feature given the difficulty to find highly specific primary antibodies against a high number of proteins such as VDAC2 as discussed before. Capture arrays, on the other hand, include a sample labelling step, which is technically difficult and often leads to the introduction of experimental artefacts. For application of reverse proteins in diagnostic processes standardized, array production (spotting of the samples onto the glass substrate) in different laboratories represents a major challenge as it is costly and technically difficult. Further standardization of assays (including sample drawing and sample preparation) and the development of universal references that can be applied across clinical laboratories and time are more big issues possibly counteracting a widespread application of reverse protein arrays in clinical proteomics or diagnostic procedures [86]. An ideal universal reference would serve as a positive control for antibody specificity and staining procedures, be fully renewable, and still resemble the test samples to the biggest possible extent. For human tissue samples this is practically not feasible as normally only very limited sample sizes are available, and even lysates from cell lines do not overcome the problem of long-term reproducibility. However,

this problem is not unique to reverse protein arrays but exists also in Western blotting or IHC assay procedures. Alternatively, immunogenic peptides might serve as highly reproducible and renewable internal standard [86].

In conclusion, our results show that the quantitative measurement of dystrophin and DGC proteins in muscle tissue and cultured myotubes can be carried out in a reverse protein array format. The saving of sample material is a great advantage over currently used methods such as Western blotting or IHC, in particular when numerous biopsies are to be analyzed for a wide range of proteins thus providing an excellent tool to collect valuable and comprehensive information about proteins and protein patterns in patient samples. The analysis of a wide range of proteins in small tissue samples might be of particular interest in the assessment of therapeutic effects on the protein level in clinical trials where biopsies have to be repeated after treatment such as exon skipping therapies [61].

4.2. 2DE / HPLC-MS/MS proteomic profiling of DMD skeletal muscle tissue

The loss of sarcolemmal integrity in DMD patients appears to cause various downstream effects in metabolic pathways and cellular signaling. The application of 2DE and MS aims at the elucidation of these downstream effects in order to find new disease markers for diagnostic purposes and for the monitoring of preclinical and clinical trials. As mass-spectrometry based proteomics experiments are considered poorly reproducible, especially in combination with preceding 2DE separation, we have first performed analyses of landmark spots on representative gels from human skeletal muscle tissue in order to compare our 2-D maps to reference maps from literature. Our overall protein pattern corresponded well a reference map for human *vastus lateralis* [114]. Prefractionation using the ZOOM isoelectric fractionator did not increase the resolution in the first dimension but rather caused horizontal streaking and overall higher background staining and was therefore omitted in subsequent experiments. We have found 500-1000 spots on each silver-stained gel which is consistend with the general conception that conventional gel stains such as Coomassie or silver stains normally visualize around a few hundred protein spots [114]. Most sophisticated DIGE approaches are probably capable of presenting a few thousand spots in one single experiment [82, 85]. The dynamic protein range in In a study using dialysis-assisted two-dimensional gel electrophoresis (DIGE), a dynamic range of protein expression of about 1000 was seen in over 1000 spots [78]. In our 2DE experiments using silver staining we have seen a slightly higher dynamic range (about 3000), however, we detected lower total spot numbers.

In our 2DE experiments we have found four differentially expressed proteins in DMD tissue that were reproducible in our experiment series. Evidence that the differences in protein expressions for these proteins are “real” differences between DMD and control tissue samples comes from the fact that in the two BMD samples intermediate spot intensities are measured (except for HSPβ2 where like in DMD samples no protein was detected, and for GPD1L where the protein level was slightly higher in DMD than in BMD). This might to a certain extent compensate the problem of unmatched tissue samples of often unknown muscle origin in our study as the BMD phenotype represents a milder disease progression of DMD similar to different stages of a disease as suggested by Schiess et al. in order to follow disease progression [115]. HSPβ2 and GPD1L appeared particularly interesting because their differential expression in DMD patients was not seen in either LGMD2A or LGMD2I and are therefore discussed in detail below.

4.2.1. HSPβ2 in DMD and HSPs in muscular dystrophies

We have found HSPβ2, a 20.2kDa member of the sHSP family to be dramatically increased in DMD muscle compared to controls (>8.51 fold). The protein was mostly not detectable on

2DE gels from control muscle tissue and it was not significantly increased in other muscular dystrophies. In particular, we have seen a significantly higher expression in DMD muscle than in LGMD2A muscle when the two diseases were compared in the same experiment run. HSPβ2, therefore, represents a candidate disease-specific marker of muscle degeneration in DMD and BMD patients. HSPβ2 was not identified on 2DE gels in previous studies on *mdx* skeletal muscle tissue [82] or human vastus lateralis muscle [114].

Other HSPs identified in our experiments on the 2DE gels include α-crystallin β chain HSP27 (HSPβ1, in two isoforms), and HSP90-β (HSP84). The authors of [82] state that decreased HSP90 in *mdx* mice might be associated with impaired cell growth. We could, however, not find differential expression of HSP90 in muscle tissue from DMD patients.
Generally, the transcription of HSPs is induced by cellular stress (such as “heat”, differentiation, growth, oxidative stress, ischemia, etc.). HSPs can be divided into five major families: the four high-molecular-weight families HSP100, HSP90, HSP70, HSP60, and the large family of small heat shock proteins (sHSPs) characterized by an α-crystallin domain of about 100 amino acids [116]. Many HSPs are molecular chaperones involved in the prevention of aggregation of misfolded proteins but also in intracellular protein transport. In muscular dystrophies HSPs are believed to play this dual role by targeting denatured or misfolded muscle proteins thereby initiating cellular repair and by chaperoning newly synthesized muscle proteins during regeneration. In many pathological processes the up-regulation of stress factors is a response to cellular injury. Muscle cells in general are frequently exposed to severe cellular stresses caused by mechanical stress during activity and exercise and therefore must be protected from damage by specialized mechanisms such as HSPs. Skeletal muscle in muscular dystrophy patients is particularly subjecte to constant severe conditions from sarcolemmal instability and HSPs have been found to be differentially expressed in a number of diseases and experiments: Doran et al. [82] found drastic increase (8.09 fold) in cardiovascular HSP (cvHSP) in *mdx* mice and examined also other key HSPs (HSP20 (↓) , HSP25 (-) (equal to HSP27 in humans [117]) , HSP60 (-), HSP70 (-) , HSP90 (↓), HSP110 (↑), GRP75 (↓)), but not HSPβ2. cvHSP was also found to be increased in aged gastrocnemius muscle from rats by immunoblotting indicating that stress response and muscle degeneration correlate, however, it was in this study not possible to identify the corresponding spot in a 2DE gel by MS [118]. Other differences in expressions of HSPs include induction of HSP70 due to muscle necrosis (reviewed in [117]) and oxidative stress [119], HSP47 upregulation in membranes of regenerating muscle in various muscular disorders [112], induction of other stress proteins such as GRP due to high calcium concentration (discussed in [120]), increased levels of HSPβ1 during myotube differentiation [78] and increased levels of p20 (HSPβ6) and HSP27 associated with high muscle activity in

fast-twitch muscles in *dy* mice [120]. HSP27 and α-crystallin β chain levels are generally higher in slow-twitch than in fast-twitch muscle [117] giving further evidence on the importance of matched muscle samples for the evaluation of candidate marker proteins. HSP90 and HSP27 bind to actin and might therefore have a stabilizing actin filaments in muscle cells and mitochondrial HRPs have an important role in skeletal muscle metabolism (reviewed in [117]). Most of the members of the small HSP family mediate stabilisation of cytoskeletal protein folding and transport. If these proteins are upregulated, it appears that damaged muscle fibers attempt to rescue cellular integridy via modulation and repair of the cellular network [82]. A-crystallin β, HSP27 and other sHSPs are induced in differentiating skeletal muscle under the influence of MyoD, and HSP27 and HSP70 are induced in skeletal muscle after exercise (reviewed in [117]).

HSPβ2/MKBP was identified at the same time by two independent groups [121, 122].

It was suggested that two independent stress response systems for muscle maintenance and differentiation based on oligomerization properties coexist [123]. The authors conclude that the system consisting of HSP27/αB-crystallin/p20 is induced by heat and/or other stresses while the system consisting of HSPβ2 and HSPβ3 may work dominantly under normal conditions and does not show heat inducibility. The authors hypothesize further that HSPβ2 interacts directly with myofibrils (localization not only at the NMJ where DMPK is localized but also at the Z-band of myofibrils) and contributes to myofibril integrity. The complex of HSPβ2 and HSPβ3 was indeed shown not to interact with other sHSPs, while HSPβ2 alone can interact with HSP20 independent of HSP27 and αB-crystallin [121, 124]. The HSPβ2/HSPβ3-complex has very low chaperoning activity [124] but HSPβ2 alone associates specifically with DMPK and protects it from heat-induced inactivation [121]. Interestingly, DMPK expression increased dramatically upon exercise-induced muscle damage in a gene expression profiling study [125]. Though HSPβ2 expression does not seem to be heat inducible it behaves like a stress-responsive protein when after heat treatment, a redistribution of protein to the insoluble cell fraction takes place [121].

HSPβ2 is expressed in skeletal and heart muscle [122] and possibly to a lower extent in prostate, testis, ovary, intestine, and colon tissue (mRNA, [123]). In pig muscle HSPβ2 and cvHSP are expressed in heart and muscle only [126]. HSPβ2 expression is induced during the initial phase of skeletal muscle differentiation but still later than αB-crystallin [123]. The authors showed in the same study that the induction of HSPβ2 upon serum depletion in muscle cells is actually the result of myogenic differentiation and not due to the stress stimulus caused by the serum removal. In pig developing muscle HSPβ2 temporally increased the first day after birth and then showed a developmental expression of upregulation with age [126], HSPβ2 stains only differentiated multinuclear myotubes in IHC,

but even after pre-treatment with 0.5% Triton-X which worked for HSP27 and αB-crystallin no filamentous localization could be detected [123].

In myotonic dystrophy type 1 (DM1) an abnormal expansion of CTG repeats in the 3' untranslated region of the dystrophia myotonica protein kinase (DMPK) causes face-, neck, and distal-dominant limb weakness and atrophy with decreased expression of DMPK. Histologically, there are only few necrotic and regenerating fibers [127]. The accumulation of mutant RNA containing the CUG repeats interferes with alternative splicing of several genes such as the insulin receptor or chloride channels contributing to clinical features of DM1. ER stress was suggested to be involved in the muscle wasting seen in DM1 but disrupted intracellular Ca^{2+}-homeostasis did not seem to be the only reason for it. HSPβ2 was found to be increased about 2.5 folds in Western blots in DM1 patients but not in patients suffering from polymyositis [121], indicating a specific change in HSPβ2 that does not result from muscle degeneration itself. Our results suggest, however, that an increase in HSPβ2 due to muscle degeneration cannot be excluded and further experiments on HSPβ2 expression in muscular dystrophies should be carried out.

4.2.2. Lower GPD1L expression in DMD/BMD patients

A protein that was identified as GPD1L at the mass spectrometry facility at the Biozentrum in Basel was found to be significantly reduced on 2DE gels in DMD patients with an average fold-change of 0.11 while not showing any differential expression in either LGMD2A or LGMD2I patients (see Figure 28). We have, however, not been able to identify this protein mass spectrometrically in our laboratory with the given instrumental setup.

Mutations in the GPD1L gene are the cause of Brugada syndrome type 2 [128] and a cause of sudden infant death syndrome [129]. Brugada syndrome is a rare autosomal-dominant, male predominant form of ventricular fibrillation characterized by ventricular arrythmias, syncope, a high incidence in sudden deaths, and coved-type ST-segment elevation in the right precordial leads of the electrocardiogram (ECG, reviewed in [128]). Mutations in the SCN5A (encoding for the α-subunit of the heart sodium channel) have first been linked to Brugada syndrome and then a second locus on chromosome 3 was identified in a single pedigree with a progressive conduction disease and a relatively good prognosis, later being identified as GPD1L [128, 130]. Most known mutations for Brugada syndrome decrease inward Na^{+} current, and mutations in the cardiac Ca^{+} channels that decrease inward Ca^{2+} current have been shown to cause similar symptoms. In general, only ion channel-related genes have been shown to cause Brugada syndrome. Arrythmias and ST elevations are likely to be caused by inadequate depolarizing current in the epicardium of the left right ventricle where the transient outward repolarizing current is greatest [131]. ECG abnormalities that can lead to ST-segment elevations are also seen in DMD patients [128, 132].

GPD1L is concentrated in the membrane fraction in heart tissue (most highly expressed) and at lower levels in skeletal muscle, kidney, lung, and some other organs [131]. For the heart sodium channel SCN5A, the A280V mutation in GPD1L decreased inward Na^+ current, but this does not hold true for the skeletal muscle sodium channel SCN4A. Surface expression of SCN5A (but not total SCN5A protein) was reduced by almost 50% by the A280V mutation in GPD1L. No direct interactions between SCN5A and GPD1L could be shown though [131]. On the protein level, GPD1L has to our knowledge not been shown to be reduced in DMD patients. GPD and GPD1L RNA levels were shown to be changed 0.63 and 0.54 fold respectively in muscle biopsies from young DMD patients [133]. A study on microRNAs in skeletal muscle tissue found a two-fold increase in microRNA targeting GPD1L resulting in a predicted two-fold reduction in GPD1L RNA in DMD patients [134]. On the other hand, an increase in GPD RNA was measured in rabbit muscle after denervation due to accumulation of white adipose tissue [135]. The authors of this study stated that the denervation of muscle followed by the development of white adipose tissue in fast but also in slow-twitch muscle could represent an interesting model for myodystrophic diseases with fatty degeneration of muscle tissue. Unfortunately, the commercially available goat polyclonal antibody against GPD1L that we have evaluated in order to confirm the results from 2DE by Western blotting and/or reverse protein arrays proved to be highly unspecific and produced multiple bands in Western blots. GPD1L might not be particularly suitable as a diagnostic marker because an absence or reduction in protein levels in the disease state is more challenging to monitor than an increase and suitable positive controls have to be carefully evaluated. However, it would be interesting to analyze the role of GPD1L in the molecular pathways underlying muscular dystrophies in order to find out whether GPD1L reduction is a decisive secondary factor responsible for the DMD phenotype and particularly cardiac involvement.

4.2.3. Other candidate markers found to be differentially expressed in DMD patients

The significant increase in α-enolase in DMD patients that was seen on 2DE gels has been observed to a lesser extent also in other muscular dystrophies. The glycolytic enzyme enolase consists of three tissue-specific isozyme subunits (α/β/γ) forming homo- (α/α in embryo and most adult tissues, β/β in striated muscle, γ/γ in neurons) and heteordimers (α/β in striated muscle and α/γ in neurons). During ontogenesis in muscle, a transition from the embryonic α/α isoform to the α/β and β/β isoforms takes place with a precise organization of the β-enolase expression according to the energy requirements in the different muscle fiber types [136]. In fast type IIB fibers expression of β-enolase was highest, intermediate in type IIA and IIX, and lowest in slow type I fibers [136]. Muscle-specific β-enolase (ENO3) mRNA was found to be changed 0.64 fold in DMD patients whereas α-enolase (ENO1) was found to be changed 1.70 fold [133]. On the protein level it was seen that during the differentiation of human myoblasts the expression of ENO3 increased dramatically [78]. Myoblasts from fetal

tissues have been shown to express predominantly α-enolase whereas myoblasts from postnatal tissues express mostly β-enolase [137]. Therefore, higher levels of α-enolase in DMD patients that are also seen on 2DE gels of other muscular dystrophies (see Figure 28), probably come along with the fact that fetal-like isozyme patterns are frequently observed in neuromuscular disorders, particularly in severe forms [138]. The isozyme pattern found for enolase in [138] was, however, fetal-like in only one out of four DMD cases and intermediate in two out of four. This might have occurred due to the fact that the biopsies did not really show the typical regenerating fibers which gives further importance of sample drawing from the patients and controls.

The isoform of troponin T from fast skeletal muscle that we have found to be reduced in DMD patients was also slightly reduced in LGMD2A and LGMD2I (see Figure 28) and might therefore represent a general indicator of muscle damage. As we have identified this protein in more than one spot on the 2DE gels more than one isoform is obviously present in skeletal muscle from muscular dystrophy patients. Different isoform patterns in muscle can either represent different contractile properties of the muscle types used in the experiments as for example the characteristic patterns of myosin and tropomyosin in deltoideus and vastus lateralis muscle [139] but may also constitute possible novel markers of muscle disease. However, highly specific antibodies recognizing only one isoform would be needed if isoform patterns are to be taken into consideration as diagnostic approach for example on reverse protein arrays.

We have also found annexin-A5 to be increased 3.5 fold in DMD patients compared to control samples. Only a slight increase was was seen in LGMD2I patients and conflicting results were obtained in two experiments analyzing LGMD2A patients.
Annexins are Ca^{2+}/lipid-binding proteins with a highly conserved protein core and variable domains at the N-terminus [140]. Annexins exert different physiological functions mostly related to their membrane-binding properties as membrane-membrane or membrane-cytoskeleton linker. Annexin-A1 and annexin-A2 play a role in dysferlin-mediated membrane repair [11] and show higher expression in dysferlinopathies [141]. The positive correlation of annexin A1 and A2 levels with clinical severity in LGMD2B but also in DMD and BMD patients indicates that they might be prognostic markers of disease [141].
Annexin-A5 can form calcium channels and mediates calcium-dependent apoptosis as well as probably the Ca^{2+}-uptake in hypertrophic chondrocytes [140, 142]. It assumedly plays a role in skeleton growth and development which was however not confirmed in an experiment generating an annexin-A5 deficient mouse model [140]. The facts that annexin-A5 is an intracellular protein that can be secreted and is also found in blood [140] and it was reported

to be increased almost six-fold in DMD patients in a gene expression study [101] make it a valuable candidate in the panel of candidate indicators of disease severity in DMD and other muscular dystrophies.

We have furthermore found a protein that was identified as VDAC2 at the Biozentrum mass spectrometry facility to be completely undetectable on 2DE gels from DMD muscle tissue, an effect that has not been seen in LGMD2A or LGMD2I. MS-analysis in our laboratory failed to confirm this result, and the position of the spot on the gel is not fully compliant with VDAC2 MW and pI. VDACs are mitochondrial outer membrane proteins and exist in three isoforms (VDAC 1, 2, 3). VDAC1 is localized in skeletal muscle of mice and humans in the SR and mitochondria where VDAC1 antibodies and Mitotracker stained virtually identical regions but not in the sarcolemma [143]. In Western blots no differences in VDAC1 expression could be demonstrated between control and *mdx* mice. As at the time of this study specific antibodies against VDAC2 and VDAC3 were not available the authors carried out Northern blots of total RNA after RT-PCR and found no significant changes for both VDAC1 and VDAC2 between control and *mdx* mice except for a slight reduction in 90-days old *mdx* mice with respect to their age-matched controls. In contrast, VDAC3 was markedly reduced in mdx mice in all age groups tested. Due to the very high sequence homology between VDAC1, VDAC2 and VDAC3, the preparation of specific antibodies against either one of the VDACs seems to be very challenging. Yamamoto et al. [144] tried to produce specific antibodies against the three rat VDACs (30.6, 31.6, and 30.7 kDa for VDAC1, 2 and 3 respectively) but were not successful except for VDAC1. Furthermore, they found that recombinant VDAC1 and VDAC2 show a very similar migration pattern in SDS-PAGE and VDAC3 unexpectedly seems to migrate slightly faster. VDAC1 was the most abundant isoform in the mitochondria of all tissues examined but considerable differences in relative levels between tissues were found and they did not analyze skeletal muscle. VDAC1 and VDAC2 were divided into three and two spots in their 2-DE experiments. Antibody specificity is obviously an issue for VDAC1, 2 and 3 respectively. It is hard to make a statement on VDAC2 levels in control versus patient samples in western blots because of the very high sequence identities of all VDAC isoforms. BLAST (bl2seq) alignments [145] using compositional score matrix adjustment [146] show 74% identity (91% positives) between VDAC1 and VDAC2, 67% identity (85% positives) between VDAC 1 and VDAC3 and 73% identity (88% positives) between VDAC2 and VDAC3. The commercially available VDAC2 (a) antibody from abcam was produced using GST-tagged recombinant full length human protein as antigen. VDAC2 (b) was produced against a synthetic peptide corresponding to the C-terminal amino acids 298/309 of Human VDAC2. BLAST predicts for the length of the peptide 66% identity (83% positives) with VDAC1 and 83% identity (83% positives) with VDAC3. Gene expression profiling studies

showed a 0.55 fold change reduction in VDAC1 [133] in RNA extracted from muscle biopsies from young DMD patients (under two years, however, four- and five-year-old patients did not show different expression patterns) and a -2.5 fold change in VDAC1 pseudogene in muscle biopsies from 5-7 year old males [101].
Despite these obvious challenges to produce specific antibodies against VDACs, the marked reduction in DMD patients makes them an interesting candidate disease marker.
Mitochondrial oxidative phosphorylation is impaired in DMD and mitochondrial proteins are largely reorganized. Elevated intracellular calcium and subsarcolemmal calcium levels have been found to be increased in muscle cells/muscle fibers from dystrophic mice. Mitochondria in muscle cells undergo a so-called “permeability transition” in response to persistent elevated calcium concentrations. In a regulated process, a large pore complex spanning the inner and outer mitochondrial membrane is formed which leads to loss of matrix and intermembrane content and swelling of the mitochondria. If this process is not stopped, mitochondria eventually break apart and cause necrotic and/or apoptotic cell death. This raises the question whether absence of the spot likely representing VDAC2 on the DMD 2DE gels is a secondary consequence of general lower expression of mitochondrial proteins in DMD patients as seen for example in the tissue-specific downregulation of eight mitochondrial mRNAs in *mdx* mice [147]. As seen in Figure 30, other mitochondrial proteins such as mitochondrial ATP synthase or mitochondrial malate dehydrogenase that we have identified on 2DE gels do not reflect the absence of VDAC2 in DMD patients indicating that the possible reduction in VDAC2 in DMD is more specific than just reduction in overall mitochondrial protein. Moreover, HSPβ2 has an association with mitochondria that is enhanced by head shock (and probably other cellular stress) [148] and the strong increase in HSPβ2 levels that we have seen in DMD patients would also not conform to the hypothesis of overall mitochondrial protein reduction. Further investigation on the drastic reduction of VDAC2 and probably other VDACs on the protein level should include first of all the definitive identification of the corresponding spot on the gel as VDAC2 and the evaluation of suitable antibodies.

Two unknown proteins were furthermore found to be differentially expressed in DMD patients compared to healthy controls. We have so far not been able to identify these proteins mass spectrometrically. In order to get the complete picture of candidate novel markers it would be interesting to identify the proteins corresponding to the respective spots in the 2DE gels.

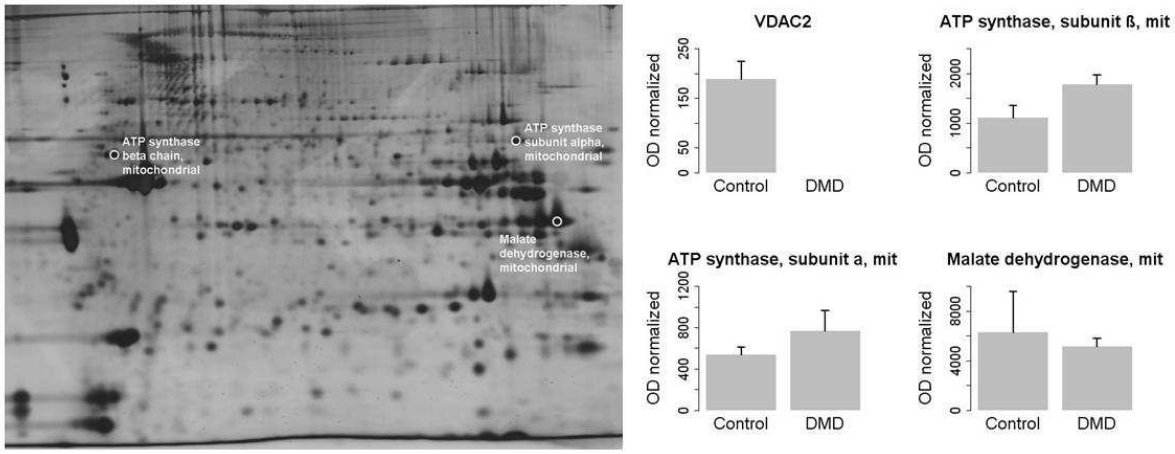

Figure 30: Mitochondrial proteins in DMD patients. Left panel: Position of mitochondrial proteins on gel. Right panel: VDAC2, ATP Synthase (mitochondrial) subunits alpha and beta, and malate dehydrogenase (mitochondrial) in EXP II, mit=mitochondrial, error bars are SEM. VDAC2 absence is probably not an effect of lower mitochondrial number.

4.2.4. Considerations on sampling

For the interpretation of the changes found between normal and diseased tissue it is necessary to rule out the possibility that differences might be caused by sample properties or characteristics rather than by the primary genetic mutation. The expression of genes on the mRNA level changes along the progression of the disease [133]. This might be evidence that by comparing controls with patients (not age-matched) some early markers of DMD could be missed. On the other hand, the same authors report that most of the molecular aspects seen in the pathophysiology in DMD are already seen in very young infant patients. Muscle protein levels and isoform patterns are strongly dependent on muscle innervation (reviewed in [85]): The loss of the connection of a muscle fiber unit to its motor neuron causes atrophy whereas artificial electro-stimulation causes considerable changes in muscle activity and fiber type shifting is observerd in various neuromuscular disorders and as adaptions to functional requirements in normal muscle tissue. Moreover, it was shown previously that the patterns of contractile protein isoforms in vastus lateralis and deltoideus muscles are reflective of their relative contents of fast- and slow-twitch muscle fibers [139]. A a number of proteins associated with glycolysis, the tricarboxylic acid cycle, and oxidative phosphorylation have been shown to be increased in vastus lateralis and the authors associate this phenomenon to the greater metabolic potential of vastus lateralis compared to deltoideus. Mitochondria are more abundant in slow-twitch (type I) muscle than in fast-twitch (type II) muscle [1] and oxidative enzymes are typically more abundant in slow-type muscle than in fast-type.
For dystrophin deficiency and in DMD/BMD patients the effect of muscle type in the biopsy does not seem to be significant [109], no considerable differences were found between a biopsy from the quadriceps taken at the time of the diagnosis and two follow-up biopsies from both the left and the right extensor digitorum brevis ten years later [108]. Dystrophin

deficiency is obviously such a dominant effect that muscle fiber differences in the samples do not have a considerable influence the outcome of analyses. This might be different for candidate marker proteins serving for the elucidation of secondary pathobiochemical abnormalities in DMD musce. Fast muscle fibers generally tend to be more affected in DMD patients than slow-twitch [149]. As a relevant proportion of our sample set consists of biopsies from unknown muscles alterations in protein patterns might be influenced by the muscle type that in the worst case would outbalance the alterations caused by the disease. The relative amount of fast- and slow-twitch fibers in muscle biopsies varies not only depending on the muscle that is used for the biopsy but also on the region (deep or superficial) of the muscle [2], a variable that is impossible to control in our study. From the samples with a known origin muscle none was a biopsy from typical type I-fibre muscle such as the soleus from a typical type II-fibre muscle such as orbicularis oculi. Samples in our study consisted of some vastus lateralis (depending on the region of the biopsy between 58 and 70% type II fibers), deltoideus (40-50%), biceps brachii (50-58%), tibialis anterior (27-28) [2] and quadriceps femoris. For HSPβ2 expression for example the only case where the protein was detectable (at a low level) in a control sample on a 2DE gel was sample CONT 5 which is from tibialis anterior. In EXP V in sample CONT 2 consisting of tibialis anterior muscle, no spot corresponding to HSPβ2 was detected whereas in the same experiment in DMD 12 (tibialis anterior) increased HSPβ2 was found. This suggests that in the case of HSPβ2 muscle fiber type differences probably not account for the higher protein levels in DMD patient tissue. Consequently, including the differences that come from the fact whether the muscle biopsy is from deep or superficial muscle biopsy it is not likely that the hardly assessable type of muscle used in our samples account for all of the differentially expressed proteins that we have found. However, in further studies aiming at the validation of markers of disease, samples should be matched as good as possible as a common problem to many approaches in clinical proteomics (utilizing eiter body fluid or tissue samples) is the assembly of a sample set from clinically well-defined individuals [84].

4.2.5. Proteomic approaches to (muscle) biomarker discovery

Functional genomic studies applying methods as DNA microarrays and profiling the transcriptome make the assumption that changes on the mRNA level are directly reflected in the proteome. This might not always be true, for example if protein levels are determined by the rate of their degradation or if changes are due to protein modifications (reviewed in [81]). Furthermore, rather than from changes in gene expression many short-term changes in the proteome originate from protein modifications such as phosphorlyation or acetylation representing the actual phenotype or disease state of the organism. Proteomic approaches aim at the evaluation of protein patterns in order to understand pathways and mechanisms underlying diseases, therapeutic strategies, and the discovery of new biomarkers.

Biomarkers are not only applied in diagnostic procedures but also in research processes and clinical trials, when therapeutic potential of novel drugs or treatments should be assessed. However, the process of biomarker discovery is lengthy and cost-intensive and in many cases many candidate biomarkers do not reach validation due to lack of specificity or sensitivity. Many proteins are identified and classified as potential biomarker but the problem remains that potential biomarkers reported by one group of researchers are not identified by other groups, even though if they are using similar methods [84, 150, 151]. We have for example not identified adenylate kinase that was reported to be dramatically decreased in *mdx* skeletal [82, 152]. It is of course possible that this decrease in *mdx* mice is not seen in humans as to our knowledge a decrease in adenylate kinase has not been observed in proteomic studies or in gene expression analysis [101]. Desmin was found to be increased in mdx diaphragm 2.14 fold [82] and 2.1 fold [83] and desmin upregulation is a known feature of dystrophinopathies. We have not found desmin to be significantly increased on our 2DE gels. The gels obtained after ZOOM isoelectric prefractionation revealed higher desmin expressions in the DMD patients included in the experiment, however, as there was only one gel from pooled DMD samples and controls respectively we cannot make a statement on significance (see Figure 31). In any case, these observations emphasize the need for careful evaluation and validation of candidate marker proteins that are found in 2DE experiments. There is a risk of generation of low-quality data increasing “background noise” in biomarker discovery rather than contribution to real progress in clinical proteomics if candidate biomarkers are not validated. A potential way out of this situation is the validation using independent assays such as ELISA, quantitative Western blotting, and confocal microscopy [23, 84].

MS-based proteomics have become the method of choice for many comparative and exploratory investigations in biological sciences. The accessible part of the proteome in serum or tissue at a given time or disease state is often separated prior to MS-based

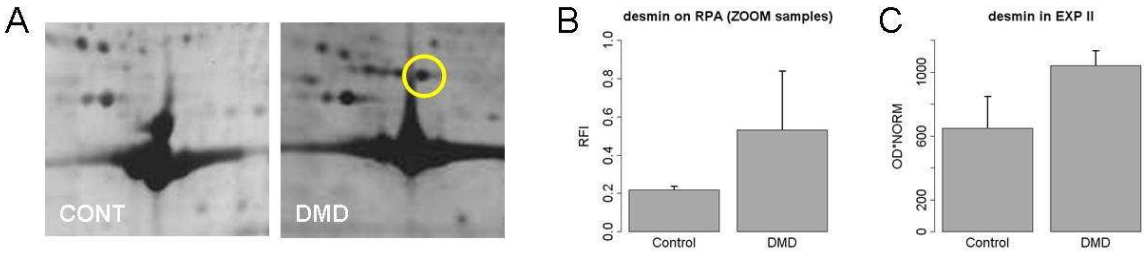

Figure 31: Higher desmin expression in DMD patients compared to control muscle tissue. A: Spot corresponding to desmin on narrow-range pI 2DE gels from control and DMD muscle tissue. B: Reverse protein array (RPA) RFI from the same samples that were pooled in A; C: Desmin spot intensities from 2DE gels in EXP II. No significant differences for desmin spot intensities or RFI signals on reverse protein arrays were found in DMD samples.

analytical methods, most commonly fractionated by chromatography and/or gel electrophoresis in order to reduce sample complexity. Fractionation methos such as 2DE again have a number of limitations. Skeletal muscle in particular consists of extremely large cellular structures as well as a considerable amount of insoluble proteins and it is relatively tough for preparing cell extracts [83, 85]. Proteins that are present at low concentrations can be hidden by highly abundant proteins or simply not detectable by the staining method of choice. It has become widely accepted that in order to identify diagnostic biomarkers the dynamic range of the samples included in the discovery experiment has to be reduced [84, 115]. Prefractionation methods have been applied in a number of studies in order to remove highly abundant proteins that are masking underlying less abundant spots or in order to expand the dynamic range of detection. However, all these procedures by their nature possibly introduce artefacts to subsequent analysis. In addition, by removing highly abundant serum proteins (e.g. albumin) other potentially interesting compounds bound to these proteins can be removed in the same step and therefore be missed in subsequent analyses [84]. In serum samples immunodepletion did so far not lead to the desired increased discovery of low-abundance biomarkers due to the introduction of variability in sample preparation. We carried out a prefractionation step according to isoelectrical point and the subsequent analyis of narrow-range pI fractions on separate gels did not lead to higher resolution but rather to higher background staining and horizontal streaking on gels. This was most possibly due to protein degradation in the time-consuming experiment with many steps carried out at room temperature. Another disadvantage of the prefractionation of the complex protein sample in solution is the relatively high sample consumption. For the ZOOM isoelectric fractionator an amount of 1.95mg total protein is necessary for one fractionation run which is hardly obtainable from a single patient (when lysing a large biopsy of 15-20mg, resulting amounts of protein in the lysate are around 1.5mg [114]). We therefore omitted prefractionation steps in subsequent experiments to obtain the most complete information about protein alterations in skeletal muscle tissue from patients with various muscular dystrophies compared to controls.

The range for plasma protein concentrations comprises about 12 order of magnitude from classical serum proteins (>10mg/ml) to interleukins and cytokines (<pg/ml). Tissue leakage proteins are found at concentrations around ng/ml [153] already presenting a major challenge to currently used technologies and methods aiming at biomarker discovery. Prostate specific antigen (PSA), probably the best known biomarker for the detection of prostate cancer, would be assumed to be present in blood due to tissue leakage at a concentration about 1000fold lower than in the prostate just because of the volume difference of the organs [115]. It was stated relatively early that elevated levels of serum CK do not directly reflect a change in the gene expression pattern [138], but the presence of the

MB isozyme in muscle is caused by regenerating muscle and the elevated serum CK is caused by leakage from damaged muscle. Advantages of biomarker discovery in tissue, on the other hand, include a more “direct” contact to the actual site of disease the disease and an overall lower range of protein concentrations in tissue (reviewed in [115]).
To overcome the high complexity of biological samples targeted approaches focus on a subproteome, e.g. on proteins that are N-linked glycosylated (reviewed in [115]) or in skeletal muscle on Ca^{2+}-binding proteins rather than on global protein expression patterns [56], while new emerging MS-based technologies as selected reaction monitoring (SRM, also referred to as multiple reaction monitoring, MRM) are promising new approaches for the sensitive detection of pre-defined analytes in complex samples [115].
The extent of the difference between controls and patient samples that is considered a “real” different is often discussed in literature. A two-fold increase or decrease in protein expression on 2DE gels is usually called relevant. The degree of experimental variation that is introduced in a 2DE experiment is at least 20% in terms of average CV and another 25%-50% comes from the biological variation depending on sample origin [154]. As biological variation in our sample set is hard to assess we have consideret a threshold of four-fold increase or decrease in protein expression relevant in our 2DE experiments.

4.3. Conclusions and Outlook

In conclusion, we have identified a set of candidate marker proteins that could after validation be applied in future diagnostic processes or in the monitoring of success in clinical trials evaluating emerging therapeutic approaches to muscular dystrophies. In case the highly sensitive antibodies to the respective proteins are available, assays could be carried out in a reverse protein array format that we have evaluated. Bringing a candidate biomarker to the level of a validated disease or even diagnostic marker is an ambitious goal and faces many methodological challenges. As muscle tissue is not readily obtainable future efforts that aim at the identification of biomarkers for muscular dystrophies in serum rather than in tissue are particularly interesting. In *mdx* serum coagulation factor XIIIa has been identified as a candidate marker of muscular dystrophy [155]. In the simplest case higher peak intensities in mass spectra might be characteristic for dystrophic sera like it is the case for serum CK. Whether factor XIIIa constitutes a serum biomarker for dystrophinopathies in humans remains to be demonstrated in translational studies where its specificity also needs to be addressed.
The concept of muscle-specific proteins are detectable in serum due to muscle damage is well known and provides the rationale for routine serum CK tests in various neuromuscular disorders [111, 155]. Blood circulating in the body collects proteins that are secreted or released from tissue, however, concentrations of tissue leakage proteins compared to classical serum proteins are lower by several orders of magnitude (reviewed in [115]). This

might be also the case for the muscle-specific HSPβ2 that could be found as a disease marker in serum due to leakage from damaged muscle tissue in DMD/BMD patients. Even though HSPβ2 is present at relatively high concentrations around 0.3μg/mg total protein in rat skeletal muscle [123] the concentration in serum due to leakage from damage tissue is unclear. Moreover, HSPβ2 is a cytosolic protein but is redistributed to the unsoluble protein fraction upon cellular stress [121], and poor solubility for purified recombinant HSPβ2 from E. coli has been reported [124]. We are currently aiming at the quantification of HSPβ2 in tissue lysates from primary human myotubes from DMD patients and controls. Unique peptides of HSPβ2 were detected previously in a shotgun LC-MS/MS experiment in primary human myotubes from DMD patients (data not shown) and preliminary experiments are carried out for the establishment of a selective SRM assay.

5. REFERENCES

1. Zierz S, Jerusalem F, Muskelerkrankungen (in German). 3., neu bearb. Aufl. ed. Neurologie: Klinische Neurologie, ed. S. Zierz. 2003, Stuttgart: Georg Thieme Verlag.
2. Johnson MA, Polgar J, Weightman D, Appleton D. Data on the distribution of fibre types in thirty-six human muscles: An autopsy study. Journal of the Neurological Sciences 1973; 18: 111-129.
3. Craig RW, Padron R, Molecular Structure of the Sarcomere, in *Myology: basic and clinical*, A.G. Engel and C. Franzini-Armstrong, Editors. 2004, McGraw-Hill: New York. p. 129-166.
4. Franzini-Armstrong C, Horwitz AR, The Cytoskeleton: Maintenance of Muscle Fiber Integrity, in *Myology: basic and clinical*, A.G. Engel and C. Franzini-Armstrong, Editors. 2004, McGraw-Hill: New York. p. 443-451.
5. Goldman YE, Homsher E, Molecular Physiology of the Cross-Bridge Cycle, in *Myology: basic and clinical*, A.G. Engel and C. Franzini-Armstrong, Editors. 2004, McGraw-Hill: New York. p. 187-202.
6. Batchelor CL, Winder SJ. Sparks, signals and shock absorbers: how dystrophin loss causes muscular dystrophy. Trends in Cell Biology 2006; 16: 198-205.
7. Franzini-Armstrong C, The Membrane Systems of Muscle Cells, in *Myology: basic and clinical*, A.G. Engel and C. Franzini-Armstrong, Editors. 2004, McGraw-Hill: New York. p. 232-256.
8. Banker BQ, Engel AG, Basic Reactions of Muscle, in *Myology: basic and clinical*, A.G. Engel and C. Franzini-Armstrong, Editors. 2004, McGraw-Hill: New York. p. 691-747.
9. Wallace GQ, McNally EM. Mechanisms of Muscle Degeneration, Regeneration, and Repair in the Muscular Dystrophies. Annual Review of Physiology 2009; 71: 37-57.
10. Bischoff R, Franzini-Armstrong C, Satellite and Stem Cells in Muscle Regeneration, in *Myology: basic and clinical*, A.G. Engel and C. Franzini-Armstrong, Editors. 2004, McGraw-Hill: New York. p. 66-86.
11. Bansal D, Campbell KP. Dysferlin and the plasma membrane repair in muscular dystrophy. Trends in Cell Biology 2004; 14: 206-213.
12. Sellers JR. Myosins: a diverse superfamily. Biochimica et Biophysica Acta (BBA) - Molecular Cell Research 2000; 1496: 3-22.
13. Schiaffino S, Reggiani C. Myosin isoforms in mammalian skeletal muscle. Journal of Applied Physiology 1994; 77: 493-501.
14. Pette D, Staron RS. Myosin Isoforms, Muscle Fiber Types, and Transitions. Microscopy Research and Technique 2000; 50: 500-509.
15. Sewry CA. Immunocytochemical Analysis of Human Muscular Dystrophy. Microscopy Research and Technique 2000; 48: 142-154.
16. Ervasti JM, Ohlendieck K, Kahl SD, Gaver MG, Campbell KP. Deficiency of a glycoprotein component of the dystrophin complex in dystrophic muscle. Nature 1990; 345: 315-319.
17. Martin PT. Dystroglycan glycosylation and its role in matrix binding in skeletal muscle. Glycobiology 2003; 13: 55R-66R.
18. Emery AEH. Fortnightly review: The muscular dystrophies. British Medical Journal 1998; 317: 991-995.
19. Hoffmann EP, Brown RH, Jr., Kunkel LM. Dystrophin: The Protein Product of the Duchenne Muscular Dystrophy Locus. Cell 1987; 51: 919-928.
20. Ohlendieck K, Campbell KP. Dystrophin constitutes 5% of membrane cytoskeleton in skeletal muscle. FEBS Journal 1991; 283: 230-234.
21. Campbell KP. Three Muscular Dystrophies: Loss of Cytoskeleton-Extracellular Matrix Linkage. Cell 1995; 80: 675-679.
22. Engel AG, Ozawa E, Dystrophinopathies, in *Myology: basic and clinical*, A.G. Engel and C. Franzini-Armstrong, Editors. 2004, McGraw-Hill: New York. p. 961-1025.

23. Lewis C, Carberry S, Ohlendieck K. Proteomic profiling of x-linked muscular dystrophy. Journal of Muscle Research and Cell Motility 2009; 30: 267-279.
24. Holt KH, Crosbie RH, Venzke DP, Campbell KP. Biosynthesis of dystroglycan: processing of a precursor propeptide. FEBS Letters 2000; 468: 79-83.
25. Brancaccio A, Schulthess T, Gesemann M, Engel J. Electron microscopic evidence for a mucin-like region in chick muscle α-dystroglycan. FEBS Letters 1995; 368: 139-142.
26. Ervasti JM, Campbell KP. Membrane organization of the dystrophin-glycoprotein complex. Cell 1991; 66: 1121-1131.
27. Henry MD, Campbell KP. Dystroglycan: an extracellular matrix receptor linked to the cytoskeleton. Current Opinion in Cell Biology 1996; 8: 625-631.
28. Helliwell TR, Nguyen thi M, Morris GE. Expression of the 43 kDa dystrophin-associated glycoprotein in human neuromuscular disease. Neuromuscular Disorders 1994; 4: 101-113.
29. Barton ER. Impact of sarcoglycan complex on mechanical signal transduction in murine skeletal muscle. The American Journal of Physiology - Cell Physiology 2006; 209: 411-419.
30. Matsumura K, Tomé FMS, Collin H*, et al.* Deficiency of the 50K dystrophin-associated glycoprotein in severe childhood autosomal recessive muscular dystrophy. Nature 1992; 359: 320-322.
31. Roberds SL, Leturcq F, Allamand V*, et al.* Missense mutations in the adhalin gene linked to autosomal recessive muscular dystrophy. Cell 1994; 78: 625-633.
32. Piccolo F, Roberds SL, Jeanpierre M*, et al.* Primary adhalinopathy: a common cause of autosomal recessive muscular dystrophy of variable severity. Nature Genetics 1995; 10: 243-245.
33. Anastasi G, Cutroneo G, Sidoti A*, et al.* Sarcoglycan subcomplex in normal human smooth muscle: an immunohistochemical and molecular study. International Journal of Molecular Medicine 2005 16: 367-374.
34. Lin S, Gaschen F, Burgunder J-M. Utrophin is a regeneration-associated protein transiently present at the sarcolemma of regenerating skeletal muscle fibers in dystrophin-deficient hypertrophic feline muscular dystrophy. Journal of Neuropathology and Experimental Neurology 1998; 57: 780-790.
35. Taylor J, Muntoni F, Dubowitz V, Sewry CA. The abnormal expression of utrophin in Duchenne and Becker muscular dystrophy is age related. Neuropathology and Applied Neurobiology 1997; 23: 399-405.
36. Weir AP, Morgan JE, Davies KE. A-utrophin up-regulation in mdx skeletal muscle is independent of regeneration. Neuromuscular Disorders 2004; 14: 19-23.
37. Fanin M, Nascimbeni AC, Fulizio L, Trevisan CP, Meznaric-Petrusa M, Angelini C. Loss of Calpain-3 Autocatalytic Activity in LGMD2A Patients with Normal Protein Expression. The American Journal of Pathology 2003; 163: 1929-1936.
38. Taveau M, Bourg N, Sillon G, Roudaut C, Bartoli M, Richard I. Calpain 3 Is Activated through Autolysis within the Active Site and Lyses Sarcomeric and Sarcolemmal Components. Molecular and Cellular Biology 2003; 23: 9127-3135.
39. Ravulapalli R, Garcia Diaz B, Campbell RL, Davies PL. Homodimerization of calpain 3 penta-EF-hand domain. The Biochemical Journal 2005; 388: 585-591.
40. Kinbara K, Ishiura S, Tomioka S*, et al.* Purification of native p94, a muscle-specific calpain, and characterization of its autolysis. The Biochemical Journal 1998; 335: 589–596.
41. Chan Y-m, Tong H-Q, Beggs AH, Kunkel LM. Human Skeletal Muscle-Specific [alpha]-Actinin-2 and -3 Isoforms Form Homodimers and Heterodimersin Vitroandin Vivo. Biochemical and Biophysical Research Communications 1998; 248: 134-139.
42. Beggs AH, Byers TJ, Knoll JHM, Boyce FM, Bruns GAP, Kunkel LM. Cloning and Characterization of Two Human Skeletal Muscle a-Actinin Genes Located on Chromosomes 1 and 11. The Journal of Biological Chemistry 1992; 267: 9281-9288.

43. Endo T, Masaki T. Differential Expression and Distribution of Chicken Skeletal- and Smooth-Muscle-type a-Actinins during Myogenesis in Culture. The Journal of Cell Biology 1984; 99: 2322-2332.
44. Nagano A, Koga R, Ogawa M*, et al.* Emerin deficiency at the nuclear membrane in patients with Emery-Dreifuss muscular dystrophy. Nature Genetics 1996; 12: 254-259.
45. Manilal S, Man Nt, Sewry CA, Morris GE. The Emery-Dreifuss muscular dystrophy protein, emerin, is a nuclear membrane protein. Human Molecular Genetics 1996; 5: 801-808.
46. Weilbach FX, Kress W, Strassburg HM, Müller CR, Gold R. Diagnostic approach to muscular dystrophies-recent developments and case reports. Nervenarzt 1999; 70: 89-1000.
47. Beedle AM, Nienaber PM, Campbell KP. Fukutin-related Protein Associates with the Sarcolemmal Dystrophin-Glycoprotein Complex. The Journal of Biological Chemistry 2007; 282: 16713-16717.
48. Brockington M, Blake DJ, Prandini P*, et al.* Mutations in the Fukutin-Related Protein Gene (FKRP) Cause a Form of Congenital Muscular Dystrophy with Secondary Laminin [alpha]2 Deficiency and Abnormal Glycosylation of [alpha]-Dystroglycan. The American Journal of Human Genetics 2001; 69: 1198-1209.
49. Brockington M, Yuva Y, Prandini P*, et al.* Mutations in the fukutin-related protein gene (FKRP) identify limb girdle muscular dystrophy 2I as a milder allelic variant of congenital muscular dystrophy MDC1C. Human Molecular Genetics 2001; 10: 2851-2859.
50. Bushby K, Anderson L, Pollitt C, Naom I, Muntoni F, Bindoff L. Abnormal merosin in adults. A new form of late onset muscular dystrophy not linked to chromosome 6q2. Brain 1998; 121: 581-588.
51. Brown SC, Torelli S, Brockington M*, et al.* Abnormalities in alpha-Dystroglycan Expression in MDC1C and LGMD2I Muscular Dystrophies. American Journal of Pathology 2004; 164: 727-737.
52. Rando TA. The dystrophin-glycoprotein complex, cellular signaling, and the regulation of cell survival in the muscular dystrophiesq. Muscle Nerve 2001; 24: 1575-1594.
53. Prior TW, Bridgeman SJ. Experience and Strategy for the Molecular Testing of Duchenne Muscular Dystrophy. Journal of Molecular Diagnostics 2005; 7: 317-326.
54. Kirschner J. Diagnosis and therapy of Duchenne and Becker forms of muscular dystrophy (in German). Medizinische Genetik 2009; 21: 322-326.
55. Matsumura K, Campbell KP. Deficiency of dystrophin-associated proteins: A common mechanism leading to muscle cell necrosis in severe childhood muscular dystrophies. Neuromuscular Disorders 1993; 3: 109-118.
56. Doran P, Dowling P, Lohan J, McDonnel K, Poetsch S, Ohlendieck K. Subproteomics analysis of Ca2+-binding proteins demonstrates decreased calsequestrin expression in dystrophic mouse skeletal muscle. Eur. J. Biochem 2004; 271: 3943-3952.
57. Judge LM, Haraguchi M, Chamberlain JS. Dissecting the signaling and mechanical functions of the dystrophin-glycoprotein complex. Journal of Cell Science 2006; 119: 1537-1546.
58. Ohlendieck K, Campbell KP. Dystrophin-associated Proteins Are Greatly Reduced in Skeletal Muscle from mdx Mice. The Journal of Cell Biology 1991; 115: 1685-1694.
59. Kuznetsov AV, Winkler K, Wiedemann FR, von Bossanyi P, Dietzmann K, Kunz WS. Impaired mitochondrial oxidative phosphorylation in skeletal muscle of the dystrophin-deficient mdx mouse. Molecular and Cellular Biochemistry 1998; 183: 87-96.
60. Muntoni F, Wells D. Genetic treatments in muscular dystrophies. Current Opinion in Neurology 2007; 20: 590-594.
61. van Deutekom JC, Janson AA, Ginjaar IB*, et al.* Local Dystrophin Restoration with Antisense Oligonucleotide PRO051. The New England Journal of Medicine 2007; 357: 2677-2686.
62. Kinali M, Arechavala-Gomeza V, Feng L*, et al.* Local restoration of dystrophin expression with the morpholino oligomer AVI-4658 in Duchenne muscular dystrophy:

a single-blind, placebo-controlled, dose-escalation, proof-of-concept study. Lancet Neurology 2009; 8: 918-928.
63. Doran P, Wilton SD, Fletcher S, Ohlendieck K. Proteomic profiling of antisense-induced exon skipping reveals reversal of pathobiochemical abnormalities in dystrophic mdx diaphragm. Proteomics 2009; 9: 671-685.
64. Emery AEH. The muscular dystrophies. The Lancet 2002; 359: 687-695.
65. Schara U, Mortier W. Neuromuscular diseases. Part 2: muscular dystrophies (MD) (in German). Nervenarzt 2004; 75: 219-239.
66. Nicholson LVB, Davison K, Johnson MA*, et al.* Dystrophin in skeletal muscle II. Immunoreactivity in patients with Xp21 muscular dystrophy. Journal of the Neurological Sciences 1989; 94: 137-146.
67. Klein CJ, Coovert DD, Bulman DE, Ray PN, Mendell J, Burghes AH. Somatic reversion/suppression in Duchenne muscular dystrophy (DMD): evidence supporting a frame-restoring mechanism in rare dystrophin-positive fibers. The American Journal of Human Genetics 1992; 50: 950-959.
68. Flanigan K, von Niederhausern A, Dunn D, Alder J, Mendell J, Weiss R. Rapid Direct Sequence Analysis of the Dystrophin Gene. The American Journal of Human Genetics 2003; 72: 931–939.
69. Mendell J, Buzin C, Feng J*, et al.* Diagnosis of Duchenne dystrophy by enhanced detection of small mutations. Neurology 2001; 57: 645-650.
70. Griggs R, Bushby K. Continued need for caution in the diagnosis of Duchenne muscular dystrophy. Neurology 2005; 64: 1498-1499.
71. Muntoni F. Is a muscle biopsy in Duchenne dystrophy really necessary? Neurology 2001; 57: 574-575.
72. Monaco A, Bertelson C, Liechti-Gallati S, Moser H, Kunkel L. An Explanation for the Phenotypic Differences between Patients Bearing Partial Deletions of the DMD Locus. Genomics 1988; 2: 90-95.
73. Guglieri M, Bushby K. How to go about diagnosing and managing the limb-girdle muscular dystrophies. Neurology India 2008; 56: 271-280.
74. Engel AG, The Muscle Biopsy, in *Myology: basic and clinical*, A.G. Engel and C. Franzini-Armstrong, Editors. 2004, McGraw-Hill: New York. p. 681-690.
75. Pogue R, Anderson LVB, Pyle A*, et al.* Strategy for mutation analysis in the autosomal recessive limb-girdle muscular dystrophies. Neuromuscular Disorders 2001; 11: 80-87.
76. Anderson LVB, Harrison RM, Pogue R*, et al.* Secondary reduction in calpain 3 expression in patients with limb girdle muscular dystrophy type 2B and Miyoshi myopathy (primary dysferlinopathies). Neuromuscular Disorders 2000; 10: 553-559.
77. Urish K, Kanda Y, Huard J. Initial Failure in Myoblast Transplantation Therapy Has Led the Way Toward the Isolation of Muscle Stem Cells: Potential for Tissue Regeneration. Current Topics in Developmental Biology 2005; 68: 263-280.
78. Gonnet F, Bouazza B, Armel Millot G*, et al.* Proteome analysis of differentiating human myoblasts by dialysis-assisted two-dimensional gel electrophoresis (DAGE). Proteomics 2008; 8: 264-278.
79. Decary S, Mouly V, Ben Hamida C, Sautet A, Barbet JP, Butler GS. Replicative Potential and Telomere Length in Human Skeletal Muscle: Implications for Satellite Cell-Mediated Gene Therapy. Human Gene Therapy 1997; 8: 1429-1438.
80. Bulfield G, Siller WG, Wight PAL, Moore KJ. X chromosome-linked muscular dystrophy (mdx) in the mouse. PNAS 1984; 81: 1189-1192.
81. Griffin JL, Des Rosiers C. Applications of metabolomics and proteomics to the *mdx* mouse model of Duchenne muscular dystrophy: lessons from downstream of the transcriptome. Genome Medicine 2009; 1: Article 32.
82. Doran P, Martin G, Dowling P, Jockusch H, Ohlendieck K. Proteome analysis of the dystrophin-deficient MDX diaphragm reveals a drastic increase in the heat shock protein cvHSP. Proteomics 2006; 6: 4610-4621.
83. Doran P, Dowling P, Donoghue P, Buffini M, Ohlendieck K. Reduced expression of regucalcin in young and aged mdx diaphragm indicates abnormal cytosolic calcium

handling in dystrophin-deficient muscle. Biochimica et Biophysica Acta 2006; 1764: 773-785.
84. Silberring J, Ciborowski P. Biomarker discovery and clinical proteomics. Trends in Analytical Chemistry 2010; 29: 128-140.
85. Doran P, Donoghue P, O'Connell K, Gannon J, Ohlendieck K. Proteomic profiling of pathological and aged skeletal muscle fibres by peptide mass fingerprinting (Review). International Journal of Molecular Medicine 2007; 19: 547-564.
86. Sheehan KM, Calvert VS, Kay EW*, et al.* Use of Reverse Phase Protein Microarrays and Reference Standard Development for Molecular Network Analysis of Metastatic Ovarian Carcinoma. Molecular and Cellular Proteomics 2005; 4: 346-355.
87. Pawlak M, Schick E, Bopp M, Schneider M, Oroszlan P, Ehrat M. Zeptosens' protein microarrays: A novel high performance microarray platform for low abundance protein analysis. Proteomics 2002; 2: 383-393.
88. Sinha P, Poland J, Schnölzer M, Rabilloud T. A new silver staining apparatus and procedure for matrix-assisted laser desorption/ionization-time of flight analysis of proteins after two-dimensional electrophoresis. Proteomics 2001; 1: 835-840.
89. R Development Core Team 2009. R: A language and environment for statistical computing. R Foundation for Statistical Computing, Vienna, Austria. ISBN 3-900051-07-0, http://www.R-project.org
90. White SJ, Den Dunnen JT. Copy number variation in the genome; the human DMD gene as an example. Cytogenetic and Genome Research 2006; 115: 240-246.
91. Ramelli GP, Joncourt F, Luetschg J, Weis J, Tolnay M, Burgunder J-M. Becker muscular dystrophy with marked divergence between clinical and molecular genetic findings: case series. Swiss Medical Weekly 2006; 136: 189-193.
92. Guglieri M, Straub V, Bushby K, Lochmüller H. Limb-girdle muscular dystrophies. Curr Opin Neurol 2008; 21: 576-584.
93. Klinge L, Dekomien G, Aboumousa A*, et al.* Sarcoglycanopathies: Can muscle immunoanalysis predict the genotype? Neuromuscular Disorders 2008; 18: 934-941.
94. Carrié A, Piccolo F, Leturcq F*, et al.* Mutational diversity and hot spots in the alpha-sarcoglycan gene in autosomal recessive muscular dystrophy (LGMD2D). J Med Genet 1997; 34: 470-475.
95. Manzur AY, Muntoni F. Diagnosis and new treatments in muscular dystrophies. J Neurol Neurosurg Psychiatry 2009; 80: 706-714.
96. Kolski HK, Hawkins C, Zatz M*, et al.* Diagnosis of limb-girdle muscular dystrophy 2A by immunohistochemical techniques. Neuropathology 2007; 28: 264-268.
97. Charlton R, Henderson M, Richards J*, et al.* Immunohistochemical analysis of calpain 3: Advantages and limitations in diagnosing LGMD2A. Neuromuscular Disorders 2009; 19: 449-457.
98. Gailly P, De Backer F, Van Schoor M, Gillis JM. In situ measurements of calpain activity in isolated muscle fibres from normal and dystrophin-lacking mdx mice. The Journal of Physiology 2007; 582: 1261-1275.
99. Ueyama H, Kumamoto T, Fujimoto S, Murakami T, Tsuda T. Expression of three calpain isoform genes in human skeletal muscles. Journal of Neurological Sciences 1998; 155: 163-169.
100. Spencer MJ, Croall DE, G. TJ. Calpains are activated in necrotic fibers from mdx dystrophic mice. The Journal of Biological Chemistry 1995; 270: 10909-10914.
101. Haslett JN, Sanoudou D, Kho AT*, et al.* Gene expression comparison of biopsies from Duchenne muscular dystrophy (DMD) and normal skeletal muscle. PNAS 2002; 99: 15000-15005.
102. Paulin D, Huet A, Khanamyrian L, Xue Z. Desminopathies in muscle disease. Journal of Pathology 2004; 204: 418-427.
103. Paulin D, Li Z. Desmin: a major intermediate filament protein essential for the structural integrity and function of muscle Experimental Cell Research 2004; 301: 1-7.
104. Zanotti S, Saredi S, Ruggieri A*, et al.* Altered extracellular matrix transcript expression and protein modulation in primary Duchenne muscular dystrophy myotubes. Matrix Biology 2007; 26: 615-624.

105. Schuierer MM, Mann CJ, Bildsoe H, Huxley C, Hughes SM. Analyses of the differentiation potential of satellite cells from myoD-/-, mdx, and PMP22 C22 mice. BMC Musculoskeletal Disorders 2005; 6:
106. Bachrach E, Li S, Perez AL*, et al.* Systemic delivery of human microdystrophin to regenerating mouse dystrophic muscle by muscle progenitor cells. PNAS 2004; 101: 3581-3586.
107. Danowski BA, Imanaka-Yoshida K, Sanger JM, Sanger JW. Costameres Are Sites of Force Transmission to the Substratum in Adult Rat Cardiomyocytes. The Journal of Cell Biology 1992; 118: 1411-1420.
108. Arechavala-Gomeza V, Kinali M, Feng L*, et al.* Immunohistological intensity measurements as a tool to assess sarcolemma-associated protein expression. Neuropathology and Applied Neurobiology 2009; Accepted Article, doi: 10.1111/j.1365-2990.2009.01056.x:
109. Williams MW, Resneck WG, Bloch RJ. Membrane Skeleton of Innervated and Denervated Fast- and Slow-Twitch Muscle. Muscle Nerve 2000; 23: 590-599.
110. Ferguson R, Carroll H, Harris A, Maher E, Selby P, Banks R. Housekeeping proteins: A preliminary study illustrating some limitations as useful references in protein expression studies. Proteomics 2005; 5: 566-571.
111. Morandi L, Angelini C, Prelle A*, et al.* High plasma creatine kinase: review of the literature and proposal for a diagnostic algorithm. Neurological Sciences 2006; 27: 303-311.
112. Higuchi I, Hashiguchi A, Matsuura E*, et al.* Different pattern of HSP47 expression in skeletal muscle of patients with neuromuscular diseases. Neuromuscular Disorders 2007; 17: 221-226.
113. Espina V, Woodhouse EC, Wulfkuhle J, Asmussen HD, Petricoin EF, Liotta LA. Protein microarray detection strategies: focus on direct detection technologies. Journal of Immunological Methods 2004; 290: 121-133.
114. Gelfi C, De Palma S, Cerretelli P, Begum S, Wait R. Two-dimensional protein map of human vastus lateralis muscle. Electrophoresis 2003; 21: 286-295.
115. Schiess R, Wollscheid B, Aebersold R. Targeted proteomic strategy for clinical biomarker discovery. Molecular Oncology 2009; 3: 33-44.
116. Mounier N, Arrigo A. Actin cytoskeleton and small heat shock proteins: how do they interact? Cell Stress & Chaperones 2002; 7: 167-176.
117. Nishimura RN, Sharp FR. Heat shock proteins and neuromuscular disease. Muscle Nerve 2005; 32: 693-709.
118. Doran P, Gannon J, O'Connell K, Ohlendieck K. Aging skeletal muscle shows a drastic increase in the small heat shock proteins [alpha]B-crystallin/HspB5 and cvHsp/HspB7. European Journal of Cell Biology 2007; 86: 629-640.
119. Bornman L, Rossouw H, Gericke GS, Polla BS. Effects of iron deprivation on the pathology and stress protein expression in murine x-linked muscular dystrophy. Biochemical Pharmacology 1998; 56: 751-757.
120. Sakuma K, Watanabe K, Totsuka T, Kato K. Pathological changes in levels of three small stress proteins, [alpha]B crystallin, HSP 27 and P20, in the hindlimb muscles of dy mouse. Biochimica et Biophysica Acta (BBA) - Molecular Basis of Disease 1998; 1406: 162-168.
121. Suzuki A, Sugiyama Y, Hayashi YK*, et al.* MKBP, a Novel Member of the Small Heat Shock Protein Family, Binds and Activates the Myotonic Dystrophy Protein Kinase. The Journal of Cell Biology 1998; 10: 1113-1124.
122. Iwaki A, Nagano T, Nakagawa M, Iwaki T, Fukumaki Y. Identification and Characterization of the Gene Encoding a New Member of the [alpha]-Crystallin/Small hsp Family, Closely Linked to the [alpha]B-Crystallin Gene in a Head-to-Head Manner. Genomics 1997; 45: 386-394.
123. Sugiyama Y, Suzuki A, Kishikawa M*, et al.* Muscle Develops a Specific Form of Small Heat Shock Protein Complex Composed of MKBP/HSPB2 and HSPB3 during Myogenic Differentiation. The Journal of Biological Chemistry 2000; 275: 1095-1104.

124. den Engelsman J, Boros S, Dankers PYW*, et al.* The Small Heat-Shock Proteins HSPB2 and HSPB3 Form Well-defined Heterooligomers in a Unique 3 to 1 Subunit Ratio. Journal of Molecular Biology 2009; 393: 1022-1032.
125. Mohoney DJ, Safdar A, Parise G*, et al.* Gene expression profiling in human skeletal muscle during recovery from eccentric exercise. The American Journal of Physiology - Regulatory, Integrative and Comparative Physiology 2008; 294: 1901-1910.
126. Verschuure P, Tatard C, Boelens W, Grongnet J-F, David JC. Expression of small heat shock proteins HspB2, HspB8, Hsp20 and cvHSP in different tissues of the perinatal developing pig. European Journal of Cell Biology 2003; 82: 523-530.
127. Ikezoe K, Nakamori M, Furuya H*, et al.* Endoplasmic reticulum stress in myotonic dystrophy type 1 muscle. Acta Neuropathologica 2007; 114: 527-535.
128. Antzelevitch C. Brugada Syndrome. Pacing and Clinical Electrophysiology 2006; 29: 1130-1159.
129. van Nostrand DW, Valdivia CR, Tester DJ*, et al.* Molecular and Functional Characterization of Novel Glycerol-3-Phosphate Dehydrogenase 1–Like Gene (GPD1-L) Mutations in Sudden Infant Death Syndrome. Circulation 2007; 116: 2253-2259.
130. Weiss R, Barmada MM, Nguyen T*, et al.* Clinical and Molecular Heterogeneity in the Brugada Syndrome: A Novel Gene Locus on Chromosome 3. Circulation 2002; 105: 707-713.
131. London B, Michalec M, Mehdi H*, et al.* Mutation in Glycerol-3-Phosphate Dehydrogenase 1–Like Gene (GPD1-L) Decreases Cardiac Na+ Current and Causes Inherited Arrhythmias. Circulation 2007; 116: 2260-2268.
132. Perloff JK, Henze E, Schelbert HR. Alterations in regional myocardial metabolism, perfusion, and wall motion in Duchenne muscular dystrophy studied by radionuclide imaging. Circulation 1984; 69: 33-42.
133. Pescatori M, Broccolini A, Minetti C*, et al.* Gene expression profiling in the early phases of DMD: a constant molecular signature characterizes DMD muscle from early postnatal life throughout disease progression. The FASEB Journal 2007; 21: 1210-1226.
134. Eisenberg I, Eran A, Nishino I*, et al.* Distinctive patterns of microRNA expression in primary muscular disorders. PNAS 2007; 104: 17016-17021.
135. Dulor JP, Cambon B, Vigneron P*, et al.* Expression of specific white adipose tissue genes in denervation-induced skeletal muscle fatty degeneration. FEBS Letters 1998; 439: 89-92.
136. Keller A, Demeurie J, Merkulova T*, et al.* Fibre-type distribution and subcellular localisation of α and β enolase in mouse striated muscle. Biology of the Cell 2000; 92: 527-535.
137. Peterson CA, Cho M, Rastinejad F, Blau HM. [beta]-Enolase is a marker of human myoblast heterogeneity prior to differentiation. Developmental Biology 1992; 151: 626-629.
138. Edwards YH, Tipler TD, Morgan-Hughes JA, Neerunjun JS, Hopkinson DA. Isozyme patterns and protein profiles in neuromuscular disorders. Journal of Medical Genetics 1982; 19: 175-183.
139. Capitanio D, Viganò A, Ricci E, Cerretelli P, Wait R, Gelfi C. Comparison of protein expression in human deltoideus and vastus lateralis muscles using two-dimensional gel electrophoresis. Proteomics 2005; 5: 2577-2586.
140. Brachvogel b, Dikschas J, Moch H*, et al.* Annexin A5 Is Not Essential for Skeletal Development. Molecular and Cellular Biology 2003; 23: 2907-2913.
141. Cagliani R, Magri F, Toscano A*, et al.* Mutation Finding in Patients With Dysferlin Deficiency and Role of the Dysferlin Interacting Proteins Annexin A1 and A2 in Muscular Dystrophies. Human Mutation 2005; 26: 283.
142. Rescher U, Gerke v. Annexins – unique membrane binding proteins with diverse functions. Journal of Cell Science 2004; 117: 2631-2639.

143. Massa R, Marlier LN, Martorana A*, et al.* Intracellular localization and isoform expression of the voltage-dependent anion channel (VDAC) in normal and dystrophic skeletal muscle. Journal of Muscle Research and Cell Motility 2000; 21: 433-442.
144. Yamamoto T, Yamada A, Watanabe M*, et al.* VDAC1, Having a Shorter N-Terminus Than VDAC2 but Showing the Same Migration in an SDS-Polyacrylamide Gel, Is the Predominant Form Expressed in Mitochondria of Various Tissues. Journal of Proteome Research 2006; 5: 3336-3344.
145. Altschul SF, Madden TL, Schäffer AA*, et al.* Gapped BLAST and PSI-BLAST: a new generation of protein database search programs. Nucleic Acids Research 1997; 25: 3389-3402.
146. Altschul SF, Wootton JC, Gertz EM*, et al.* Protein database searches using compositionally adjusted substitution matrices. FEBS Journal 2005; 272: 5101-5109.
147. Gannoun-Zaki L, Fournier-Bidoz S, Le Cam G*, et al.* Down-regulation of mitochondrial mRNAs in the mdx mouse model for Duchenne muscular dystrophy. FEBS Letters 1995; 375: 268-272.
148. Nakagawa M, Tsujimoto N, Nakagawa H, Iwaki T, Fukumaki Y, Iwaki A. Association of HSPB2, a Member of the Small Heat Shock Protein Family, with Mitochondria. Experimental Cell Research 2001; 271: 161-168.
149. Webster C, Silberstein L, Hays AP, Blau HM. Fast muscle fibers are preferentially affected in Duchenne muscular dystrophy. Cell 1988; 52: 503-513.
150. Aebersold R. A stress test for mass spectrometry-based proteomics. Nature Methods 2009; 6: 411-412.
151. Bell AW, Deutsch EW, Au CE*, et al.* A HUPO test sample study reveals common problems in mass spectrometry-based proteomics. Nature Methods 2009; 6: 423-430.
152. Ge Y, Molloy MP, Chamberlain JS, Andrews PC. Proteomic analysis of mdx skeletal muscle: Great reduction of adenylate kinase 1 expression and enzymatic activity. Proteomics 2003; 3: 1895-1903.
153. Anderson NL, Anderson NG. The Human Plasma Proteome: History, Character, and Diagnostic prospects. Molecular and Cellular Proteomics 2002; 1: 845-867.
154. Molloy MP, Brzezinski EE, Hang J, McDowell MT, VanBogelen RA. Overcoming technical variation and biological variation in quantitative proteomics. Proteomics 2003; 3: 1912-1919.
155. Alagaratnam S, Mertens BJA, Dalebout J*, et al.* Serum protein profiling in mice: Identification of Factor XIIIa as a potential biomarker for muscular dystrophy. Proteomics 2008; 8: 1552-1563.

6. ACKNOWLEDGEMENTS

First of all, I would like to thank Prof. Daniel Gygax for giving me the opportunity to do my PhD in his group. I am very happy he set up this interesting project for me and trusted me with the carrying out of this work. I appreciated his support, commitment, and straightforwardness very much.

I am very grateful to Prof. Markus Rüegg for being a highly professional, supportive, and inspiring mentor. I appreciated his expertise, interest in my work and support very much. Moreover, I would like to thank Markus for his encouragement, cordiality and a great sense of humour.

Many thanks go to Prof. Ruedi Aebersold for being the co-referee of my dissertation. I highly appreciate his interest in my work and his advice during my PhD.

I would like to thank Prof. Mike Hall for taking the chair of my PhD exam.

Furthermore, my thanks go to Dr. Markus Ehrat for letting me carry out the reverse protein array experiments at Zeptosens and everybody at his company for their help.

Thanks to all the members of the bioanalytics laboratories at the University of Applied Sciences Northwestern Switzerland for creating a motivating atmosphere and for being helpful in many situations. I would like to thank especially Daniela Tobler and Peter Spies for their patient supervision of my first steps in a bioanalytics laboratory and for excellent support in bioanalytical methods. Special thanks go also to Prof. Eric Kübler for inspiring discussions and for reviewing the manuscript of my thesis.

Thanks to Prof. Hansruedi Schmutz and Benjamin Gygax for letting me carry out the analytics in their laboratory and for giving me an excellent introduction to instrumental analytics.

My sincere thanks go to all the people who helped me with this project, especially Reto Ossola for LC-MS/MS support and Dr. Elizaveta Fasler for the excellent introduction to immunofluorescence

I would like to thank Anna Weston, Kristina Kufner and Sibylle Tschumi for being friends and colleagues at the same time. They all made my day more than just once.

Many thanks go to all of my friends for being there, especially Stefi Omlin. I'm a very lucky person to have a friend like her.

Finally, I would like to express my deepest gratitude to my parents. Their love and support are the basis of my happy life.

7. APPENDIX

7.1. Appendix I – Peptide list of all proteins identified in 2DE experiments

Nr	Unique Peptides	Percent Coverage	MW [kDa]	pI	Uniprot Nr	Name	Peptides	Remarks
1	12	48	29.6	6.86	P07451	Carbonic anhydrase 3	(R)HDPSLQPWSVSYDGGSAK(T), (R)DGIAVIGIFLK(I), (R)VVFDDTYDR(S), (K)DIRHDPSLQPWSVSYDGGSAK(T), (K)IGHENGEFQIFLDALDK(I), (K)GENQSPVELHTK(D), (K)FDPSCLFPACR(D), (K)YAAELHLVHWNPK(Y), (R)GGPLPGPYR(L), (K)EPMTVSSDQMAK(L), (R)HDPSLQPWSVSYDGGSAK(T), (K)YNTFKEALK(Q)	*******
2	11	30	43.1	6.77	P06732	Creatine kinase M-type	(K)FEEILTR(L), (K)GGDDLDPNYVLSSR(V), (K)GQSIDDMIPAQK(-), (K)LNYKPEEEYPDLSK(H), (K)LSVEALNSLTGEFK(G), (K)LSVEALNSLTGEFKGK(Y), (K)VLTLELYK(K), (K)VLTLELYKK(L), (R)FCVGLQK(I), (R)GTGGVDTAAVGSVFDVSNADR(L), (R)LGSSEVEQVQLVVDGVK(L)	****, ******
3	12	32	47.0	7.58	P13929	B-enolase	(K)VNQIGSVTESIQACK(L)*, (K)FMIELDGTENK(S), (K)DATNVGDEGGFAPNILENNEALELLK(T), (K)ACNCLLLK(V), (K)LAMQEFMILPVGASSFK(E), (K)VDKFMIELDGTENK(S), (K)TAIQAAGYPDK(V), (K)YNQLMR(I), (K)VVIGMDVAASEFYR(N), (R)GNPTVEVDLHTAK(G), (K)TAIQAAGYPDKVVIGMDVAASEFYR(N), (R)AAVPSGASTGIYEALELR(D)*	***
3a	2	5	47.0	7.58	P13929	B-enolase	(K)TAIQAAGYPDK(V), (K)VNQIGSVTESIQACK(L)	
4	32	54	69.4	5.92	P02768	Serum Albumin	(K)AACLLPK(L), (K)AAFTECCQAADK(A), (K)ADDKETCFAEEGKK(L), (K)AEFAEVSK(L), (K)AVMDDFAAFVEK(C), K)CCAAADPHECYAK(V), (K)CCTESLVNR(R), (K)DLGEENFK(A), (K)FQNALLVR(Y), (K)KVPQVSTPTLVEVSR(N), (K)LCTVATLR(E), (K)LDELRDEGK(A), (K)LKECCEKPLLEK(S), (K)LVAASQAALGL(-), (K)LVNEVTEFAK(T), (K)LVTDLTK(V), (K)QNCELFEQLGEYK(F), (K)QNCELFEQLGEYKFQNALLVR(Y), (K)QTALVELVK(H), (K)SHCIAEVENDEMPADLPSLAADFVESK(D), (K)SLHTLFGDKLCTVATLR(E), (K)TCVADESAENCDK(S), (K)TYETTLEK(C), (K)VFDEFKPLVEEPQNLIK(Q), (K)VPQVSTPTLVEVSR(N), (K)YICENQDSISSK(L), (K)YLYEIAR(R), (R)ETYGEMADCCAK(Q), (R)FKDLGEENFK(A), (R)MPCAEDYLSVVLNQLCVLHEK(T), (R)RPCFSALEVDETYVPK(E), (R)YKAAFTECCQAADK(A)	
5	3	20	22.8	5.98	P04792	Heat shock protein β-1	(K)LATQSNEITIPVTFESR(A), (R)VSLDVNHFAPDELTVK(T), (R)LFDQAFGLPR(L)	
5a	5	34	22.8	5.98	P04792	Heat shock protein β-1	(K)LATQSNEITIPVTFESR(A)*, (R)AQLGGPEAAKSDETAAK(-), (R)LFDQAFGLPR(L), (R)QLSSGVSEIR(H), (R)VSLDVNHFAPDELTVK(T)*	****, ******
6	11	72	19.0	4.91	Q96A32	Myosin regulatory light chain 2, skeletal muscle isoform	(K)GADPEDVITGAFK(V), (K)LKGADPEDVITGAFK(V), (K)FLEELLTTQCDR(F), (K)EAFTVIDQNR(D), (K)NEELDAMMK(E), (K)NMWAAFPPDVGGNVDYK(N), (R)TVEGGSSSVFSMFDQTQIQEFK(E), (K)NICYVITHGDAKDQE(-), (R)DTFAAMGR(L), (R)LNVKNEELDAMMK(E), (R)DGIIDKEDLR(D)	***
7	9	48	21.9	5.03	P08590	Myosin light chain 3	(K)AAPAPAPPPEPERPK(E), (K)AAPAPAPPPEPERPKEVEFDASK(I), (K)DTGTYEDFVEGLR(V), (K)ITYGQCGDVLR(A), (K)NKDTGTYEDFVEGLR(V)*, (R)ALGQNPTQAEVLR(V)*, (R)HVLATLGER(L), (R)LTEDEVEK(L), (R)VFDKEGNGTVMGAEIR(H)	
8	4	16	36.4	6.91	P40925	Malate dehydrogenase, cytoplasmic	(K)VIVVGNPANTNCLTASK(S), (K)ELTEEKESAFEFLSSA(-), (K)FVEGLPINDFSR(E), (K)LGVTANDVK(N)	***

Nr	Unique Peptides	Percent Coverage	MW [kDa]	pI	Uniprot Nr	Name	Peptides	Remarks
9	5	15	36.7	8.44	P00338	L-lactate dehydrogenase A chain	(K)VTLTSEEEAR(L), (K)LVIITAGAR(Q), (K)QVVESAYEVIK(L), (K)SADTLWGIQK(E), (R)VIGSGCNLDSAR(F)	****
9a	6	17	36.7	8.44	P00338	L-lactate dehydrogenase A chain	(K)VTLTSEEEAR(L), (K)LVIITAGAR(Q), (K)QVVESAYEVIK(L), (K)SADTLWGIQK(E), (R)VIGSGCNLDSAR(F), (R)LNLVQR(N)	
10	4	32	20.2	6.76	P02511	A-crystallin β chain	(R)IPADVDPLTITSSLSSDGVLTVNGPR(K), (R)FSVNLDVK(H), (R)APSWFDTGLSEMR(L), (K)HFSPEELKVK(V)	
11	6	32	26.7	6.45	P60174	Triosephosphate isomerase	(K)VVLAYEPVWAIGTGK(T), (R)IIYGGSVTGATCK(E), (K)IAVAAQNCYK(V), (K)QSLGELIGTLNAAK(V), (K)VTNGAFTGEISPGMIK(D), (K)SNVSDAVAQSTR(I)	
11a	2	12	26.7	6.45	P60174	Triosephosphate isomerase	(K)SNVSDAVAQSTR(I), (K)VPADTEVVCAPPTAYIDFAR(Q)	
12	1	6	18.1	4.06	P02585	Troponin C, skeletal muscle	(K)SEEELAECFR(I)	
13	2	13	18.4	4.04	P63316	Troponin C, slow skeletal and cardiac muscles	(K)SEEELSDLFR(M), (K)NADGYIDLDELK(I)	
14	4	21	18.8	4.92	P10916	Myosin regulatory light chain 2, ventricular/cardiac muscle isoform	(K)GADPEETILNAFK(V), (K)LKGADPEETILNAFK(V), (K)VFDPEGK(G), (K)NLVHIITHGEEKD(-)	***
14a	3	15	18.8	4.92	P10916	Myosin regulatory light chain 2, ventricular/cardiac muscle isoform	(R)DTFAALGR(V), (K)VFDPEGK(G), (K)EAFTIMDQNR(D)	
15	12	30	56.6	5.26	P06576	ATP synthase subunit β, mitochondrial	(K)IGLFGGAGVGK(T), (K)TVLIMELINNVAK(A), (K)VALVYGQMNEPPGAR(A)*, (K)VLDSGAPIKIPVGPETLGR(I), (K)VVDLLAPYAK(G), (R)AIAELGIYPAVDPLDSTSR(I)*, (R)FTQAGSEVSALLGR(I), (R)IMDPNIVGSEHYDVAR(G)*, (R)IMNVIGEPIDER(G), (R)IMNVIGEPIDERGPIK(T), (R)LVLEVAQHLGESTVR(T), (R)TIAMDGTEGLVR(G)	***, ******
16	3	8	49.8	4.79	P68371	Tubulin β-2 chain	(R)FPGQLNADLR(K), (R)EIVHIQAGQCGNQIGAK(F), (R)INVYYNEATGGK(Y)	***
17	5	35	21.1	7.01	P30086	Phosphatidylethanolamine-binding protein 1	(K)LYTLVLTDPDAPSR(K), (K)CDEPILSNR(S), (K)GNDISSGTVLSDYVGSGPPK(G)*, (K)NRPTSISWDGLDSGK(L), (K)LYEQLSGK(-)	****
18	6	19	32.9	4.66	P07951	Tropomyosin β chain	(K)CGDLEEELK(I), (K)LVILEGELER(S), (K)TIDDLEDEVYAQK(M), (R)IQLVEEELDR(A), (R)RIQLVEEELDR(A), (K)ATDAEADVASLNR(R)	
19	4	15	32.7	4.69	P09493	Tropomyosin α-1 chain	(K)SIDDLEDELYAQK(L), (K)QLEDELVSLQK(K), (K)CAELEEELK(T), (R)IQLVEEELDR(A)	
20	8	26	39.4	8.3	P04075	Fructose-bisphosphate aldolase A	(K)GILAADESTGSIAK(R), (R)ALANSLACQGK(Y), (R)ALQASALK(A), (K)ADDGRPFPQVIK(S), (R)LQSIGTENTEENRR(F), (R)QLLLTADDR(V), (K)YTPSGQAGAAASESLFVSNHAY(-), (K)VLAAVYK(A)	****
20a	3	10	39.4	8.3	P04075	Fructose-bisphosphate aldolase A	(K)ADDGRPFPQVIK(S), (K)GILAADESTGSIAK(R), (R)ALANSLACQGK(Y)	
21	2	8	25.0	6	P30041	Peroxiredoxin-6	(R)VVFVFGPDK(K), (K)LSILYPATTGR(N)	
22	3	6	46.7	5.4	P01009	A-1 antitrypsin	(K)LSITGTYDLK(S), (K)AVLTIDEK(G), (K)QINDYVEK(G)	******
22a	5	12	46.7	5.4	P01010	A-1 antitrypsin	(K)SVLGQLGITK(V), (K)LSITGTYDLK(S), (K)AVLTIDEK(G), (K)QINDYVEK(G), (K)VFSNGADLSGVTEEAPLK(L)	******
23	15	nd	38.4	6.61	Q8N335	Glycerol-3-phosphate dehydrogenase 1-like protein	(K)ALGITLIK(G), (K)ELLQTPNFR(I), (K)FC*ETTIGSK(V), (K)GIDEGPEGLK(L), (R)IC*DEITGR(V), (K)KALGITLIK(G), (R)KLTDIINNDHENVK(Y), (R)LGLM#EM#IAFAR(I), (K)LISDIIR(E), (K)LQGPQTSAEVYR(I), (K)LTDIINNDHENVK(Y), (K)MWVFEETVNGR(K), (K)NIVAVGAGFC*DGLR(C), (K)VC*IVGSGNWGSAVAK(I), (R)TVDNLLEVSAR(H)	*****

Nr	Unique Peptides	Percent Coverage	MW [kDa]	pI	Uniprot Nr	Name	Peptides	Remarks
24	3	nd	30.4	7.5	P45880	VDAC2	(R)NNFAVGYR(T), (K)LTLSALVDGK(S), (K)YQLDPTASISAK(V)	*****
	3	nd	36.4	6.91	P40925	Malate dehydrogenase, cytoplasmic	(K)GEFVTTVQQR(G), (K)VIVVGNPANTNC*LTASK(S), (K)LGVTANDVK(N)	*****
	2	nd	36.1	8.57	P04406	Glyeraldehyde-3-phosphate dehydrogenase	(R)VPTANVSVVDLTC*R(L), (R)GALQNIIPASTGAAK(A)	*****
25	2	4	47.2	7.01	P06733	A-enolase	(K)YNQLLR(I), (R)GNPTVEVDLFTSK(G)	**
26	2	15	16.0	6.74	P68871	Hemoglobin subunit β	(K)VNVDEVGGEALGR(L), (R)LLVVYPWTQR(F)	
27	7	13	57.9	7.95	P14618	Pyruvate kinase isozymes M1/M2	(R)LDIDSPPITAR(N), (R)NTGIICTIGPASR(S), (R)GDLGIEIPAEK(V), (K)GDYPLEAVR(M), (R)APIIAVTR(N), (R)GIFPVLCK(D), (K)DPVQEAWAEDVDLR(V)	
28	4	8	59.8	9.16	P25705	ATP synthase subunit α, mitochondrial	(R)VLSIGDGIAR(V), (R)VVDALGNAIDGK(G), (K)AVDSLVPIGR(G), (R)ILGADTSVDLEETGR(V)	
29	19	46	42.1	5.23	P68133	Actin, α skeletal muscle	(K)CDIDIR(K), (K)DSYVGDEAQSK(R), (K)DSYVGDEAQSKR(G)*, (K)EITALAPSTMK(I), (K)EKLCYVALDFENEMATAASSSSLEK(S), (K)IKIIAPPER(K), (K)LCYVALDFENEMATAASSSSLEK(S), (K)QEYDEAGPSIVHR(K)*, (K)QEYDEAGPSIVHRK(C), (R)DLTDYLMK(I), (R)GYSFVTTAER(E), (R)HQGVMVGMGQK(D), (R)LDLAGRDLTDYLMK(I), (R)MQKEITALAPSTMK(I)*, (R)VAPEEHPTLLTEAPLNPK(A), (K)AGFAGDDAPR(A), (K)RGILTLK(Y), (K)SYELPDGQVITIGNER(F)*, (R)AVFPSIVGRPR(Q)	*******
30	3	8	52.7	6.05	Q6ZMU5	Tripartite motif-containing protein 72	(R)ALVCGVCASLGSHR(G), (K)NAQPLLLVGPEGAEA(-), (K)ILAESPPPAR(L)	
31	2	8	30.8	5.56	P02647	Apolipoprotein A-I	(R)DYVSQFEGSALGK(Q), (R)THLAPYSDELR(Q)	***
32	10	39	35.5	8.92	P40926	Malate dehydrogenase, mitochondrial	(K)VAVLGASGGIGQPLSLLLK(N)*, (K)VDFPQDQLTALTGR(I), (K)TIIPLISQCTPK(V), (K)GCDVVVIPAGVPR(K), (K)MISDAIPELK(A), (K)IFGVTTLDIVR(A), (K)SQETECTYFSTPLLLGK(K), (K)GYLGPEQLPDCLK(G), (K)AGAGSATLSMAYAGAR(F), (K)EGVVECSFVK(S)	
33	1	3	35.9	4.94	P08758	Annexin A5	(R)GTVTDFPGFDER(A)	***
34	5	22	36.1	8.57	P04406	Glyceraldehyde-3-phosphate dehydrogenase	(R)VPTANVSVVDLTCR(L), (K)IISNASCTTNCLAPLAK(V)*, (R)GALQNIIPASTGAAK(A), (K)LVINGNPITIFQER(D)*, (K)LISWYDNEFGYSNR(V)	
35	2	7	32.9	5.86	P13805	Troponin T, slow skeletal muscle	(K)YEINVLYNR(I), (R)KKEEEELVALK(E)	
35a	4	10	32.9	5.86	P13805	Troponin T, slow skeletal muscle	(K)YEINVLYNR(I), (R)KKEEEELVALK(E), (K)EEEELVALK(E), (R)VDFDDIHR(K)	
	2	7	36.6	5.71	P07195	L-lactate dehydrogenase B chain	(R)GLTSVINQK(L), (K)LIAPVAEEEATVPNNK(I)	
35b	1	3	32.9	5.86	P13805	Troponin T, slow skeletal muscle	(K)YEINVLYNR(I)	
35c	2	7	32.9	6.86	P13806	Troponin T, slow skeletal muscle	(K)YEINVLYNR(I), (R)KKEEEELVALK(E)	******
36	11	19	77.1	6.81	P02787	Serotransferrin	(K)DGAGDVAFVK(H), (R)FDEFFSEGCAPGSK(K), (K)IECVSAETTEDCIAK(I), (K)EDPQTFYYAVAVVK(K), (K)SVIPSDGPSVACVK(K), (K)SASDLTWDNLK(G), (K)ASYLDCIR(A), (R)EGTCPEAPTDECKPVK(W), (R)DDTVCLAK(L), (K)EGYYGYTGAFR(C), (K)CSTSSLLEACTFR(R)	
37	2	3	83.3	4.97	P08238	Heat shock protein HSP 90-β	(R)ELISNASDALDK(I), (K)EQVANSAFVER(V)	***

Nr	Unique Peptides	Percent Coverage	MW [kDa]	pI	Uniprot Nr	Name	Peptides	Remarks
38	2	14	17.1	5.95	O14558	Heat shock protein β-6	(R)ASAPLPGLSAPGR(L), (K)HFSPEEIAVK(V)	
39	2	10	31.8	5.71	P45378	Troponin T, fast skeletal muscle	(K)IPEGEKVDFDDIQK(K), (K)ALSSMGANYSSYLAK(A)	
39a	5	17	31.8	5.71	P45378	Troponin T, fast skeletal muscle	(K)IPEGEKVDFDDIQK(K), (K)YDITTLR(S), (K)VDFDDIQK(K), (K)ALSSMGANYSSYLAK(A), (R)KKEEEELVALK(E)	
39b	3	16	31.8	5.71	P45378	Troponin T, fast skeletal muscle	(K)ALSSMGANYSSYLAK(A), (K)IPEGEKVDFDDIQK(K), (K)DLMELQALIDSHFEAR(K)	
39c	1	2	31.8	5.71	P45378	Troponin T, fast skeletal muscle	(K)YDITTLR(S)	
40	8	57	17.2	7.14	P02144	Myoglobin	(K)ALELFRK(D), (K)DMASNYKELGFQG(-), (K)GHPETLEKFDK(F), (K)GHPETLEKFDK(F)*, (K)HGATVLTALGGILKK(K), (K)HPGDFGADAQGAMNK(A)*, (K)SEDEMKASEDLKK(H), (K)VEADIPGHGQEVLIR(L)*	
41	4	14	37.6	5.81	P21695	Glycerol-3-phosphate dehydrogenase [NAD+], cytoplasmic	(K)IVGGNAAQLAQFDPR(V*, (K)LISEVIGER(L), (K)ANATGISLIK(G), (K)FCETTIGCKDPAQGQLLK(E)	
42	1	7	34.9	9.31	A8MVS1	Zinc finger protein 705F	(K)HMISMHPIIRKDASTSMTMSK(T)	
43	19	41	53.5	5.21	P17661	Desmin	(K)EEAENNLAAFR(A), (K)NISEAEEWYK(S), (K)VELQELNDR(F), (K)VSDLTQAANK(N), (R)ADVDAATLAR(I), (R)AQYETIAAK(N), (R)AQYETIAAK(N), (R)FANYIEK(V), (R)FASEASGYQDNIAR(L), (R)FLEQQNAALAAEVNR(L)*, (R)HQIQSYTCEIDALK(G), (R)INLPIQTYSALNFR(E), (R)QVEVLTNQR(A), (R)RIESLNEEIAFLK(K), (R)TNEKVELQELNDR(F), (R)TSGGAGGLGSLR(A), (R)VAELYEEELR(E), (K)IEEEIR(Q)	*******
44	3	7	55.9	8.54	P02675	Fibrinogen β chain	(K)DNENVVNEYSSELEK(H), (R)TPCTVSCNIPVVSGK(E), (K)ECEEIIR(K)	****
45	3	10	28.9	6.59	P00915	Carbonic anhydrase 1	(K)VLDALQAIK(T), (K)YSSLAEAASK(A), (K)GGPFSDSYR(L)	
48	1	8	20.2	5.07	Q16082	Heat shock protein β-2	(R)AALSHDGILNLEAPR(G)	**, ***
47	2	10	21.9	5.66	P32119	Peroxiredoxin-2	(K)ATAVVDGAFK(E), (R)QITVNDLPVGR(S)	
47a	2	10	21.9	5.66	P32119	Peroxiredoxin-2	(K)ATAVVDGAFK(E), (R)QITVNDLPVGR(S)	****

* different parent charges; ** confirmed by experiments at the Biozentrum, Basel (Suzette Moes); *** confirmed by an additional experiment (at least one more unique peptide); **** confirmed by an additional experiment (at least one unique peptide), ***** identified the Biozentrum, Basel (Suzette Moes); ****** data from ZOOM experiment; ******* confirmed in ZOOM experiment